Keck Adaptive Optics Note 455

Keck Next Generation Adaptive Optics Science Case Requirements Document

Release 2.2

Version 1
March 28, 2008

Keck Adaptive Optics Note 455

Keck Next Generation Adaptive Optics Science Case Requirements Document
Release 2.2

Table of Contents

List of Figures

List of Requirements Tables

Revision History

Version	Date	Author	Reason for revision / remarks
Release 1 v 10b	June 6, 2007	Max	Official "Release 1", KAON 455
Release 2 v 1	June 29, 2007	Max	Added Science Requirements tables that have been developed to date
Release 2 v 4	December 7, 2007	McGrath	Re-organized science cases into KSD vs. SD and updated Requirements Tables
Release 2 v 5	December 14, 2007	McGrath	Added science cases for Ice and Gas Giant Planets, Gravitational Lensing
Release 2 v 6	December 17, 2007	McGrath	Re-ordered science cases from extra-galactic to solar system
Release 2 v 9	January 23, 2008	McGrath and Max	Revised many requirements tables, revised sections 2.1.2, 2.1.4, 2.1.5, 2.2.1, 2.2.2, 2.2.6, 2.2.7, 2.2.8, 2.2.9, 2.3
Release 2 v 10	January 24, 2008	McGrath and Max	Inserted revised Rainbow Chart (v8)
Release 2.1 v1	February 1, 2008	McGrath and Max	Placed KSD and SD into different sections
Release 2.1 v2	March 12, 2008	McGrath	Removed section 4, Rainbow Chart, which is now KAON 548; updated section 3.2 on Gravitational Lensing
Release 2.1 v3	March 18, 2008	McGrath	Fixed Figure 15 and updated figure references.
Release 2.1 v4	March 19, 2008	McGrath	Added Young Stellar Objects and Debris Disk science. Updated Gravitational Lensing case.
Release 2.1 v5	March 20, 2008	McGrath & Wizinowich	Added current Keck AO publication statistics.
Release 2.1 v6	March 23, 2008	Max	Added more details about science cases, from NGAO Proposal. Renumbered figures.
Release 2.1 v7	March 25, 2008	Max	Added science case for Resolved Stellar Populations.
Release 2.1 v8	March 26, 2008	McGrath and Max	Added science case for Astrometry Science. Corrected inconsistencies in required enclosed energy for the High z Galaxy science case: now all are 0.07 arc sec.
Release 2.1 v10	March 28, 2008	McGrath	Fixed formatting and list of figures.
Release 2.2 v1	March 28, 2008	Max	Reformatted footer, renamed to Release 2.2

1 Introduction

1.1 Background

The Science Team of the Keck Next-Generation Adaptive Optics (NGAO) project is charged with 1) identifying compelling science cases that will set the requirements for NGAO performance, 2) deriving from these cases the science requirements for the NGAO system, and 3) when design trade-offs must be made, ensuring that the NGAO system will be built with capabilities that enable key science cases to be carried out to the greatest extent possible.

This document, which will be referred to as the Science Case Requirements Document (SCRD), is a "living document" and will be updated as the science cases are developed with increasing fidelity. Initial versions of this SCRD relied upon and heavily referenced the science cases developed for the Proposal to the Keck Science Steering Committee prepared in June 2006 (KAON 455). Later versions are considerably more concrete with respect to requirements, and include additional science drivers that will influence the operations modes of the NGAO system but not the central AO performance requirements. Key issues continue to be (a) the importance of the science enabled by the NGAO system and its accompanying instruments; (b) the advances offered by NGAO relative to AO systems being developed on other telescopes (discovery space); and (c) complementarity to the James Webb Space Telescope (JWST) and the Atacama Large Millimeter Array (ALMA), which will be commissioned on the same timescale as Keck NGAO.

Since June 2006, the Project Scientist has assembled a Science team and met with subgroups thereof to re-examine the initial science cases, to add new ones where appropriate, to develop solid performance requirements, and to look in more detail at the associated Instrument and Observatory requirements. This document, Release 2.1 of the SCRD, describes AO and instrument requirements for a subset of NGAO science that is anticipated to have impact on the following AO system error budgets and instrument requirements:

- AO and instrument background requirements
- wavefront error
- Point Spread Function (PSF) knowledge and stability
- astrometric error budget
- field of view and field of regard
- spectral resolution and multiplicity for the deployable integral field unit instrument
- AO capabilities at visible wavelengths

We begin with an overview of the capabilities expected for the James Webb Space Telescope (JWST), and for the Atacama Large Millimeter Array (ALMA), both of which are expected to be commissioned within a year or two of the anticipated NGAO commissioning date.

1.2 James Webb Space Telescope Capabilities

The James Webb Space Telescope (JWST) is a cryogenic 6.5-m space telescope currently scheduled to be launched in 2013. It will have considerably higher faint-source sensitivity than Keck NGAO due to its low backgrounds. Its NIRCAM instrument will image in 14 filters in the 0.6-2.3 μm wavelength range that overlaps with Keck NGAO. NIRCAM will have a 2.2 x 2.2 arc-minute field of view, a pixel scale of 0.035 arc sec for 0.6-2.3 μm wavelengths, and coronagraphic capability. NIRCAM has diffraction-limited imaging for wavelengths between 2.4 and 5 μm, but not below 2 μm due both to the primary mirror quality specification and to the undersampled pixel scale (0.035 arcsec) within NIRCAM. Thus there is an interesting part of parameter space in which Keck NGAO can complement JWST's imaging capabilities: diffraction limited imaging at wavelengths below 2 μm, over a field of order 2 arc-minutes on a side, and with a smaller diffraction limit due to Keck's larger diameter.

NIRSpec is a near infrared multi-object spectrograph for JWST in the 0.6 - 5 μm band. The primary goal for NIRSpec is enabling large surveys of faint galaxies ($1<z<5$) and determining their metallicity, star formation rate, and reddening. The NIRSpec design provides three observing modes for slit spectroscopy: a low resolution R=100 prism mode, an R=1000 multi-object mode, and an R=2700 mode. In the R=100 and R=1000 modes NIRSpec provides the ability to obtain simultaneous slit spectra of more than 100 objects in the 3.4 x 3.5 arcmin field of view. Spatial pixel size will be 0.1 arc sec. There will be only one integral field spectrograph with field of view 3" x 3", using 0.1 arc sec pixels, and a spectral resolution of R=2700.

Areas of parameter space in which Keck NGAO would complement JWST's spectroscopic capabilities include the following: 1) Spectroscopy (either slit or IFU) that benefits from spatial resolution better than 0.1 arc sec; 2) multi-IFU spectroscopy; 3) spectroscopy (slit or IFU) near the Keck diffraction limit at wavelengths 0.6 - 2 μm. It would be very difficult for Keck NGAO to compete with JWST at wavelengths longer than K band, because JWST will have far lower backgrounds. Even at the long-wavelength end of K band where the thermal background is important, NGAO will have difficulty competing in sensitivity with JWST's NIRSpec.

1.3 ALMA Capabilities

ALMA will be a powerful new facility for mm and sub-mm astrophysics, currently scheduled to begin science operations in 2012. It will consist of 54 12-m and 12 7-m antennas located at an altitude of 5000 m (16,500 feet) in the Atacama desert of Chile. ALMA will observe, with very high sensitivity and resolution, the cold regions of the Universe which are optically dark, yet shine brightly in the millimeter portion of the electromagnetic spectrum. With baselines ranging from 150 m to 18 km, it will have spatial resolution down to 0.01 arc-seconds (0.004 arc-seconds at the highest frequencies), with typical resolution of 0.1 arc-second or better. It is expected to operate within atmospheric windows from 0.35 to 9 mm.

The design of the ALMA is being driven by three key science goals:

1. The ability to detect spectral line emission from CO or CII in a normal galaxy like the Milky Way at a redshift of z = 3, in less than 24 hours of observation.

2. The ability to image the gas kinematics in protostars and in protoplanetary disks around young Sun-like stars at a distance of 150 pc (roughly the distance of the star-forming clouds in Ophiuchus or Corona Australis), enabling the study of their physical, chemical and magnetic field structures and to detect the tidal gaps created by planets undergoing formation in the disks.

3. The ability to provide precise images at an angular resolution of 0.1 arcsec. Here the term "precise image" means being able to represent, within the noise level, the sky brightness at all points where the brightness is greater than 0.1% of the peak image brightness.

ALMA will excel at the study of chemical evolution in star-forming regions at $z \sim 3$, dust-gas interactions, molecules surrounding stars, and molecular clouds. With its high sensitivity it will detect redshifted continuum dust emission out to z=10. It will reveal kinematics of obscured AGNs and quasi-stellar objects on spatial scales of 10 - 100 pc. It will use line emission from CO to measure the redshift of star-forming galaxies throughout the universe. It will image the formation of molecules and dust grains in the circumstellar shells and envelopes of evolved stars, novae, and supernovae.

ALMA's spatial resolution in the mm and sub-mm bands will be competitive with Keck NGAO's diffraction limit at wavelengths 0.6 – 2.4 μm. ALMA will be observing regions that are colder and more dense than can be seen in the visible or near-infrared with Keck. However Keck NGAO observations of H_2 and atomic hydrogen emission lines at H and K bands will complement ALMA by characterizing the warmer outer regions of molecular clouds and circumstellar disks. ALMA images and spectra of debris disks will complement the higher spatial resolution NGAO images at shorter wavelengths.

1.4 Next Generation AO Projects at Other Observatories

The NGAO team has done a survey of current and future AO systems worldwide. Within the scope of our science goals we would prefer to position Keck NGAO to take a leadership role in AO, rather than building the second or third version of a specific type of next-generation AO system.

The VLT and Gemini Observatories are planning Ground Layer AO and Extreme AO systems. Gemini South and (eventually) the LBT plan to have MCAO systems. By contrast *precision AO*, as in the planned Keck NGAO system, has not been emphasized in the plans of the other 8-10 meter telescopes.

Below in Table 1 we give an overview of plans of other observatories for what we call "next-generation AO systems" on 8 – 10 meter telescopes. By next-generation AO we mean those systems that go beyond single-conjugate AO with one laser guide star, or that aim for a special-purpose application such as high-contrast imaging or interferometry. We obtained our information from published papers, from web sites, and from the May 2006 SPIE meeting in Orlando FL.

Next-Generation AO Systems Under Development for 8 - 10 meter Telescopes					
Type	**Telescope**	**GS**	**Next-Generation AO Systems for 8 to 10 m telescopes**	**Capabilities**	**Dates**
High-contrast	Subaru	N/LGS	Coronagraphic Imager (CIAO)	Good Strehl, 188-act curvature, 4W laser	2007
High-contrast	VLT	NGS	Sphere (VLT-Planet Finder)	High Strehl; not as ambitious as GPI	2010
High-contrast	Gemini-S	NGS	Gemini Planet Imager (GPI)	Very high Strehl	2010
Wide-field	Gemini-S	5 LGS	MCAO	2' FOV	2007
Wide-field	Gemini	4 LGS	GLAO	Feasibility Study Completed	?
Wide-field	VLT	4 LGS	HAWK-I (near IR imager) + GRAAL GLAO	7.5' FOV, AO seeing reducer, 2 x EE in 0.1"	2012
Wide-field	VLT	4 LGS	MUSE (24 vis. IFUs) + GALACSI GLAO	1' FOV; 2 x EE in 0.2" at 750nm	2012
Narrow-field	VLT	4 LGS	MUSE (24 vis. IFUs) + GALACSI GLAO	10" FOV, 10% Strehl @ 650 nm	2012
Inter-ferometer	LBT	NGS	AO for LINC-NIRVANA (IR interferometer)	Phase 1: Single conj., 2 tel's Phase 2: MCAO 1 telescope Phase 3: MCAO both telescopes	Phase 1 in 2008

Table 1 Next-Generation AO Systems Under Development for 8 – 10 meter Telescopes

1.5 Science with the Existing Keck AO Systems

The two existing Keck AO systems, both with and without laser guide star, have been extremely fruitful. Through early March 2008 a total of 174 refereed science papers have been accepted for publication based on Keck AO data. The distribution with respect to subfield is as follows: 32% solar system, 51% galactic and 17% extragalactic as shown in Figure 1; this total includes 18 papers from the Keck Interferometer. A total of 37 laser guide star (LGS) science papers were published or accepted beginning in 2005 (12% solar system, 50% galactic and 38% extragalactic), and the number steadily increases each year.

Keck AO has had a significant impact on the young researchers in our community. A rough count was made of student participation in the author lists of the Keck AO science papers

published through 2005. The total was 26 graduate students and 20 postdocs. This educational impact continues to grow with Keck LGS AO.

Extending the benefits of AO to a greater range of science comes down to three key characteristics for a next-generation AO system: (1) very high Strehl near-IR performance to produce a stable, high-contrast PSF; (2) correction at optical wavelengths (toward the red) to achieve the highest angular resolutions and to access key physical diagnostics; and (3) and expanding the corrected field of view to open the door to statistical studies of larger samples. Enabling these new observational capabilities will advance AO from being a specialized tool to a fundamental Observatory facility, capable of meeting the demands of many quite different science programs.

The NGAO science cases have been developed based on the significant AO science experience of the Keck user community, as reflected in the scientific productivity of the existing Keck AO systems. The combination of the Keck science community and NGAO will be very powerful.

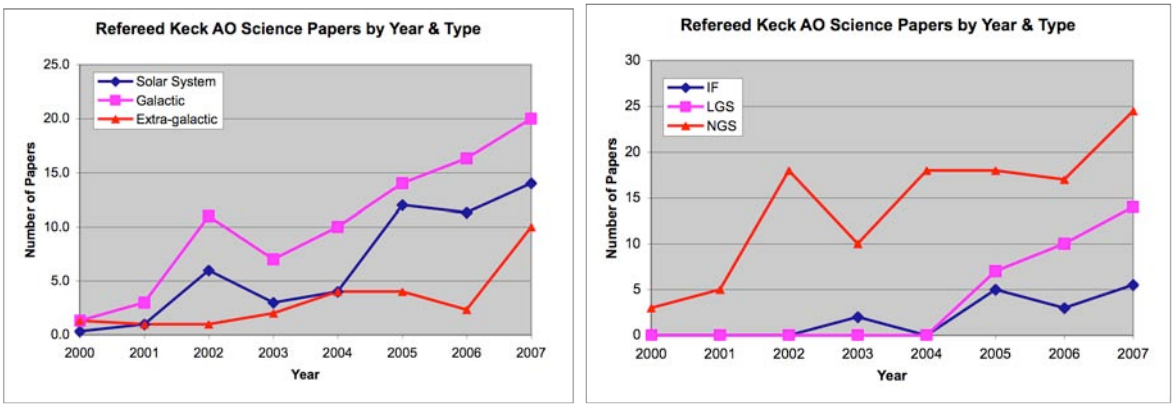

Figure 1. Keck AO science papers by year and type of science.

2 Science Cases: Key Science Drivers

"Key Science Drivers" (KSDs) are defined as those science cases which place the strongest or technologically challenging demands on the performance of the NGAO system and instruments. KSDs are the science cases that we are using to drive the performance requirements for the AO system and instruments. In Section 3 we will also discuss a number of "Science Drivers" (not Key). The latter are included in order to assure that the NGAO system is sufficiently flexible to deal with the broad range of science that users will demand, over the lifetime of the NGAO system. Typically the "Science Drivers" do not push the state of the art of the AO system itself, but rather they require specific types of coordination between the AO system, the instruments, and the telescope, or they help define parameters such as the full wavelength range or the required field of view. In the remainder of this section we discuss the "Key Science Drivers."

2.1 Galaxy Assembly and Star Formation History

Authors: D. Law. C. Steidel, J. Larkin
Editor: Claire Max

2.1.1 Introduction

Within the last decade the near infrared has become crucial for understanding the early universe and the evolution of galaxies. At redshifts $z > 1$, galaxies have shrunk to angular sizes of approximately 1 arc sec making seeing based observations almost useless at uncovering morphologies and internal kinematics. At the epoch of greatest star formation and AGN activity around a $z \sim 2.5$, traditional optical lines of Hα, OIII and OII are nicely shifted into the K, H and J bands respectively. The Keck LGS AO system with OSIRIS spatially resolved infrared spectroscopy is just now starting to dissect some of the brightest galaxies at this epoch. But with the factor of 20 - 40 in sensitivity gain possible with Keck NGAO (see below), a wealth of science topics can be addressed. These include the relationship between AGN and their host galaxies: radio galaxies and quasars have very strong emission lines and complex kinematics. In more "normal" galaxies, the redshift range from 1.5 to 2.5 is the key era for the birth of their first stars and the formation of the major architectural components of the galaxy, the bulge and disk. Measuring the morphology of star formation, the kinematics of proto-disks, the internal velocity dispersions and metallicity gradients (e.g. from the NII/Hα ratio) will allow us to witness the birth of galaxies like the Milky Way.

Table 2 shows which spectral lines are available in each near-IR band as a function of z.

Table 2

Redshift	J band	H band	K band
~ 1.2	Hα and NII		
~ 1.5	OIII	Hα and NII	
~ 2.5	OII	OIII	Hα and NII
~ 3.2		OII	OIII
~ 4.1			OII

Because JWST is optimized for faint-object IR spectroscopy and imaging, for this science case we will seek specific "sweet spots" in which Keck NGAO can make a significant contribution in the age of JWST.

Here we address science requirements flowing from one of these redshift ranges: $2 \leq z \leq 3$.

2.1.2 Scientific background and context

At high redshifts $z \sim 1 - 3$, galaxies are thought to have accumulated the majority of their stellar mass (Dickinson et al. 2003), the rate of major galaxies mergers appears to peak (Conselice et al. 2003), and instantaneous star formation rates and stellar masses range over two decades in value (Erb et al. 2006). Given the major activity at these redshifts transforming irregular galaxies into the familiar Hubble sequence of the local universe, it is of strong interest to study these galaxies in an attempt to understand the overall processes of galaxy formation and the buildup of structure in the universe.

The global properties of these galaxies have recently received considerable attention, and the star formation rate, stellar mass, gaseous outflow properties, etc. have been studied in detail (e.g. Steidel et al. 2004, Papovich et al. 2006, Reddy et al. 2006 and references therein). Beyond these global properties however, little is known about their internal kinematics or small-scale structure, particularly with regard to their mode of dynamical support or distribution of star formation. Previous observations with slit-type spectrographs (e.g. Erb et al. 2004, Weiner et al. 2006) and seeing-limited integral field spectrographs (Flores et al. 2006) suggest that kinematics are frequently inconsistent with simple equilibrium disk models. However these studies are too severely constrained by slit misalignment, spatial resolution, and the size of the atmospheric seeing halo relative to the size of the typical sources (less than one arcsecond) to obtain conclusive evidence. It is therefore unknown whether the majority of star formation during this epoch is due to rapid nuclear starbursts driven by major merging of gas-rich protogalactic fragments, circumnuclear starbursts caused by bar-mode or other gravitational instabilities, or piecemeal consumption of gas reservoirs by overdense star forming regions in stable rotationally-supported structures.

Here we investigate the general capabilities of Keck NGAO for the study of these high-redshift galaxies, via simulations of the integral field spectrographs used to dissect these galaxies and to study their kinematics and chemical composition.

2.1.3 Scientific goals

The study of high-redshift galaxies is a powerful driver for multiplexed observations, for example via deployable integral field unit (IFU) spectrographs. Given the areal densities of 1 to 10 targets per square arcminute on the sky (depending on the target selection criteria, Table 3), multiplexing multi-conjugate or multi-object adaptive optics (MCAO/MOAO) systems would be capable of simultaneously observing 6 to 12 targets within a several square arcminute field, permitting the compilation of a large representative sample with a minimum of observing time. In order to take best advantage of the high areal densities of targets, it is desirable to be able to deploy of order 6-12 IFUs over a ~ 2 square arcminute field of view.

Table 3

Space Densities of Various Categories of Extragalactic Targets.

Type of Object	Approx density per square arc minute	Reference
SCUBA sub-mm galaxies to 8 mJy	0.1	Scott et al. 2002
Old and red galaxies with $0.85 < z < 2.5$ and $R < 24.5$	2	Yamada et al. 2005; van Dokkum et al. 2006
Field galaxies w/ emission lines in JHK windows $0.8 < z < 2.6$ & $R < 25$	> 25	Steidel et al. 2004; Coil et al. 2004
Center of distant rich cluster of galaxies at $z > 0.8$	> 20	van Dokkum et al. 2000
All galaxies $K < 23$	> 40	Minowa et al. 2005

Such observations would permit the study of the chemical composition and distribution of star formation within the target galaxies (e.g. through mapping the measured [N II]/Hα ratios), in addition to mapping the velocity fields of the galaxies. Velocity data will enable us to detect AGN through chemical signatures and broadening of nuclear emission lines, to differentiate chaotic major mergers from starbursting galaxies in dynamical equilibrium, to determine the location of major star forming regions within any such rotationally supported systems, and to distinguish between chaotic and regular velocity fields to help ascertain whether observed star formation is commonly a consequence of major tidal interaction as predicted in current theories of galaxy formation.

With current-generation instruments, it is extremely challenging to observe a representative sample of sources due to the uncertainties inherent in long-slit spectroscopy (i.e. slit misalignment with kinematic axes), seeing-limited integral field spectroscopy (i.e. loss of information on scales smaller than the seeing disk), or a single-object IFU with current-generation adaptive optics (for which integration times are prohibitive for obtaining a large sample). A high-Strehl NGAO system with multi-object IFU capability and lower background would represent a major advance towards reliable kinematic and chemical data for a large sample of high redshift galaxies. These data could then be productively integrated with the known global galaxy properties to further our understanding of galaxy formation in the early universe.

2.1.4 Proposed observations and targets

At redshifts z = 0.5-3, major rest-frame optical emission lines such as Hα, [N II], and [O III] fall in the observed frame near-IR, and in order to study the evolution of galaxies across this range of cosmic times it is important to have wavelength coverage extending from 1 to 2.5 microns. Hα line emission from the well-studied redshift z ~ 2-3 galaxy sample falls in the K band, emphasizing the importance of optimizing observations at these wavelengths by reducing thermal backgrounds and increasing system throughput as much as possible.

A typical observing strategy could entail simultaneous spatially resolved spectroscopy of approximately 6 high-redshift galaxies within a given field, using a dithered set of exposures designed to move each object around on the detectors permitting maximum on-source integration time while simultaneously measuring accurate background statistics for sky subtraction. Based on the numerical simulations of Law et al. (2006) and the observed performance of the OSIRIS spectrograph, we anticipate that typical observations (assuming a K-band Strehl of roughly 60-70% from the NGAO system) would last approximately < 3 hours per set of targets (for bright star-forming galaxies at redshift z ~ 2) permitting a sample of 40 - 50 targets in a given night of dedicating observing.

Figure 2 shows the significant improvement in signal to noise ratio predicted for the NGAO system, relative to today's Keck 2 laser guide star AO. NGAO will yield a signal to noise ratio 3 - 6 times higher than the current Keck LGS AO system, for the same exposure times. For background-limited measurements this means an exposure-time reduction of a factor of 9 to 36. Adding multiple IFUs in the system will multiply the efficiency yet again. Thus our nominal 6 IFU MOAO system will yield a dramatic total gain of a factor of 50 to 200 in the completion rate for survey-level programs, relative to the current LGS AO OSIRIS system. This is an astounding advance in the potential of AO systems to finish deep spectroscopic surveys of the distant universe.

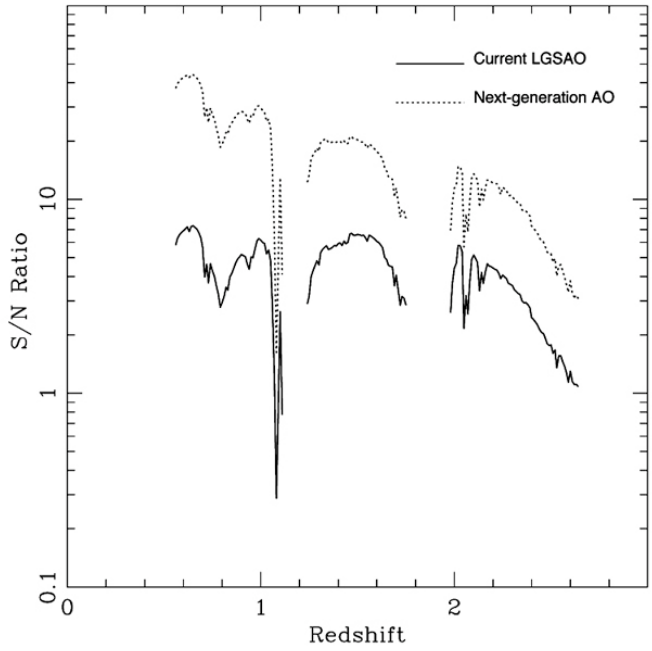

Figure 2. Predicted signal to noise ratios for an OSIRIS-like IFU.
Signal-to-noise for NGAO (upper curve) is compared with that for today's OSIRIS with LGS AO (bottom curve) in a calculation by David Law. For 0.6 < z < 2.3, NGAO shows a factor of 3 to 6 times improvement in signal to noise ratio. Here we have assumed IFU lenslet sizes of 0.1 arcsec, and the requirement that the added background due to the NGAO system be less than 30% of the unattenuated background due to the telescope plus sky.

We have used results from merger simulations by P. Jonsson, T. J. Cox, G. Novak, and J. Primack (Jonsson et al. 2006) to feed IFU simulations by David Law (using the methods in Law et al. 2006) to compare the relative capabilities of NGAO and present Keck LGS AO in the study of high-z galaxy mergers. The merger simulations include dust extinction, radiative transfer, star formation, and metallicity, and assume an AGN-free merger. Figure 3 shows simulated IFU-derived images and velocity fields for a merger in progress. With NGAO, images similar to the kinematic maps below will also be derived for star formation rates, metallicity distributions, velocity dispersion, and age., thus allowing us to address the issue of whether the observed peak in star formation at z ~ 2.5 is stimulated by galaxy mergers.

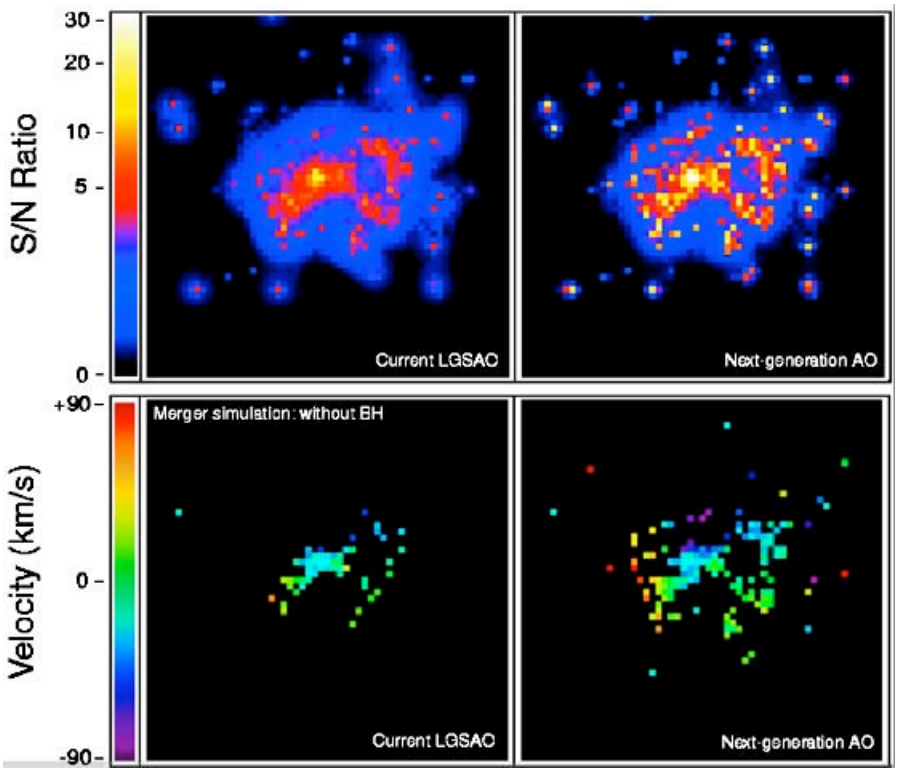

Figure 3. Improvements in SNR and velocity measurements with NGAO.
Top: Signal to noise ratio for Hα emission line from simulated major merger at z = 2.2, midway through the merger process, observed with the current LGS AO system (left) and with the proposed Keck NGAO system (right). Using current LGS AO there are only a few pixels with SNR ≥ 10 (yellow), but with NGAO there are an order of magnitude more such pixels. Lower panels: Kinematic maps for the same cases as the upper panels, showing velocities for those pixels with SNR > 5. Note the difficulty with current LGS AO of determining whether the lower left panel is kinematically differentiated from a typical ordered rotation map with smooth transition across the galaxy from red (positive velocities) to violet (negative velocities). The NGAO panel brings out the spatially complex velocity field which characterizes a major merger.

2.1.5 AO and instrument requirements

2.1.5.1 AO requirements

Using the Gemini model of the Mauna Kea near-IR sky background coupled with a mathematical model of the thermal contributions from warm optical surfaces in the light path, Law et al. (2006) have demonstrated that the current K-band performance of AO-fed

instruments is limited primarily by thermal emission from the warm AO system (which constitutes the majority of the total interline K band background). It is therefore a priority to reduce this emission to a lower fraction of the intrinsic background from the night sky and thermal radiation from the telescope itself. Using a combination of high-throughput optical components and AO system cooling, we require the following:

Spectrograph Requirement: The total background seen at the focal plane of all spectrographs being fed by NGAO shall be less than 130% of the current unattenuated sky plus telescope background (at 2209 nm and at a spectral resolution $\lambda/\Delta\lambda = 5000$).

Goal: less than 120%

Implications of requirement: cool the NGAO system to about 260K

This requirement is motivated by Figure 4, which shows that the K-band integration time for an IFU spectrum of a z=2.6 galaxy would be about 3 hours with the 130% requirement described above. The current integration time for OSIRIS is more than 6 hours.

Calculations by David Law of Caltech indicate that this should be achievable for AO system cooling to -18 C if the AO transmission is 65%, or to -14 C if the AO transmission is 75%, as shown in Figure 5.

Broadband imaging requirement: Background (mag/arcsec^2) at J: 15.9, at H: 13.7, at K in wide field mode: 13.6, at K in narrow field mode: 13.2 . Source: KAON 501 (A. Bouchez).

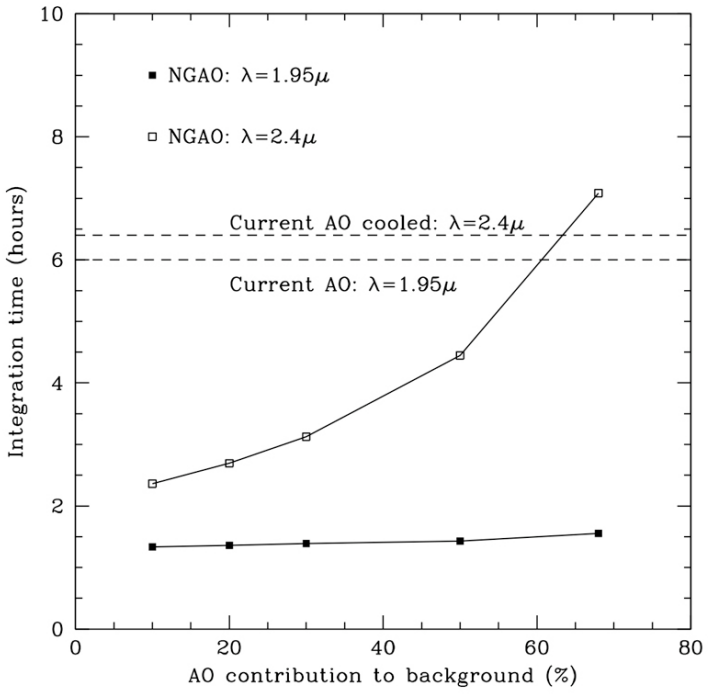

Figure 4. Required integration time to obtain an OSIRIS-like IFU spectrum of a z=2.6 galaxy, for varying AO contributions to the instrument background.
At K band with a 30% AO contribution to background, the integration time is about 3 hours, much shorter than the current >6 hr integration time.

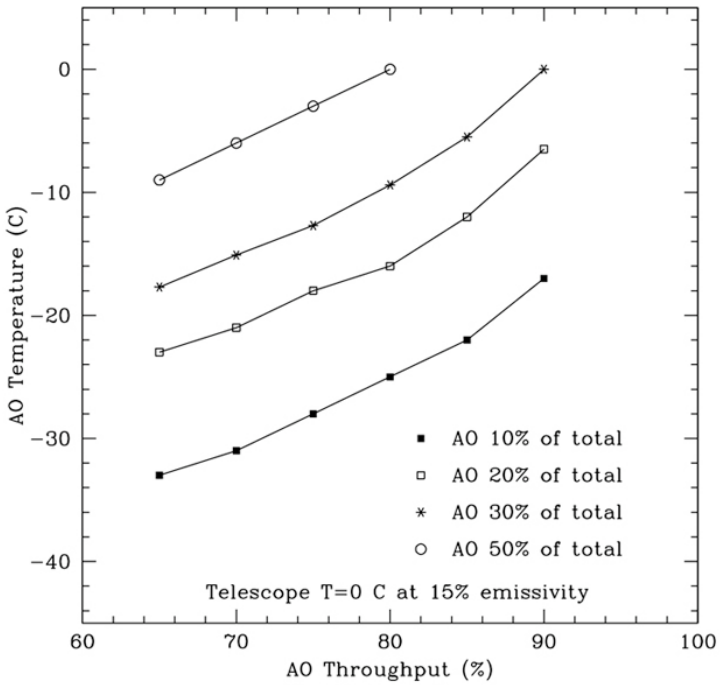

Figure 5. Required cooling of the NGAO system

Required cooling of the NGAO system in order to achieve an AO background that is 10% through 50% of the total, for varying values of the AO throughput.

Sky background subtraction is key to obtaining quantitative spectral information. There are two ways to achieve this: 1) Given the typical size of the target galaxies (less than or of order an arcsecond), the field of view of each IFU could be suitably large to permit accurate sky subtraction (via on-IFU dithering) while sampling the target on the smallest scales permitted by detector noise characteristics. In this approach, each IFU should have a field of view measuring at least 3 x 1 arcseconds in order to avoid costly dedicated sky exposures. 2) The deployable integral field spectrograph could include one or more arms that would be dedicated to taking spectra of the sky at the same time that galaxy spectra are being obtained on the other IFU arms. In this case each unit would only need to subtend 1 x 1 arcsecond on the sky. In the process of designing the deployable IFU spectrograph, there needs to be a trade study to evaluate and compare these two approaches to sky subtraction, as well as any other concepts that appear to be viable. It is not yet clear to us that option 2), using separate IFU heads in order to measure sky backgrounds, will yield accurate enough sky measurements.

The individual IFU units could be sampled on scales of as small as the diffraction limit (~ 50 mas) to permit accurate characterization of structure on small scales without introducing excessive instrumental contribution to the total noise budget. Spectral resolution should be greater than R~3000 in order to effectively resolve out OH sky features and distinguish Hα from [N II] emission.

Specifying AO requirements such as spatial resolution and encircled energy is not straightforward for the high-z galaxy science case. This is because the width of the core of the PSF will be limited by the availability of adequately bright tip-tilt stars. One can obtain very high spatial resolution and encircled energy over that small fraction of the sky where excellent tip-tilt stars are available, or more modest spatial resolution and encircled energy over a larger fraction of the sky where tip-tilt stars are dimmer and/or farther away. AO requirements that deal with resolution alone are less useful than those that can be phrased in terms of "spatial resolution of xx achieved over a sky coverage fraction larger than yy".

2.1.5.2 AO Requirements: Near-IR

Nominal spaxel size (IFU spectroscopy)	70 mas
Field of view of one IFU unit	
Two options	1) 3 x 1 arc sec or greater (object size ~ 1", but need 3" in at least one dimension to get good sky meas't), or 2) one or more dedicated IFU units for sky measurement, with each unit 1 x 1 arc sec
Spectrograph Backgrounds	The total background seen at the focal plane of all instruments being fed by NGAO shall be less than 130% of the current unattenuated sky plus telescope background (at 2209 nm and at a spectral resolution $\lambda/\Delta\lambda = 5000$). Goal: less than 120%
Broadband Imager Backgrounds:	Background (mag/arcsec^2) at J: 15.9, at H: 13.7, at K in wide field mode: 13.6, at K in narrow field mode: 13.2. Source: KAON 501.
Field of regard	As large as needed to get required tip-tilt stars
Is a contiguous field required?	no
Encircled energy	70 mas with optimal tip-tilt stars
Sky coverage fraction	at least 30% with encircled energy radius < 70 mas
(Photometric accuracy)	
(Astrometric accuracy)	
(Polarimetry)	
(Contrast sensitivity)	

2.1.5.3 Instrument Requirements:

Field of view (spectroscopy)	3 x 1 arcsec or greater if sky subtraction is to be done within each IFU head. If there are separate IFU heads dedicated

	to sky subtraction, then field of view of 1 x 1 arcsec could be adequate.
Field of regard	As large as needed for good tip-tilt
IFU or imager multiplicity	6-12
Wavelength coverage	JHK
Spectral resolution	3000 - 4000
Data reduction pipeline	Required
Other considerations	Atmospheric dispersion: may be able to avoid a dispersion corrector through appropriate data reduction pipeline software. The performance needs to be compared with that of a "real" ADC.

2.1.6 Summary of Requirements

The requirements for the *high-z galaxy* science case are summarized in the following table. In the following tables the desired 50% enclosed energy diameter and spaxel size are specified to be 70 mas, based on considerations of what is achievable for >30% sky coverage and the expected tip-tilt sensor performance.

Requirements Table 1. High-Redshift Galaxies derived requirements

#	Science Performance Requirement	AO Derived Requirements	Instrument Requirements
1.1	*Spectral Sensitivity.* SNR ≥ 10 for a z = 2.6 galaxy in an integration time ≤ 3 hours for a spectral resolution R = 3500 with a spatial resolution of 70 mas	Sufficiently high throughput and low emissivity of the AO system science path to achieve this sensitivity. Background due to AO less than 30% of unattenuated (sky + telescope) at wavelength of 2209 nm and at a spectral resolution $\lambda/\Delta\lambda$ = 5000.	

#	Science Performance Requirement	AO Derived Requirements	Instrument Requirements
1.2	*Target sample size* of ≥ 200 galaxies in ≤ 3 years (assuming a target density of 4 galaxies per square arcmin)	Multi-object AO system: one DM per arm, *or* an upstream MCAO system correcting the entire field of regard. 6-12 arms on 5 square arc minutes patrol field.	Multiple (6-12) IFUs, deployable on the 5 square arc minute field of regard
1.3	Spectroscopic and imaging observing wavelengths = J, H and K (to 2.4 μm)[1]	AO system must transmit J, H, and K bands[1]	Infrared imager and IFUs designed for J, H, and K.[1] Each entire wavelength band should be observable in one exposure.
1.4	Spectral resolution = 3000 to 4000		Spectral resolution of >3000 in IFUs
1.5	Narrow field imaging: diffraction limited at J, H, K	Wavefront error 170 nm or better	Nyquist sampled pixels at each wavelength
1.6	Encircled energy at least 50% in 70 mas for sky coverage of 30% (see 1.12)	Wavefront error sufficiently low (~170 nm) to achieve the stated requirement in J, H, and K bands.	IFU spaxel size: either 35 or 70 mas, to be determined during the design study for the multiplexed IFU spectrograph
1.7	Velocity determined to ≤ 20 km/sec for spatial resolutions of 70 mas	PSF intensity distribution known to ≤ 10% per spectral channel.	
1.8	IFU field of view ≥ 1" x 3" in order to allow sky background measurement at same time as observing a ~1" galaxy	Each MOAO IFU channel passes a 1"x3" field.	Each IFU unit's field of view is 1" x 3"
1.9	Simultaneous sky background measurements within a	See #1.8	

[1] Note that z band (central wavelength 912 nm) and Y band (central wavelength 1020 nm) are of interest as well, since Hα falls in z (Y) band for redshift 0.4 (0.55). The importance of including these two bands in addition to J, H, K is currently being assessed.

#	Science Performance Requirement	AO Derived Requirements	Instrument Requirements
	radius of 3" with the same field of view as the science field		
1.10	Relative photometry to ≤ 5% for observations during a single night	Knowledge of ensquared energy in IFU spaxel to 5%. Telemetry system that monitors tip/tilt star Strehl and other real-time data to estimate the EE vs. time, or other equivalent method to determine PSF to the required accuracy.	
1.11	Sky coverage ≥30% at 170 nm wavefront error, to overlap with data sets from other instruments and telescopes	Infrared tip/tilt sensors with AO correction of tip/tilt stars	
1.12	Should be able to center a galaxy to ≤ 10% of science field of view		
1.13	Should know the relative position of the galaxy to ≤ 20% of spaxel size		
1.14	Target drift should be ≤ 10% of spaxel size in 1 hr		
1.15	The following observing preparation tools are required: PSF simulation and exposure time calculator		
1.16	The following data products are required: calibrated spectral data cube		

2.1.7 References

Coil, A. L. et al. 2004, ApJ, 617, 765

Conselice. C. et al. 2003, AJ, 126, 1183
Dickinson, M. et al. 2003, ApJ, 587, 25
Erb, D. K. et al. 2004, ApJ, 612, 122
Erb, D. K. et al. 2006, ApJ, 647, 128
Flores, H. et al. 2006, A&A, 455, 107
Law, D. et al. 2006, AJ, 131, 70
Minowa, Y. et al. 2005, ApJ, 629, 29
Papovich, C. et al. 2006, ApJ, 640, 92
Reddy et al. 2006, ApJ, 644, 792
Scott, S. E. et al. 2002, MNRAS, 331, 817
Steidel, C. C. et al. 2004, ApJ, 604, 534
van Dokkum, P. G. et al 2000, ApJ, 541, 95
van Dokkum, P. G. et al. 2006, ApJ, 638, L59
Weiner, B. J. et al. 2006, ApJ, 653, 1027 and ApJ, 653, 1049
Yamada et al. 2005

2.2 Nearby Active Galactic Nuclei

Authors: Aaron Barth, Claire Max, Elizabeth McGrath

2.2.1 Introduction

During the past several years it has become increasingly clear that black holes play a key role in galaxy formation and evolution. The most important evidence for a close connection between black hole growth and galaxy evolution comes from the observed correlations between black hole mass and the bulge velocity dispersion of the host galaxy (the "M-σ relation"), and from the correlation between black hole mass and bulge mass. Despite the fact that black holes contain only about 0.1% of the mass of their host bulge, their growth is evidently constrained very tightly by the kiloparsec-scale properties of their environment. In addition, simulations and theory have highlighted the importance of feedback from active galactic nuclei (AGNs), in the form of winds or outflows which can serve to shut off AGN fueling and potentially expel a significant fraction of the host galaxy's gas into the intergalactic medium following a major merger. AGN feedback is frequently invoked as a mechanism to limit black hole growth and to shut off star formation in early-type galaxies, but observational evidence for this scenario remains sketchy.

Key observational goals in this field include:

- Accurate determination of the demographics of black holes in nearby galaxies, over the widest possible range in black hole mass
- Investigations of the redshift evolution of the M-σ relation
- Studies of the host galaxies of AGNs out to high redshifts to determine bulge luminosities, stellar populations, and emission-line kinematics.

AO observations will be crucial in addressing these issues over the next decade. Currently, with no spectroscopic capability on HST, AO observations are the *only* way to pursue dynamical measurements of black hole masses, apart from the very few special cases of AGNs that host water megamaser disks. AO data are already beginning to play an important role in this field and near-IR observations have the important advantage of being able to probe the central regions of dust-obscured galaxies, for example in Centaurus A (Silge et al. 2005). AO observations in the near-IR will be used to search for starlight from quasar host galaxies at high redshifts, but to date results have been severely limited by the quality of AO corrections available with current-generation facilities.

Here we discuss AGN and black hole projects that will benefit from NGAO at Keck. For the observations described below, the most desirable AO capability will be a high-Strehl AO correction in the near-IR and in the red with a highly stable PSF, even if only over a narrow field of view (~15 arcsec). An AO correction operating at wavelengths as short as the Ca II triplet (8500 A) will have important applications for black hole mass measurements.

2.2.2 Black hole masses in nearby galaxies

Detections of the black holes in the Milky Way and in the megamaser galaxy NGC 4258 remain the "gold standard" in this field, but the majority of black hole detections to date have been done with HST, and are limited to galaxies without significant dust obscuration. In the best cases, observations of spatially resolved stellar or gas kinematics can yield black hole masses with uncertainties in the range ~10-20%, which is sufficient for an accurate determination of the M-σ relation. Currently, although there are about 30 kinematics-based detections of massive black holes, the slope and the amount of scatter in the M-σ relation remain somewhat controversial. In particular, the extreme ends of the black hole mass spectrum, above 10^9 and below 10^7 solar masses, remain poorly determined. Improvements in angular resolution lead directly to increased accuracy in black hole mass measurements, and NGAO at Keck will be the next significant new capability in this field.

In order to detect a black hole with high significance, the observations must resolve the black hole's dynamical sphere of influence -- the region in which the black hole dominates the gravitational potential. As an example, the projected radius of the gravitational sphere of influence for a 10^8 solar mass black hole in a galaxy with σ = 200 km/sec at D = 20 Mpc is ~0.2 arcsec. Currently, black holes with masses below 10^7 solar masses can only be detected out to distances of a few Mpc, severely limiting the opportunities to measure the low-mass end of the M-σ relation. At the high-mass end, for black holes above 10^9 solar masses there are only a handful of potential targets within reach of current observations. The diameter of the gravitational sphere of influence is given by

$$a_{BH} \approx \frac{2GM_{BH}}{\sigma^2} \approx \left(\frac{M_{BH}}{10^9 M_{sun}}\right)\left(\frac{100\ \text{km/sec}}{\sigma}\right)^2\ \text{kpc}$$

$$\theta_{\text{BH}} \approx 1.''5\ \left(\frac{M_{BH}}{10^9 M_{sun}}\right)\left(\frac{100\ \text{km/sec}}{\sigma}\right)^2\left(\frac{100\ \text{Mpc}}{\text{D}}\right)$$

The region of interest for spatially resolved spectroscopy is within the gravitational sphere of influence of the central black hole: generally we will need at least two resolution elements across this distance.

For black hole detection, NGAO offers two important advantages over current capabilities. First in the near-IR, compared with current LGS AO the improved PSF quality and stability will significantly reduce the measurement uncertainty in black hole masses. Second, an AO capability in the I band will open up the possibility of using the Ca II triplet lines, giving a PSF core that is narrower than in the near-IR, and which will extend the distance out to which the most massive black holes can be detected. The minimum black hole mass detectable with a given angular resolution can be roughly estimated under the assumption that black holes lie on the M-σ relation. As Figure 6 shows, Keck NGAO in the K-band can offer better sensitivity to black holes than that of HST/STIS. In comparison with NGAO at K-band, for a

given limiting distance an I-band NGAO capability with a PSF core FWHM of ≤ 0.035" can allow detections of black holes smaller by approximately a factor of two.

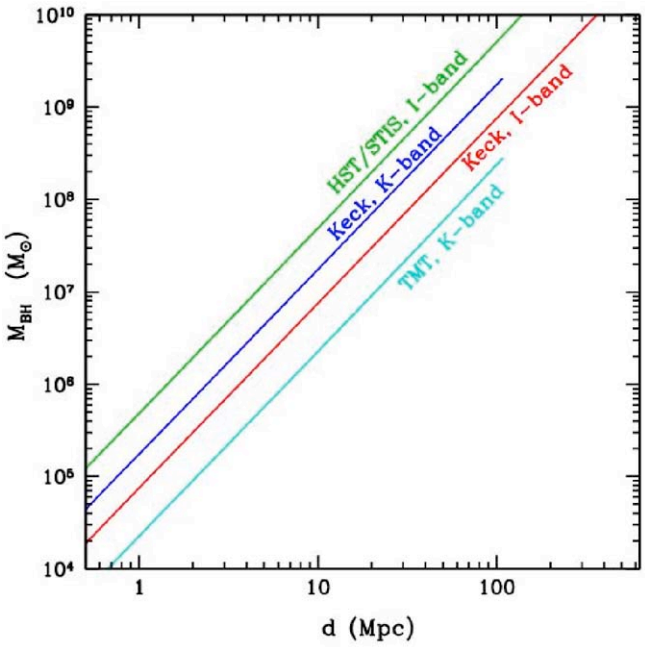

Figure 6. Minimum detectable black hole mass as a function of galaxy distance.
We assumed that the black holes follow the local M-σ relation, and assuming a minimum of two resolution elements across the black hole's radius of influence. For Keck NGAO, this figure assumes a PSF core with FWHM = 0.053" in K, and 0.035" in I. Minimum detectable black hole mass scales approximately as (distance * angular resolution)^2. For distances beyond ~100 Mpc, the CO bandhead is redshifted out of the K-band and is no longer observable. The line for TMT (optimistically) assumes a diffraction-limited PSF core in the K-band.

2.2.3 Proposed observations and targets

Supermassive black holes: Numerous nearby galaxies will be promising targets for observation with NGAO. Many galaxies previously observed with HST or other AO systems will be re-observed with Keck NGAO, to improve the accuracy of the black hole mass measurements. Giant ellipticals at distances less than ~100 Mpc will be good candidates for studying the high-mass end of the M-σ relation.

Spectral features useful for kinematic measurements include:

1. Stellar dynamics: the CO bandhead (2.29 μm), and the Ca II triplet (~8500 A)
2. Gas dynamics: [S III] (9533 A), [Fe II] (1.26 μm), Pa β (1.28 μm), H_2 (2.12 μm), Br γ (2.17 μm)

For stellar-dynamical detections of black holes, S/N = 30 or better (per resolution element) is typically needed for the stellar continuum. For nearby galaxies this can typically be accomplished in a few hours of observing with OSIRIS. For gas dynamics, the S/N requirements for a given galaxy are lower since emission lines rather than absorption lines are

used, but only about ~10% of nearby galaxies have sufficiently "clean" rotation in their emission-line velocity fields to be good targets for gas-dynamical studies.

In addition to the spectroscopic data, AO imaging of the host galaxies is needed in order to determine the distribution of stellar mass in the host galaxy. For the imaging, either NIRC2 or an upgraded IR imaging camera would be used.

One galaxy sample of particular interest is the set of 17 Seyfert galaxies having black hole mass estimates from reverberation mapping (Peterson et al. 2004). This sample serves as the bottom rung on a "distance ladder" of indirect techniques used for estimating black hole masses in quasars. Since all estimates of black hole masses in quasars are calibrated against this sample, it is important to verify the accuracy of the reverberation-based black hole masses by performing stellar-dynamical observations on these same galaxies. With NGAO, approximately 10 of these galaxies should be within reach. Current reverberation-mapping surveys under way will increase the sample size accessible to NGAO by the time the new AO system is commissioned.

2.2.4 Comparison of NGAO w/ current LGS AO

Black hole science will benefit greatly from both the higher Strehl ratio and the better PSF stability of NGAO in comparison with current LGS AO. Figure 7 illustrates one example: the improvement in the measurement of the velocity field of an emission-line disk around a black hole. To detect the black hole with high significance, it is imperative to resolve the central, nearly Keplerian region of the disk. In this simulated example of a 10^8 solar mass black hole at distance 20 Mpc, the current LGS AO capability would detect a steep velocity gradient across the nucleus due to the presence of the black hole, but would not detect the nearly Keplerian rise in velocity toward the nucleus. With NGAO, the rise in velocity toward the nucleus is detectable, and provides the "smoking gun" evidence for the presence of an unresolved central mass. With HST, this central Keplerian rise in velocity in emission-line disks has only previously been detected clearly in 2 giant elliptical galaxies, M84 and M87. Stellar-dynamical observations at the CO bandhead will similarly benefit from the enhanced ability of NGAO to resolve the black hole's sphere of influence in nearby galaxies.

The improvement in PSF stability in the near IR will be particularly beneficial for stellar-dynamical observations of the most massive elliptical galaxies, which have flat cores rather than strongly peaked cusps in the stellar light profile. For these objects, it is essential to minimize the flux in the PSF wings in order to measure accurate line-of-sight velocity profiles at the smallest radii.

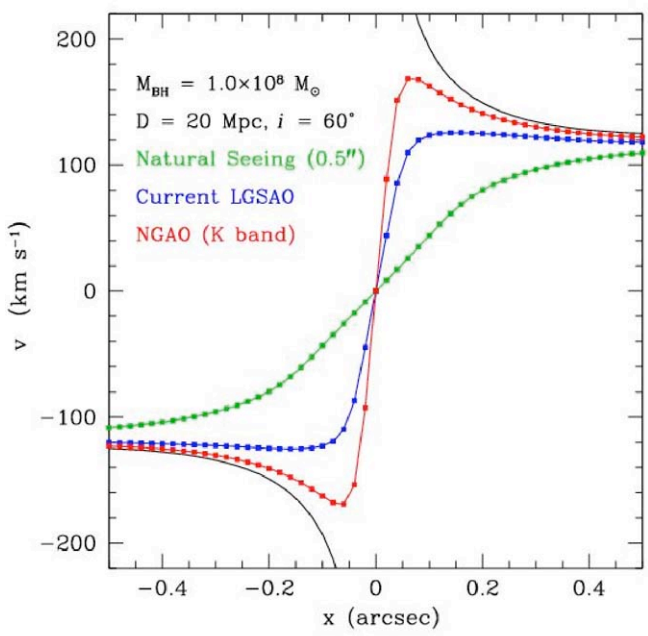

Figure 7. Simulation of radial velocities observed along the major axis of an emission-line disk surrounding a black hole in a galaxy center.
This simulation is similar to disks observed in M87 and other early-type galaxies. The black hole has mass 10^8 solar masses, and is surrounded by a bulge with a power-law mass profile. The galaxy is at D = 20 Mpc and the disk is inclined by 60° to the line of sight. The simulation was performed for observations of an emission line in the K-band (e.g., Br γ) with OSIRIS using a spatial sampling of 0.02"/pixel. The black curve shows the true major-axis velocity profile of the disk with no atmospheric or instrumental blurring. The blue and red curves show the velocity curves obtained from a 1-pixel wide cut along the disk major axis, after convolution of the intrinsic spectral data cube with a typical K-band PSF for current LGS AO (assuming a PSF core containing 30% of the total flux), and for NGAO (assuming a PSF core containing 72% of the total flux). The green curve shows the velocity profile that would be measured without any AO correction.

2.2.5 Summary of Requirements

The requirements for the *Nearby AGN* science case are summarized in the following table.

Requirements Table 2. Nearby AGNs Derived Requirements, Spectroscopy and Imaging

#	Science Performance Requirement	AO Derived Requirements	Instrument Requirements
2.1	Number of targets required: to be specified in future versions of this document		
2.2	Required wavelength range 0.85 – 2.4 microns		
2.3	Required spatial sampling at least two resolution elements	50% enclosed energy radius < ½ gravitational sphere of influence. Wavefront error	Spectral and imaging pixels/spaxels < ½ gravitational sphere of

	across gravitational sphere of influence.	requirement to be specified in future versions of this document.	influence (in the spatial dimension)
2.4	Required field of view for both spectroscopy and imaging > 10 radii of the gravitational sphere of influence. To be specified in future versions of this document		Will need to get sky background measurement as efficiently as possible. For IR, consider using a separate d-IFU on the sky.
2.5	Required SNR for spatially resolved spectroscopy of the central black hole region using stellar velocities > 30 per resolution element	PSF stability and knowledge requirements will be discussed in future releases of this document.	Spectral resolution R ~ 3000-4000 with at least two pixels per resolution element; detector limited SNR performance. Spatial sampling at least two resolution elements across the gravitational sphere of influence
2.6	Required observation planning tools: PSF simulation tools to plan for observations of Seyfert 1 galaxies which have strong central point sources		
2.7	Required data reduction pipeline for IFU		

2.2.6 References

Croom, S. M., et al. 2004, ApJ, 606, 126
Guyon, O., Sanders, D. B., & Stockton, A. 2006, astro-ph/0605079
Peterson, B. M., et al. 2004, ApJ, 613, 682
Silge, J. D., Gebhardt, K., Bergmann, M., & Richstone, D. 2005, AJ, 130, 406
Woo, J.-H., Treu, T., Malkan, M. A., & Blandford, R. D. 2006, astro-ph/0603648

2.3 Precision Astrometry: Measurements of General Relativity Effects in the Galactic Center

Authors: Andrea Ghez and Jessica Lu
Editors: Claire Max and Elizabeth McGrath

2.3.1 Scientific background and goals

The proximity of our Galaxy's center presents a unique opportunity to study a massive black hole (BH) and its environs at much higher spatial resolution than can be brought to bear on any other galaxy. In the last decade, near-IR observations with astrometric precisions of < 1 mas and radial velocity precision of 20 km/s have enabled the measurement of orbital motions for several stars near the Galactic center (GC), revealing a central dark mass of 3.7×10^6 M_{Sun} (Ghez et al. 2003, Ghez et al. 2005; Schodel et al. 2002; Schodel et al. 2003). Radio VLBA observations have now resolved the central object to within several multiples of the event horizon, indicating that the central mass is confined to a radius smaller than 1 AU (Shen et al. 2005). These observations provide the most definitive evidence for the existence of massive BHs in the centers of galaxies. The orbital motions now also provide the most accurate measurement of the GC distance R_0, constraining it to within a few percent (Eisenhauer et al. 2003).

2.3.2 General Relativistic Effects

Due to the crowded stellar environment at the GC and the strong line-of-sight optical absorption, tracking the stellar orbits requires the high angular resolution, near-IR imaging capabilities of adaptive optics on telescopes with large primary mirrors, such as Keck. Though the current orbital reconstructions are consistent with pure Keplerian motion, with improved astrometric and radial velocity precision deviations from pure Keplerian motion are expected. With Keck NGAO we will be able to detect the deviations from Keplerian motion due to a variety of effects. These will provide a unique laboratory for probing the dynamics of galactic nuclei, the properties of exotic dark matter, and the mass function of stellar-mass black holes. They will also provide the first tests of general relativity in the high mass, strong gravity, regime. Keck NGAO will measure these non-Keplerian motions to precisions that will not be greatly surpassed even in the era of extremely large (~30m) telescopes.

Of the theories describing the four fundamental forces of nature, the theory that describes gravity, general relativity (GR), is the least tested. In particular, GR has not been tested in the strong field limit, on the mass scale of massive BHs. The highly eccentric 15 yr orbit of the star S0-2 brings it within 100 AU of the central BH, corresponding to ~1000 times the BH's Schwarzschild radius (i.e., its event horizon). Studying the pericenter passage of S0-2 and the other high eccentricity stars therefore offers an opportunity to test GR in the strong gravity regime.

With Keck NGAO, the orbits can be monitored with sufficient precision to enable a measurement of post-Newtonian general relativistic effects associated with the BH. This includes the prograde precession of orbits. As Figure 8 illustrates, the General Relativistic prograde precession can be measured even for single orbits of known stars (e.g., S0-2, K=14.1 mag) if we have an astrometric precision of ~ 100 μas coupled with a radial velocity precision of 10 km/s.

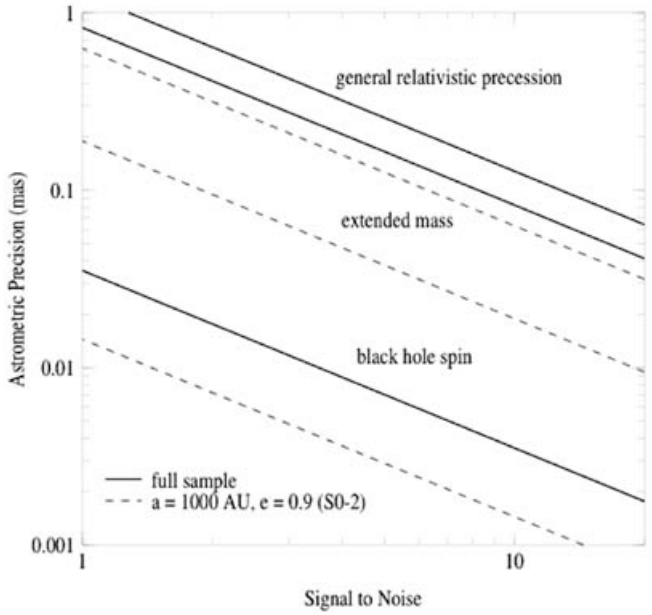

Figure 8. Required astrometric precision for detecting General Relativistic effects at the Galactic Center From top to bottom, GR effects associated with relativistic prograde precession, extended mass within the stellar orbits, and frame-dragging effects due to BH spin (based on Weinberg et al. 2005). Estimates are based on measurements of stellar orbits and positions from Keck diffraction-limited images (thick, solid lines), and assume radial velocity measurement errors of 10 km/s. The stellar orbits include 16 stars within 0.5" of Sgr A* with orbital fits obtained from speckle imaging measurements and 142 stars within 1" of Sgr A* with stellar positions obtained with new, deep AO maps. For comparison, we also show estimates based on measurements from just the short-period star S0-2 (thin, dashed line). Results are for a 10-year baseline with 10 integrations per year. Low-order GR and extended matter effects are detectable at the >7s level if an astrometric precision of ~100 mas can be achieved. Detection of BH spin requires either better precision or, at ~100 mas precision, improved SNR obtained by observation of multiple as-yet-undiscovered high-eccentricity, short-period stars over multiple orbits.

Keck NGAO will bring several important improvements to measurements at the Galactic Center:

1) Current measurements are strongly confusion limited, because the Galactic Center is a very crowded field. Higher Strehl at K-band will improve contrast and therefore reduce the confusion, improving both photometric and astrometric accuracy because the previously

undetected faint star population will cause less of a bias in the positions and magnitudes of brighter stars.

2) Higher Strehl at K-band will allow the detection of new stars, some of which may pass close enough to the black hole to contribute to the obtainable accuracy and precision of General Relativistic effects. (See figure caption.)

3) NGAO's use of multiple laser guide stars and multiple IR tip-tilt stars will decrease the field dependence of the PSF, thereby increasing both photometric and astrometric accuracy. This effect needs be quantified.

4) The accuracy of current radial-velocity measurements is limited by signal to noise. NGAO's higher Strehl and lower sky background will materially improve the radial-velocity contribution to orbit determinations.

2.3.3 R_0 and the dark matter halo

Since the orbital periods are proportional to $R_0^{3/2}M_{bh}^{-1/2}$ and the radial velocities are proportional to $R_0^{-1/2}M_{bh}^{1/2}$, where R_0 is the heliocentric distance to the BH and M_{bh} its mass, the two parameters are not degenerate and can be determined independently (Salim & Gould 1999). As shown in Figure 8, by complimenting high precision astrometric measurements with high precision radial velocity measurements with accuracies of ~10 km s^{-1}, we can measure R_0 to an accuracy of only a few parsecs (i.e., ~0.1% accuracy) with Keck NGAO. Today's radial velocity precision for the observations in hand is about 20 km/s. This could be improved to 10 km/sec with higher signal to noise observations, either from longer integration times or lower backgrounds.

Since R_0 sets the scale within which is contained the observed mass of the Galaxy, measuring it to high precision enables one to determine to equally high precision the size and shape of the Milky Way's several kpc-scale dark matter halo (Olling & Merrifield 2000). The halo shape tells us about the nature of dark matter (e.g., the extent to which it self-interacts) and the process of galaxy formation (how the dark matter halo relaxes following mergers). Currently the shape is very poorly constrained.

2.3.4 Proposed observations and targets

Target: Central 10 arc sec of the Galactic Center, centered on SgrA*. Note that this is a low-elevation target from Keck (RA 17 45 40 DEC -29 00 28).

Observing wavelengths: K band (2.2 microns)

Observing mode: Imaging for astrometry purposes, and spectroscopy for radial velocities

2.3.5 Observing plan for Astrometric Imaging

Based upon the way things are done today using 1st-generation Keck AO:

a) Guide Star Acquisition:

Current visible-wavelength guide star is USNO-A2.0 0600-28577051 (R=14.0, Separation = 19.3'')

There are a great many possible IR tip-tilt stars. The addition of multiple IR-corrected tip-tilt stars is anticipated to improve astrometric accuracy considerably.

b) 1-minute K' exposures, continuing for 3.5 hours elapsed time

c) Dither pattern is random over a 0.7'' box (small box used to minimize distortion)

d) Construct 40 arcsec mosaics to tie to radio astrometric reference frame (radio masers)

e) After the Galactic Center has set, move to a dark patch of sky at a similar airmass to obtain sky exposures.

Standard stars: none (astrometry)

Data Analysis:

1. Image reduction is standard, including distortion correction using the NIRC2 pre-ship review distortion solution. Improved distortion solution is needed and appears to be possible with data in hand.
2. Individual exposures are shifted (translations only) and added together for an entire night to produce a final map. Information from >1000 stars is included in the solution.
3. Individual exposures are also divided into 3 subsets of equal quality to produce 3 images used for determining the astrometric and photometric RMS errors.
4. Source extraction is performed using StarFinder (Diolaiti et al 2000) which iteratively estimates the PSF from several bright stars in the image and then extracts all source positions and photometry.
5. Star lists from different epochs are aligned by matching all the stars and minimizing the quad-sum of their offsets allowing for a 2nd order transformation between epochs.

2.3.6 Observing plan for Radial Velocity Measurements (IFU spectroscopy)

H and K-band IFU spectroscopy, one field
20 or 35 mas spaxel scale, R~4000
FOV at least 1.0'' x 1.0''
Exposure times are currently 15 minutes.
Sky frames of the same duration are obtained in the same mode after the Galactic Center sets in order to remove OH lines.
Obtain standards stars of A and G spectral type to remove telluric lines.
Data analysis performed with a provided pipeline to do wavelength calibration.

2.3.7 Current issues and limitations that could be further explored with existing data sets

1) Improved geometric distortion map for narrow camera on NIRC2. At present we know that the map from pre-ship review is incorrect at the half-pixel level. Improved distortion maps are under way currently.

2) Effect of differential tip-tilt error across 10 arc sec field. Present data show the expected decrease in astrometric errors as the stars get brighter (K=20 to 15), due to photon noise improvement. However for stars brighter than K=15, the astrometric error hits a plateau and does not improve further as the stars get brighter. This is illustrated in Figure 9. The Galactic Center Group at UCLA has three hypotheses for the existence of this floor: differential tip-tilt anisoplanatism across the field, differential high-order anisoplanatism across the field, and/or lack of a good enough distortion solution for the narrow camera. At present the Galactic Center Group thinks the most likely cause is differential tip-tilt anisoplanatism; they plan to test this hypothesis by further analysis of existing data.

3) In principle chromatic and/or achromatic atmospheric refraction could be adversely affecting current accuracy. These effects will also be analyzed further.

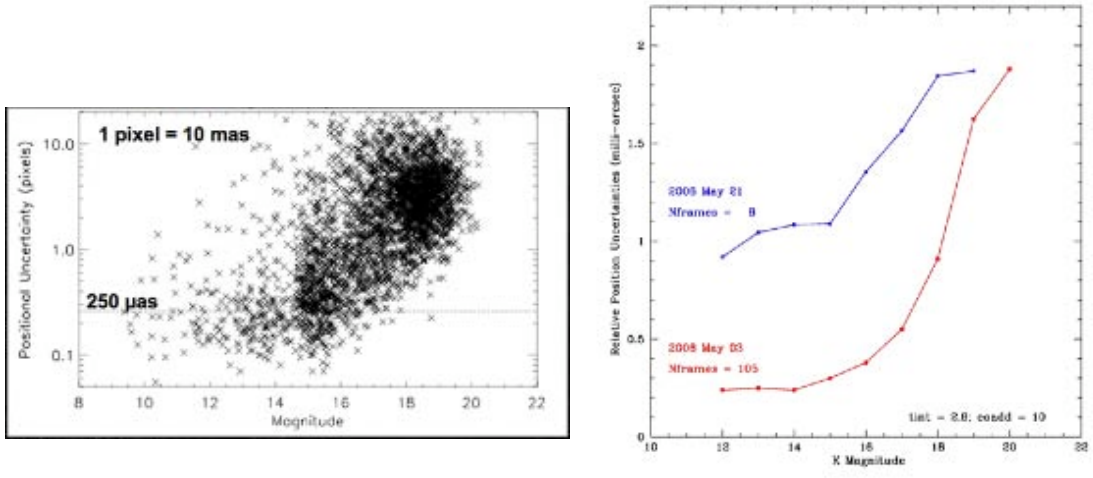

Figure 9. Currently achieved positional uncertainties at the Galactic Center, using Keck LGS AO. Left panel: positional uncertainty vs. stellar magnitude for stars near Galactic Center. Pixel scale is 0.01 arc sec/px. Right panel: average values of positional uncertainties for two different data sets. Positional uncertainty of the "floor" changes from ~ 1 mas to 0.25 mas between the two data sets shown.

2.3.8 AO requirements

2.3.8.1 Astrometry:

Astrometric precision	100 micro arc sec or better Wavefront error 170 nm or better at the elevation of the Galactic Center

Tip-tilt correction	IR tip-tilt needed; due to very strong reddening in Galactic Center, available J-band stars will be fainter than at H or K band, so either H or K is desirable for tip-tilt sensing. The total astrometric precision should be better than 0.1 mas. Therefore the required contribution from differential tip-tilt must be smaller than this. Further investigation into the astrometric error budget is required to determine the exact requirement.
Photometric precision	na
Polarimetric precision	na
Backgrounds	na (confusion dominated)

2.3.8.1.1 Comments on astrometric accuracy in an AO system with multiple deformable mirrors

The current design concept for Keck NGAO specifies a large-stroke deformable mirror within the first optical relay, plus a high-order MEMS deformable mirror either located on-axis or in multiple deployable IFU arms. The current plan is for both mirrors to be conjugate to the ground. However in the future it might be desirable to investigate the pros and cons of making one of the mirrors conjugate to a higher altitude, and to run the system in MCAO mode. Here we point out that any MCAO system with multiple DMs must consider the impacts on astrometric accuracy. The following is a quote from the TMT Science-Driven Requirements Document that seems relevant to Keck NGAO design as well (this text is a place-holder for future NGAO-specific quantitative analysis of the same topic):

"An astrometric MCAO system must constrain Zernike modes 4-6 using either a single natural guide star (NGS) which is bright enough to sense defocus and astigmatism or provide two additional tip-tilt stars, making their total number 3. The differential tilts between the three tip-tilt stars constrain these modes. This requirement occurs because the tip and tilt of laser guide stars (LGS) are undetermined. As a consequence, the information brought by them is insufficient for a full solution of the tomographic problem. In addition to tip and tilt, differential astigmatism and defocus between the two DMs is unconstrained. These three unconstrained modes do not influence on-axis image quality, but produce differential tilt between the different parts of the field of view.

If multiple tip-tilt sensors are used, the MCAO system must provide for a facility to align them. If the tip-tilt sensors for the three NGSs are misplaced, the MCAO system will compensate these errors in the closed loop, hence the field will be distorted. For example, the plate scale will change if the upper DM has a static defocus. Calibration procedures must be applied to ensure that these errors do not compromise the astrometric performance of an MCAO system (e.g., flattening of the upper DM before closing the loop).

The limitations on astrometric accuracy imposed by the atmosphere are discussed in detail in a TMT technical report (Graham 2003).

2.3.8.2 Radial Velocity

IFU with 20 or 35 mas slitlets/spaxels. Note that this is the only Key Science Driver requiring such small spaxels for the IFU; most others call for 70 mas spaxels. The issue of whether the IFU(s) should have more than one spaxel scale will be considered during the NGAO Preliminary Design phase and during the System Design phase for the deployable multiplexed IFU.

The required radial velocity accuracy is 10 km/s which is a factor of 2 improvement over current observations with OSIRIS-LGS AO. Current accuracy is limited by:

1) Signal-to-noise:
   This will be improved by higher Strehl ratios in the near IR.
2) Differential atmospheric refraction (chromatic):
   Should be compensated for by an infrared atmospheric dispersion corrector.
3) PSF estimation:
   We will investigate how to improve PSF knowledge for fields without good PSF stars.
4) Local background subtraction (diffuse Brγ gas over the entire field):
   Higher Strehls will allow sky estimates less contaminated by the halos of bright stars.
5) Spectral resolution (many lines are blends):
   Brγ (2.166 microns) and He (2.112 microns) lines are blends at R~4000. Higher spectral resolution would resolve the individual lines. Further investigation of the ideal spectral resolution is needed. In particular, if the NGAO system allows IFU spectroscopy of fainter stars, one may be able to obtain radial velocities from unblended spectral lines other than Brγ (2.166 microns) and He (2.112 microns). CO bandhead absorption at 1.619 and 2.294 microns can also be used to obtain radial velocities.

2.3.9 Instrument requirements

Essential: High contrast near-IR imager with excellent astrometric performance (better than 0.1 mas).

Essential: Infrared integral field spectrometer, R ≥ 3000 that can achieve 10 km/sec radial velocity accuracy for stars near the Galactic Center.

Desirable but not absolutely essential: High resolution (R~15000) IFU spectroscopy. With this spectral resolution, radial velocity accuracies are improved to ~1 km/s and the radial velocity measurements may themselves constrain General Relativistic effects.

Imager:

Field of view:	at least 10 x10 arc sec
Field of regard:	IR tip-tilt stars available 1-20'' from imaging field center. Tip-tilt pickoff is required to be able to deal with multiple tip-tilt stars separated by only a few arcseconds.
IFU multiplicity:	one is sufficient

Wavelength coverage: K-band

IFU Spectrometer:
Field of view: At least 1 x 1 arc sec (more is desirable but not essential)
Field of regard: as needed to meet tip-tilt correction requirements
IFU multiplicity: one is sufficient
Wavelength coverage: H, K-band
Spectral resolution: (in addition as a goal, optional R~15,000)
Type and depth of required data pipeline: IFU pipeline for wavelength/flux calibration

2.3.10 Summary of Requirements

The requirements for the *Measurement of General Relativity Effects in the Galactic Center science case* on both precision astrometry and radial velocities are summarized in the following two tables, respectively.

Requirements Table 3a. General relativity effects in the Galactic Center derived requirements

#	Science Performance Requirement	AO Derived Requirements	Instrument Requirements
3a.1	*Astrometric* accuracy ≤ 100 μas for objects ≤ 5" from the Galactic Center	High Strehl to reduce confusion limit: rms wavefront error ≤ 170 nm at G.C. IR tip/tilt sensors. Means of aligning and measuring position of tip-tilt sensors so that they permit astrometric accuracy of ≤ 100 μas. Means of preventing WFS-blind field-distortion modes (if multi-DMs are in series). Will require ADC. Need astrometric error budget in order to determine ADC requirements.	Nyquist sampling at H and K. Instrument distortion characterized and stable to ≤ 100 μas.
3a.2	Observing wavelengths: H and K-band	Transmit H and K band to science instrument	
3a.3	Field of view ≥ 10" x 10" for imaging	Science path shall allow an unvignetted 10" x 10" field.	

#	Science Performance Requirement	AO Derived Requirements	Instrument Requirements
3a.4	Ability to construct 40'x40" mosaic to tie to radio astrometric reference frame[2]		
3a.5	The following observing preparation tools are required: PSF simulation as function of wavelength and seeing conditions, exposure time calculator.		
3a.6	The following data products are required: Calibrated PSF, data reduction pipeline, accurate distortion map (see 3a.1)		

Requirements Table 3b. Radial velocity measurements derived requirements

#	Science Performance Requirement	AO Derived Requirements	Instrument Requirements
3b.1	*Radial velocity* accuracy ≤ 10 km/sec for objects ≤ 5" from the Galactic Center	170nm wavefront error at G.C. PSF estimation sufficient to measure a radial velocity to 10 km/sec.	Spectral resolution ≥ 4000 Calibration of one IFU relative to other ones sufficient to permit 10 km/sec radial velocity measurement
3b.2	Observing wavelengths H, K-band	Transmit H, K band to science instrument	
3b.3	Spatial sampling ≤ 20 mas (H) or 35 mas (K) to control confusion within IFU field of view		20 and 35 mas spaxel scales at H and K respectively
3b.4	Field of view ≥ 1" x 1"		Field of view ≥ 1" x 1"

[2] Accuracy required needs to be determined

#	Science Performance Requirement	AO Derived Requirements	Instrument Requirements
3b.5	The following observing preparation tools are required: PSF simulation as function of wavelength and seeing conditions, exposure time calculator.		
3b.6	The following data products are required: IFU pipeline for wavelength/flux calibration		

2.3.11 References

Broderick, A. E., & Loeb, A. 2005, MNRAS, 363, 353

Diolaiti, E., 0. Bendinelli, D. Bonaccini et al. 2000, A&AS 147, 335

Eisenhauer, F., Schodel, R., Genzel, R., Ott, T., Tecza, M., Abuter, R., Eckart, A., & Alexander, T. 2003, ApJL, 597, L121

Genzel, R., Schodel, R., Ott, T., Eckart, A., Alexander, T., Lacombe, F., Rouan, D., & Aschenbach, B. 2003, Nature, 425, 934

Ghez, A. M., Salim, S., Hornstein, S. D., Tanner, A., Lu, J. R., Morris, M., Becklin, E. E., & Duchene, G. 2005, ApJ, 620, 744

Ghez, A. M., et al. 2004, ApJL, 601, L159

Ghez, A. M., et al. 2003, ApJL, 586, L127

Gondolo, P., & Silk, J. 1999, Physical Review Letters, 83, 1719

Miralda-Escude, J., & Gould, A. 2000, ApJ, 545, 847

Morris, M. 1993, ApJ, 408, 496

Olling, R. P., & Merrifield, M. R. 2000, MNRAS, 311, 361

Peebles, P. J. E. 1972, ApJ, 178, 371

Salim, S., & Gould, A.1999, ApJ, 523, 633

Schodel, R., Ott, T., Genzel, R., Eckart, A., Mouawad, N., & Alexander, T. 2003, ApJ, 596, 1015

Schodel, R., et al. 2002, Nature, 419, 694

Shen, Z.-Q., Lo, K. Y., Liang, M.-C., Ho, P. T. P., & Zhao, J.-H. 2005, Nature, 438, 62

Weinberg, N. N., Milosavljevic, M., & Ghez, A. M. 2005, ApJ, 622, 878

2.4 Imaging and Characterization of Extrasolar Planets around Nearby Stars

Authors: Bruce Macintosh and Michael Liu
Editors: Claire Max and Elizabeth McGrath

2.4.1 Scientific background and context

The unique combination of high-contrast near-IR imaging (K-band Strehl ratios of 80-90%) and large sky coverage delivered by NGAO will enable direct imaging searches for Jovian-mass planets around nearby young low-mass stars and brown dwarfs. Both the Gemini Observatory and ESO are developing highly specialized planet-finding AO systems with extremely high contrast for direct imaging of young planets. These "extreme AO" systems are very powerful, but their design inevitably restricts them to searches around bright, solar-type stars (I < 9 mag).

NGAO will strongly distinguish work at WMKO from all other direct imaging searches planned for large ground-based telescopes. By number, low-mass stars ($M \leq 0.5\ M_{Sun}$) and brown dwarfs dominate any volume-limited sample, and thus these objects may represent the most common hosts of planetary systems. Such cool, optically faint targets will be unobservable with specialized extreme AO systems because their parent stars are not bright enough to provide a high-order wavefront reference. But thousands of cool stars in the solar neighborhood can be targeted by NGAO because of its laser guide stars. Direct imaging of extrasolar planets is substantially easier around these lower mass primaries, since the required contrast ratios are smaller for a given companion mass. In addition, the very youngest stars in star-forming regions such as Taurus or Ophiucus are generally too faint for extreme AO systems but easily accessible to NGAO. However, for both these science cases, the key angular scales are relatively small (0.1-0.2 arcseconds), requiring both the large aperture of the Keck telescopes and careful coronagraph design.

2.4.2 Scientific goals

Direct imaging of extrasolar planets by NGAO would allow us to measure their colors, temperatures, and luminosities, thereby testing theoretical models of planetary evolution and atmospheres. NGAO spectroscopic follow-up will be an important means to characterize the atmospheres of extrasolar planets, which are otherwise essentially inaccessible to spectroscopy. Figure 10 summarizes the relative parameter space explored by NGAO and extreme AO. The complementarity of the two systems is very important: establishing the mass and separation distribution of planets around a wide range of stellar host masses and ages is a key avenue to understanding the planet formation process. The optical faintness of low-mass stars, brown dwarfs and the very youngest stars make them inaccessible to extreme AO systems but excellent targets for NGAO.

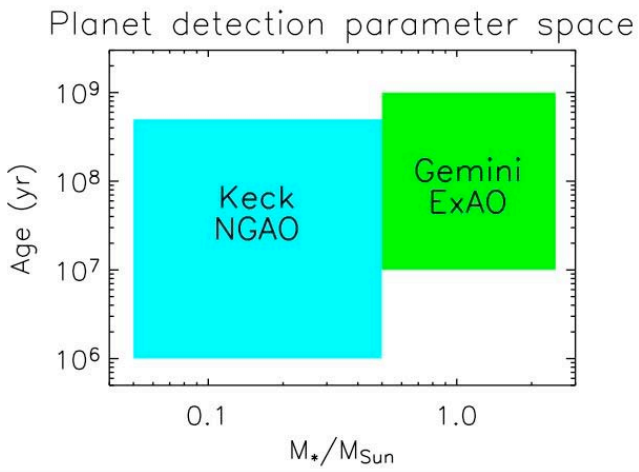

Figure 10. Schematic illustration of the parameter space of Keck NGAO and of the Gemini Planet Imager for direct imaging of extrasolar planets.

2.4.2.1 Planets around low-mass stars and brown dwarfs

Direct imaging of substellar companions (brown dwarfs and extrasolar planets) is substantially easier around lower mass primaries, since the required contrast ratios are smaller for a given companion mass. Indeed, the first bona fide L dwarf and T dwarfs were discovered as companions to low-mass stars (Becklin & Zuckerman 1988, Nakajima et al. 1995), and the first planetary-mass companion imaged orbits the brown dwarf 2MASS1207 (Chauvin et al 2004). Thus, searching for low-mass stars and brown dwarfs is an appealing avenue for planet detection and characterization. Given that low-mass stars are so much more abundant than higher mass stars, they might constitute the most common hosts of planetary systems. Figure 11 shows an estimate of the planet detection sensitivity for NGAO.

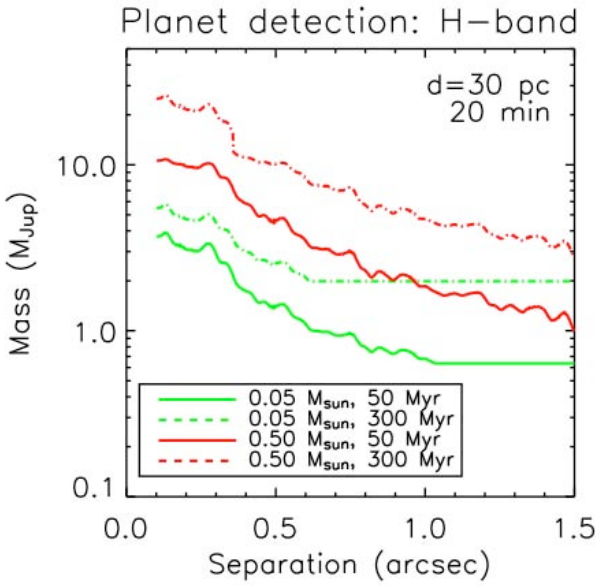

Figure 11. Estimated NGAO sensitivity for direct imaging of extrasolar planets.
Red lines: planets around low-mass stars; green lines: planets around brown dwarfs. NGAO will be able to search for Jovian-mass companions around large numbers of low-mass stars and brown dwarfs in the solar neighborhood.

Since these targets are intrinsically faint, the contrast between the primary and the planetary companion is reduced. For example, a 40 Jupiter-mass brown dwarf with an age of 1 Gyr has an absolute H magnitude of 14. A 2 Jupiter-mass planetary companion has an absolute H magnitude of 24, for a contrast of only 10^4. The known distribution of brown dwarf binaries peaks at 4 AU. Assuming a typical target distance of 20 pc, this leads to a contrast requirement of $\Delta J = 10$ at 0.2 arcseconds. If most targets come from the 2MASS catalog, they will have IR magnitudes < 15 and hence be suitable for on-axis IR tip/tilt sensing.

Spectroscopic follow-up of the coldest companions will be an important path in characterizing the atmospheres of objects in the planetary domain. Strong molecular absorption features from water and methane provide diagnostics of temperature and surface gravity at modest (R~100) spectral resolution. Below ~500 K, water clouds are expected to form and may mark the onset of a new spectral class, a.k.a. "Y dwarfs". Such objects represent the missing link between the known T dwarfs and Jupiter, but are probably too faint and rare to be detected as free-floating objects in shallow all-sky surveys such as 2MASS and SDSS. Furthermore, the coolest/lowest mass objects may not exist as free-floating objects if there is a low-mass cutoff to the initial mass function of the star formation process, e.g., from opacity-limited fragmentation of molecular clouds (M_{min} ~ 5-10 M_{Jup}; Silk 1977). Even cooler/lower mass objects might only form via fragmentation, akin to the formation of binary stars, and may only be found as companions.

2.4.2.2 Very young planets in the nearest star-forming regions

Imaging searches and characterization at the very youngest (T Tauri) stages of stellar evolution provide a unique probe of the origin of extrasolar planets, by constraining their formation timescales and orbital separations. Young stars and brown dwarfs can be enshrouded by substantial dust extinction, both from the natal molecular cloud and their own circumstellar material. Thus most young (T Tauri) stars are too optically faint for current NGS AO systems or future ExAO systems. Keck NGAO imaging will probe physical separations of ≥ 5-10 AU around these stars.

It is still an open question whether giant planets form extremely rapidly (≤ 10^4 yr) due to disk instabilities (e.g. Boss 1998) or if they first assemble as ~10 M_{earth} rocky cores and then accrete ~300 M_{earth} of gaseous material over a total timescale of ~1-10 Myr (e.g. Lissauer 1998). Potentially both mechanisms may be relevant, depending on the range of orbital separations and circumstellar disk masses. In addition, imaging searches of young T Tauri stars both with disks (classical TTS) and without disks (weak TTS) can help to constrain the formation timescale. In particular, weak T Tauri stars with planetary companions would suggest that planet formation occurs even when disk evolution/dissipation happens rapidly.

The brightness of these very young planets is highly uncertain. Marley et al (2007) show variations in the accretion history of a planet can produce changes in luminosity. Most published models have initial conditions that correspond to formation through adiabatic contraction, resulting in a "hot start" and bright planets at young ages. Planets that form through runaway accretion in a protoplanetary disk, by contrast, dissipate much of their gravitational potential energy in an accretion shock, and will be orders of magnitude dimmer. However, NGAO will be sensitive primarily to planets in wide (15-30 AU) orbits, where

contraction or gravitational instability are more likely formation mechanisms. At the age and distance of Taurus, a 1 M_J hot-start planet has an effective temperature of 300K and a J magnitude of 22 (2 M_J corresponds to J=19.5). A typical parent star would have a J magnitude of 11. A separation of 15 AU in nearby star-forming regions corresponds to 0.1 arcseconds. The contrast requirement is therefore ΔJ =8.5 mags at 0.1 arcsecond, ΔJ =11 mags at 0.2 arcseconds, with a goal of ΔJ =11 at 0.1 arcseconds. Achieving this performance at 0.1 arcseconds may require a coronagraph optimized for very small inner working angles, and perhaps multi-wavelength imaging for speckle removal.

A related science case is observations of slightly older (5-30 Myr) stars in young associations such as the TW Hydrae association or older star-forming regions. These stars will be typically 40-80 pc in distance, but it is highly desirable to probe scales similar to the orbit of Jupiter (5 AU), leading to an aggressive inner working angle of 0.07 arcseconds. High-mass young association stars will also be observable with Gemini or VLT Extreme AO, but Keck NGAO can potentially access the lower-mass members of these associations.

2.4.3 Proposed observations

For each of these science cases, observations would consist of a moderate sized (100-300 target) survey of suitable targets. To achieve this in an acceptable amount of telescope time, it would be necessary to reach the required contrast levels in 20-30 minutes per target. Follow-up observations would be used to distinguish true companions from background objects and to spectrally characterize candidate companions

2.4.4 AO and instrument requirements

The high contrast near-IR (0.9-2.5 micron) imaging required for planet imaging will require coronagraphy to suppress PSF diffraction features. For most of the science applications, this coronagraph would be optimized for moderate contrast (10^{-4}) at angular separations of 0.2". For searches for companions to young, distant stars it would be desirable to have a more ambitious inner working angle of 0.07-0.1 arcseconds. Achieving the latter contrast will require a combination of high Strehl ratio and excellent calibration of non-common-path errors.

Contrast can be further enhanced through spectral differential imaging (SDI) or angular differential imaging (ADI). In the former technique, images at various wavelengths are compared to reject artifact speckles and retain true companions. Both techniques have limitations when applied to these science cases. SDI relies on either spectroscopic differences between the star and planet, or (at large angles) the radial magnification of the speckle/diffraction pattern as a function of wavelength. Planetary companions and brown dwarf primaries may have similar spectra, and the primary search space is at small angles, reducing the leverage available for SDI. In addition, this technique could require a dedicated multi-wavelength imager, or an IFU with a suitably large (>2 arcsecond) field of view, probably only practical at low spectral resolution.

ADI takes advantage of the parallactic rotation of the field of view when the pupil is fixed on the AO bench and science camera; as a result, artifacts from the AO system and telescope

remain fixed on the detector while planetary companions move at the parallactic rate. Subtracting different images out of a long time series (Marois et al. 2006, Lafrenière et al. 2007) can remove the artifacts. However, such subtraction will also erase the planet unless enough time has elapsed for the planet image to have moved by 1 diffraction limit. At 0.2 arcseconds and a typical parallactic rate this could take 30 minutes or more – for the ADI subtraction to work, the PSF must remain extremely stable over that timescale.

In many cases, near-IR tip-tilt sensing is required given the intrinsic redness of the science targets (e.g. brown dwarfs) or the high extinction of the science regions (e.g. star-forming regions). Most targets will be brighter than H=14 mag, allowing primarily on-axis tip/tilt; for some faint brown dwarfs, off-axis tip-tilt sensing may be needed. For off-axis science applications, sky coverage of >30% (as an areal average over the entire sky) is needed at the highest image quality over a corrected field of view < 5" in size.

Low-resolution (R~100) near-IR (0.9-2.4 micron) spectroscopy is important if one is to follow-up planet discoveries, to determine their temperatures, surface gravities, and masses. The relevant spectral features have broad wavelength ranges, e.g. the broad-band SEDs of circumstellar dust needed to diagnose grain composition and sizes and the broad molecular absorption band of H_2O and CH_4 present in the atmospheres of ultracool brown dwarfs and extrasolar planets. These spectra could be produced by binning higher-resolution spectra of sufficient sensitivity. Thermal (L-band) imaging would be desirable to help measure the SEDs of the planets, but is not essential for this science.

2.4.5 Performance Requirements

2.4.5.1 Wavefront error

The key performance driver for this science case is contrast, not wavefront error. Initial simulations with an RMS wavefront error of 140 nm indicated that the required contrast could be achieved. Simulations are under way to understand how the science would degrade for wavefront errors of 170 and 200 nm (relative to 140 nm). Excellent control and calibration of internal static wavefront calibration errors and quasi-static errors due to LGS spot shape will also be required of the AO system to minimize quasi-static speckles. Preliminary analytic calculations indicate requirements of 10-30 nm residual static wavefront error and quasi-static LGS-related errors.

2.4.5.2 Encircled energy

N/A

2.4.5.3 Need for large contiguous fields

Required FOV is only a few (< 5) arc sec. A larger contiguous field is not required.

2.4.5.4 Photometric precision

Probably not a key requirement. Require relative photometry of planetary companion to primary star of better than 0.05 mag, or absolute photometry of planetary companion to the

same accuracy, to characterize planetary masses and temperatures to 10%.

2.4.5.5 Astrometric precision

Probably not a key requirement. Astrometric accuracy to ~1/10 of the PSF FWHM would suffice for proper motion confirmation that candidate planets are physically associated to their primaries.

2.4.5.6 Contrast

From a science standpoint, the required contrast can be set by the need to directly image Jupiter-mass planets around a large sample of (1) field low-mass stars and brown dwarfs at ages of <~200 Myr and (2) young stars in the nearest star-forming regions. A benchmark value of $\Delta H=13$ magnitudes at 1 arc sec separation is required.

2.4.5.7 Polarimetric precision

N/A

2.4.5.8 Backgrounds

Thermal L-band photometry is desirable, but not a key requirement. Backgrounds lower than those on the current Keck AO system would be helpful for L-band photometry; a preliminary requirement would be L=20 mag in 2 hours. Access to the CO bands at 2.3 microns is also desirable.

2.4.5.9 Overall transmission

For some targets with low-mass primaries (brown dwarfs) and relatively old ages, high sensitivity will be a benefit at separations of ≥ 1 arc sec. The baseline sensitivity numbers from the NGAO proposal of H=25 mag (5-sigma) in 20 minutes of on-source integration time are suitable for these purposes.

2.4.6 Other key design features

2.4.6.1 Required observing modes

Imaging with both on-axis and off-axis tip-tilt stars, and single-object spectroscopy will be needed. Coronagraphic imaging is required, and will need additional design consideration because one must be able to center the science target on the focal plane mask and to keep it there to high accuracy during the observations.

2.4.6.2 Observing efficiency

Good efficiency is required, i.e. 5 min or less overhead per target, since we want to be able to observe many (several dozen) targets per night.

2.4.7 Instrument requirements

Instruments needed
Primary: Near-IR diffraction limited imager, narrow field, 0.9-2.4 microns, with coronagraph

Secondary: Near-IR IFU, R~100, diffraction limited, 0.9-2.4 microns, coronagraph (Higher-resolution spectroscopy with a coronagraph could be used; quantitative calculations of sensitivities will be done during Preliminary Design phase.)

Secondary: L-band imager

Secondary: Depending on the magnitude of quasi-static optical errors in the AO system, the latter could be attenuated through differential analysis of multi-wavelength images. This would require spectral resolution of ~50-100 over the 3-5" field of view, achieved either through a multi-channel imager with 2-3 channels or a low-resolution IFU similar to that being constructed for the Gemini Planet Imager.

Field of view
No more than 5 arc sec for both the near IR imager and the R~100 IFU.

Field of regard
Determined by the need for tip-tilt stars. All-sky average sky coverage for off-axis observations should be >30%.

IFU multiplicity
One object at a time only.

Wavelength coverage
0.9-2.4 microns (extension to L-band desirable, but not essential). 0.95-1.1 microns (Y band) is highly desirable for characterization of planets

Spectral resolution
R~100 at 0.9-2.4 microns. Could be achieved by binning higher-resolution data if sufficient sensitivity is achieved

2.4.8 Summary of Requirements

The requirements for the *planets around low-mass stars* science case are summarized in the following table. The key area in which NGAO will excel is the detection of planets around low-mass stars and brown dwarfs because Keck, unlike GPI or SPHERE, will be able to use a laser guide star. NGAO will also be able to search for planets around young solar-type stars where dust extinction is significant. JWST will have coronagraphic capability in the 3 to 5 μm window, but will have significantly lower spatial resolution than Keck NGAO. In terms of the types of solar systems that can be studied, this means that JWST will focus on older, nearby main sequence stars (since older giant planets will remain visible in 3 to 5 μm for a longer time). JWST may be more limited than NGAO in doing large surveys, because of its longer slewing time and possibly a lifetime limit on the total number of slews.

Requirements Table 4. Planets Around Low Mass Stars derived requirements

	Science Performance Requirement	AO Derived Requirements	Instrument Requirements
4.1	Target sample 1: Old field brown dwarfs out to distance of 20 pc. Sample size several hundred, desired maximum survey duration 3 yrs (practical publication timescales).	Observe 20 targets per night (each with e.g. 20 min integration time). Guide on a tip-tilt star with H=14.	Near infrared imager (possibly with coronagraph). Survey primary stars at J- and H-band.
4.2	Target sample 2: Young (<100 Myr) field brown dwarfs and low-mass stars to distance of 80 pc. Sample size several hundred, desired maximum survey duration 3 yrs.	Observe 20 targets per night (each with e.g. 20 min integration time).	Near infrared imager (possibly with coronagraph). Survey primary at J- and H-band. Could benefit from dual- or multi-channel mode for rejecting speckle suppression, but not essential for this program.
4.3	Target sample 3: solar type stars in nearby star forming regions such as Taurus and Ophiuchus, and young clusters @ 100 to 150 pc distance. Bright targets (on-axis tip-tilt generally possible: V=14-15, J=10-12). Sample size several hundred, desired maximum survey duration 3 yrs.	(May not require LGS if there is a good enough near-IR wavefront sensor available).	Possible dual- or multi-channel mode for speckle suppression. Alternatively an IFU would help, provided it is Nyquist sampled at H and has FOV > 1 arc sec. Min. IFU spectral resolution is R~100. May need IR ADC for imaging or coronagraphic observations (J or H bands); typical airmass is 1.7 for Ophiuchus.
4.4	Companion Sensitivity Sample 1: assume no companions beyond 15 AU. Targets at 20 to 30 pc; companion distribution peaks at 4 AU = 0.2"; this yields 2 $M_{Jupiter}$ planets at a 0.2" separation with contrast $\Delta H = 10$.	Excellent (<10nm) calibration of both initial LGS spot size and quasi-static non-common path aberrations, especially at mid-spatial-frequencies. Needs algorithms such as phase retrieval or speckle nulling (on a fiber source + good stability). Small servo-lag error (<30nm) to avoid scattered light at 0.2 arc	Inner working angle of 6 λ/D general-purpose coronagraph with a contrast of 10^{-6}. Detailed design of coronagraph will take place during PDR stage. Speckle suppression capability (multi-spectral imaging); dual-channel imager; stability of

	Science Performance Requirement	AO Derived Requirements	Instrument Requirements
	Planets have H=24, J=24.7. Parent stars are 2MASS Brown Dwarfs with H=14.	sec. Source: Error budget and simulations by Bruce Macintosh.	static errors ~5nm per sqrt(hr) for PSF subtraction or ADI.
4.5	Companion Sensitivity Sample 2: Parent stars are T Tauri, J=11. A 1 $M_{Jupiter}$ planet is at 300K, J=22, (2 $M_{Jupiter}$ is J=19.5). This distribution could have a wider distribution of binaries a) 0.1" separation, ΔJ = 8.5 ($2M_J$) b) 0.2" separation, ΔJ = 11 ($1M_J$) c) Goal ΔJ = 11 at 0.1" separation ($1M_J$) based on properties of the planets you want to look for.	Same as #4.4	a) 6 λ/D general-purpose coronagraph b) 6 λ/D general-purpose coronagraph c) (Goal) Not achievable with a general purpose coronagraph May need small Inner Working Distance (2 λ/D) coronagraph.[3] Speckle suppression capability (multi-spectral imaging); dual-channel imager; stability of static errors ~5nm per $\sqrt{hr}$ for PSF subtraction or ADI.
4.6	Goal: Companion Sensitivity Case 3: at 5 Myr , 1 M_{sun} primary; a) goal ΔJ = 13.5 to see 1 $M_{Jupiter}$ or b) goal ΔJ = 9 for 5 $M_{Jupiter}$. 0.07" is needed. For apparent magnitudes of parent stars see 4.3 above.	Excellent (10-20nm) calibration of both initial LGS spot size and quasi-static non-common path aberrations, at both low- and mid-spatial-frequencies. Needs algorithms such as phase retrieval or speckle nulling (on a fiber source + good stability). Small servo-lag error (<30nm) to avoid scattered light at 0.2 arc sec. Tomography errors 20-30nm. Source: error budget and simulations by Bruce Macintosh.	Requires multi- λ speckle suppression; very small inner working angle coronagraph (2 λ/D); static errors in 5-10nm range.
4.7	*Sensitivity* of H=25 for 5-sigma detection in 20	Sufficiently high throughput and low emissivity to permit	

[3] Non-redundant aperture masking is an interesting approach for this, limits currently unknown, probably requires low read noise in science detector.

	Science Performance Requirement	AO Derived Requirements	Instrument Requirements
	minutes, at 1 arcsec separation from primary star. (Brown dwarf targets are limited by sky background at larger angles, of order ~1 arcsec).	detecting H=25 in 20 minutes at 5 sigma above background.	
4.8	H-band relative *photometry* (between primary and companion): accuracy ≤ 0.1 mag for recovered companions (to estimate mass of the companion); goal of measuring colors to 0.05 mags (0.03 mag per band) to measure temperatures and surface gravities sufficiently accurately (to ~10%).	Diagnostics on AO data to measure Strehl fluctuations if it takes a while to move on and off the coronagraph (a possible more attractive solution is a specialized coronagraph that simultaneously images the primary)	Induced ghost images of primary; or rapid interleaving of saturated and unsaturated images; or a partially transparent coronagraph
4.9	Requirement: Astrometric precision 2 mas (~1/10 PSF) relative between primary and planet, for initial rejection of background objects. Goal: For measuring orbits of nearby field objects, want 0.5 mas to measure masses to 10%. Note this gives you mass of primary star. Could be combined with Doppler measurements if that's practical for the brighter objects.	Ways to do this: a) Position stability requirement for star behind coronagraph (e.g., stable to 0.5 or 2 mas over 10 min.). b) Induced ghost image method. Needs a wire grating ahead of the coronagraph, or use DM to induce ghost images. (papers by Marois et al. 2006, ApJ, 647, 612; Sivaramakrishnan & Oppenheimer 2006, ApJ, 647, 620).	Stability of distortion as required for 0.5 or 2 mas. Also want ghost images of primary (as for photometry #4.8) in order to locate it accurately relative to planet.
4.10	Efficiency: 20 targets	AO system must be able to	

	Science Performance Requirement	AO Derived Requirements	Instrument Requirements
	per night (30 goal)	absolutely steer objects so they land on the coronagraph. This implies 5 mas reproducibility of field steering –or lock the tip/tilt to this accuracy relative to coronagraph field stop. Final requirement will depend on the details of the coronagraph (5 mas is consistent with GPI modeling).	
4.11	Observing wavelengths JHK bands (strong goal: Y and z for companion temperature characterization)	Transmit JHK to science instrument. Goal: Y and z.	JHK filters. Methane band filters for rapid discrimination, Y and z, and/or a custom filter for early characterization.
4.12	Able to register and subtract PSFs (with wavelength, time, etc.) for post-processing to get rid of residual speckles. Subtraction needs to be sufficient enough to meet req. #4.4.	PSF knowledge and/ or stability to meet req. #4.4.	At least 1.5 x better than Nyquist sampled at J (goal Y)
4.13	Field of view: must see companions at 100 AU scales at 30 pc (goal 20 pc)		Field of view 3" radius (goal 5" radius)
4.14	Characterization of companion		a) R ~150 IFU, sub-Nyquist sampling spectrograph, or if above not available, b) Nyquist spatial sampling IFU, R ~ 4,000, OH suppressing). c) or narrow-band filters. All must be sensitive to J = 22 or 23 in ~3 hrs.
4.15	Sky Coverage >30%. (Survey several hundred Brown Dwarfs to H=15	Technical field for low-order wavefront guidestar pickoff large enough to achieve 30%	

	Science Performance Requirement	AO Derived Requirements	Instrument Requirements
	of the ~1000 known targets.)	sky coverage at high galactic latitude. Ability to acquire and track 3 tip/tilt stars. (More lenient if parent star can be used as one of the three TT stars.) Or ability to measure everything sufficiently with a single H=15 TT star (pyramid sensors).	
4.16	The following observing preparation tools are required: guide star finder for high proper-motion stars		

2.4.9 References

Becklin, E. & Zuckerman, B. 1988, Nature 336, 656

Boss, A. 1998, ApJ 503, 923

Chauvin, G., et al. 2004, A&A, 425, L29

Lafrenière, D., Marois, C., Doyon, R., Nadeau, D., & Artigau, E. 2007, ApJ, 660, 770

Lissauer, J. 1998, in "Origins," ASP Conf. Series vol. 148, 327

Marley, M. S., Fortney, J. J., Hubickyj, O., Bodenheimer, P., & Lissauer, J. J. 2007, ApJ, 655, 541

Marois, C., Lafrenière, D., Doyon, R., Macintosh, B., & Nadeau, D. 2006, ApJ, 641, 556

Marois, C., Lafrenière, D., Macintosh, B., & Doyon, R. 2006, ApJ, 647, 612

Nakajima, T. et al. 1995, Nature 378, 463

Silk, J. 1977, ApJ 214, 152

Sivaramakrishnan, A. & Oppenheimer, B. R. 2006, ApJ, 647, 620

2.5 Multiplicity of Minor Planets

Author: Franck Marchis
Editors: Claire Max, Elizabeth McGrath

2.5.1 Scientific background and context

While space missions largely drove early progress in planetary astronomy, we are now in an era where ground-based telescopes have greatly expanded the study of planets, planetary satellites, and the asteroid and Kuiper belts. Ground-based telescopes can efficiently perform the regular observations needed for monitoring planetary atmospheres and geology, and can quickly respond to transient events.

The study of the remnants from the formation of our solar system provides insight into the proto-planetary conditions that existed at the time of solar system formation. Such information has been locked into the orbits and properties of asteroids and Kuiper Belt objects. The study of binary (and multiple) minor planets is one key path to revealing these insights, specifically by studying their kinematics and geological properties. There are no space missions currently planned to study these binaries. This important inquiry is only accessible to ground-based telescopes with AO.

2.5.2 Scientific goals

High angular resolution studies are needed of large samples of binary asteroids to understand how their enormous present-day diversity arose from their formation conditions and subsequent physical evolution, through processes such as collisional disruption and re-accretion, fragmentation, ejecta capture, and fission. Specifically one can study:

- Formation and interiors of minor planets by accurate estimates of the size and shape of minor planets and their companions
- Mass, density, and distribution of interior material by precise determination of the orbital parameters of moonlet satellites
- Chemical composition and age, by combining high angular resolution with spectroscopic analysis

2.5.3 Proposed observations and targets

Study of main-belt multiple systems: One of the main limitations of current AO observations for a large search for binary asteroids and for characterization of their orbits is the limited number of asteroids observable considering the magnitude limit on the NGS wavefront sensor. The Keck NGS AO system can use guide stars down to 13.5 magnitude, so ~1000 main-belt asteroids (to perihelion >2.15 AU and aphelion <3.3 AU) can be observed.

With NGAO providing an excellent correction up to tip-tilt star magnitudes V = 17 or J = 19 10% of the known main-belt population can be searched, corresponding to the potential discovery of 1000 multiple systems assuming the current multiplicity rate of 6% - 15%. This is a lower limit on the detection rate of new moonlets, because the NGAO system will provide

a more stable correction than current Keck LGS AO and the halo due to uncorrected phase errors will be significantly reduced.

Closer and fainter satellites should be detectable, as will be explained below. At the time of this writing, the orbits of ~15 visual binary systems are known and display considerable diversity. To better understand these differences, we propose to focus our study on 100 new binary systems in the main-belt discovered elsewhere, by light-curves or snap shot programs on HST and/or previous AO systems. The increase by an order of magnitude of known orbits will help us to understand how they formed as members of a collisional family, their distance to the Sun, their size and shape, and other parameters.

To reach a peak SNR~1000-3000 on an AO image, the typical total integration times assuming 170 nm of wavefront error are 5 min and 15 min for 13th or 17th V-magnitude targets respectively. Considering a current overhead of 25 min (Marchis et al. 2004b) to move the telescope onto the target and close the AO loop, the total telescope time per observation is ~30 min. This overhead time must be significantly improved by careful design of the NGAO system. The orbit of an asteroid can be approximated (P, a, e, i) after 8 consecutive observations taken over a period of 1-2 months to limit the parallax effect, corresponding to the need for 0.3 nights per object. The eight observations per target correspond to a discovery image, plus six epochs to constrain the orbital elements (inclination, i; longitude of the ascending node, Ω; argument of periapsis, ω; eccentricity, e; semi-major axis, a; mean anomaly at epoch, M_0), and a final observation to constrain the orbital period. If the discovery image is of sufficient quality, it can be used to constrain one of the six orbital elements or period, thus reducing the number of required observations per target to seven. If the system is face-on, only five observations would be required. Assuming eight observations per target at 30 minutes each, thirty nights of observation would be required for this program over 3 years. Fewer nights may be requested if conditions are favorable.

To illustrate the gain in quality expected with NGAO, we generated a set of simulated images of the triple asteroid system 87 Sylvia. The binary nature of this asteroid was discovered in 2001 using the Keck NGS AO system. Marchis et al. (2005) announced recently the discovery of a smaller and closer moonlet. The system is composed of a D=280 km ellipsoidal primary around which two moons describe a circular and coplanar orbit: “Romulus”, the outermost moonlet (D=18 km) at 1356 km (~0.7”) and “Remus” (D = 7 km) at 706 km (~0.35”). In our simulation we added artificially two additional moonlets around the primary: “S1/New” (D=3.5 km) located between Romulus and Remus (at 1050 km) and “S2/New” (D=12 km) closer to the primary (at 480 km). This system is particularly difficult to observe since the orbits of the moons are nearly edge-on. We blurred the image using the simulated NGAO and Keck NGS AO PSFs (with an rms error of 140 nm) and added Poisson and detector noise to reach a S/N of 2000 (corresponding to 1-3 min integration time for a V=12 target). We then estimated whether the moonlets could be detected and their intensity measured by aperture photometry. Figure 12 displays a comparison for one observation between the current Keck NGS AO, NGAO in two wavelengths, and HST/ACS. The angular resolution and thus the sensitivity of the NGAO R-band is a clear improvement and permits detection of the faintest moon of the system.

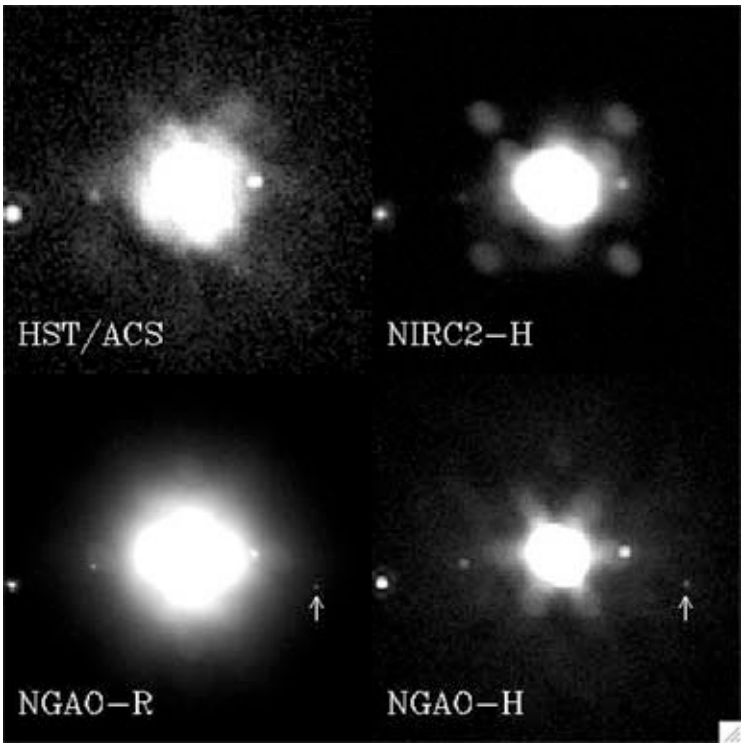

Figure 12. Simulation of pseudo-Sylvia observed with various AO systems.
We assumed here that NGAO has a wavefront error of 140 nm in this simulation.

Table 4 summarizes the 2-σ detection rate for the pseudo-Sylvia system moonlets. The photometry was done using the same technique as for real observations (aperture photometry + fitting/correction of flux lost). The detection rates for NGAO- R band are 100% for all moons. One can also notice a very good photometric recovery with this AO system. The chances to discover multiple systems and to analyze them are significantly improved with NGAO. It should be also emphasized that because the astrometric accuracy is also better, determination of the orbital elements of the moons will be also more accurate (e.g., a significant eccentricity or small tilt of the orbit).

Table 4
Detection rate and photometry on the moons of pseudo-Sylvia, assuming an NGAO system with 140 nm of wavefront error.

	Romulus		Remus		S_New1		S_New2	
	Det. rate	Δm	Det. Rate	Δm	Det. Rate	Δm	Det. Rate	Δm
Perfect image	100%	6.6	100%	8.1	100%	6.9	100%	9.6
NIRC2-H	82%	6.4±0.04	70%	8.3±0.3	11%	6.9±0.2	0%	N/A
NGAO-H	100%	7.0±0.1	70%	8.5±0.5	40%	7.1±0.2	0%	N/A
NGAO-R	100%	6.60±0.01	100%	8.3±0.1	100%	6.9±1.1	100%	10.1±0.3

2.5.4 AO requirements

2.5.4.1 Wavefront error

A wavefront error of 140 nm would provide excellent angular resolution in the visible, better than HST and adequate for our program. Table 14 of the Keck NGAO Proposal to the SSC (June 2006) indicates that the point source limiting magnitude for such AO system (5σ, 1hr integration) is 29.0 in R band. For comparison, recent observations of Pluto-Charon recorded with ACS/WFC at 0.61 μm (Weaver et al. 2006) allowed the detection of 2 new moons with R = 23.4 (SNR=35). With NGAO in R band with 140 nm of wavefront error, these moons could have been discovered with SNR~47. Such gain in sensitivity will help find more multiple systems, and also to find out if around these multiple systems there is still a ring of dust left over from the catastrophic collision that formed the multiple system. We are currently carrying out simulations to characterize the science that could be done with 170 nm and 200 nm of wavefront error. Future releases of this Science Case Requirements Document will compare the science performance for 140, 170, and 200 nm of wavefront error. Our expectation is that there will not be a "cliff" in science output as the wavefront error degrades, but rather a gradual decrease in the number of moonlets detected and in the number of primary asteroids whose shapes can be measured.

2.5.4.2 Encircled energy

N/A

2.5.4.3 Contiguous field requirement

Required FOV is ≤ 2 arc sec. There is no requirement for a larger contiguous field.

2.5.4.4 Photometric precision

Accurate photometry will lead to a better estimate of the size and shape of the moonlets, which will give strong constraints on their formation mechanism (e.g. one would be able to tell if the moonlet is synchronized and displays an equilibrium shape under tidal forces). The proposed method is to detect photometric changes due to its potential lack of sphericity over the moonlet's orbit, as we see different faces of the moonlet. With current AO systems, the photometric accuracy on the moonlet is rather poor. The accuracy of the flux estimate of the 22 Kalliope moonlet, orbiting at 0.6 arc sec with $\Delta m=3$, was only ~20% with Keck LGS AO. Assuming the same sky background and detector noise as with current Keck LGS AO, NGAO in the near IR is predicted to yield a photometric accuracy of 5% or better for the same observing situation.

2.5.4.5 Astrometric precision

The astrometric measurements for our program are relative to the primary. The maximum angular separation between the secondary and the primary is 0.7 arc sec. We require the visible instrument to provide images with at least Nyquist sampling. The relative position of the secondary, estimated by a Moffat-Gauss fit, cannot be better than a 1/4 of a pixel (since the primary is resolved). The residual distortion over the field of the detector should not be more than 1.5 mas. Uncharacterized detector distortion will be the limiting factor in these astrometric measurements.

2.5.4.6 Contrast

At the current time the faintest and closest moonlet discovered around an asteroid is Remus, orbiting at 0.2-0.5" (350-700 km) around 87 Sylvia with Δm (peak-to-peak) = 3.5. The detection of this moonlet is challenging with current Keck AO, and also with the VLT NACO system. For instance, it was detected (SNR > 3) on 10 images out of 34 recorded over 2 months with the VLT. A better contrast will increase the detection rate, allowing us to see fainter and closer moonlets but also to get a better photometric measurement on those already known. Coronagraphic observations cannot be considered in our case: the central source is not point-like so the effect of the mask will be negligible. It is assumed that the distance to the primary of a satellite is driven by tidal effects, but at the moment theoretical work fails to agree on the age of an asteroid and the position of its moonlet. This is mostly due to the lack of observed systems in which a moonlet orbits at less than 1000 km ($a / R_p < 8$). Two orders of magnitude gain in the detection limit ($\Delta m = 5.5$ at 0.5 arc sec) would lead to the possibility of detecting a half-size moonlet around (87) Sylvia.

2.5.4.7 Polarimetric precision

N/A

2.5.4.8 Backgrounds

Any background equal to or better than current Keck AO will be acceptable. Lower backgrounds are always better.

2.5.4.9 Overall transmission

Comparable to or better than with current LGS AO system.

2.5.5 Other key design features

2.5.5.1 Required observing modes

The capability of efficiently observing moving non-sidereal targets must be included in the design of NGAO, so that implementation of differential guiding when the tip-tilt source is not the object itself (and is moving relative to the target) is possible. The maximum relative velocity to be expected is 70 arc sec per hour.

We also point out that for this science case, the scientific return of the Keck telescope and the NGAO system would greatly improve if some sort of flexible or queue scheduling or service observing were to be offered. With an error budget of 140 nm the NGAO system will achieve a Strehl of ~20% in R- band under moderate seeing conditions. Bright targets like the Galilean satellites (V~6) can be observed even if the seeing conditions are lower than average in the near IR (at separations > 1.2"). Other difficult observations, such as the study of multiple TNOs (V>17) could be scheduled when the seeing conditions were excellent (< 0.7"). Finally, frequent and extremely short (half hour) direct imaging observations of a specific target such as Io, to monitor its activity over a long period of time, would be extremely valuable and are not available on HST. All these programs could be done more easily if flexible or queue or service observing were available at Keck. It would also relax the constraints on the NGAO error budget since it would be possible to take advantage of excellent atmospheric conditions to observe the faintest objects.

2.5.5.2 Observing efficiency

Current observations with Keck AO have a ~25 minute overhead when switching between targets for an on-axis LGS observation of an asteroid. It is very desirable to reduce this overhead. A goal of 10 minutes setup time when switching between LGS targets is desirable. Observing efficiency suffers in direct proportion to the time it takes to switch from one target to the next, particularly when the observing time per target is relatively short. This is an important constraint for this science case, since numerous targets must be observed per night.

2.5.6 Instrument requirements

2.5.6.1 Required instruments

Primary: Visible imager, on-axis, diffraction limited, narrow field, with coronagraph
Primary: Near IR imager, on-axis, diffraction limited, narrow field, with coronagraph
Secondary: Visible IFU, on-axis, narrow field, R~100
Secondary: Near infrared IFU, on-axis, narrow field, R~1000-4000

2.5.6.2 Field of view

No more than 4 arc sec.

2.5.6.3 Field of regard

Should be determined by the requirement to find adequate tip-tilt stars.

2.5.6.4 Pixel sampling

For both photometry and astrometry, the pixel scale of the imager that yields the best overall performance is $\lambda/3D$ for J, H, and K-bands, or $\lambda/2D$ for R and I-bands. See KAON 529 for an in-depth discussion of how these values were chosen.

2.5.6.5 IFU multiplicity

Single object mode only. Density of asteroids on the sky is not high enough for multi-object observing.

2.5.6.6 Wavelength coverage

Imaging: Wavelengths I (833 nm) or J (1.1 micron) band

2.5.7 Requirements Summary

The requirements for the *asteroid companions survey* science case are summarized in the following table.

Requirements Table 5. Asteroid Companions Survey driven requirements

#	Science Performance Requirement	AO Derived Requirements	Instrument Requirements
5.1	The *companion sensitivity* shall be $\Delta J \geq 5.5$ mag at 0.5" separation for a $V \leq 17$ asteroid ($J \leq 15.9$) (asteroid size < 0.2") with a proper motion of ≤ 50 arcsec/hour	The asteroid can be used as tip/tilt guidestar (proper motion of ≤ 50 arcsec/hour). The AO system has sufficient field of view for objects and for their seeing disks (>3 arcsec, see # 5.8). The tip-tilt residual error will be less than 10 mas (limited by resolved primary) while guiding on one V=17 (J =15.9) object with relative motion of 50 arcsec/hr (14 mas/sec). The AO system has sufficient Strehl to achieve this contrast ratio and sensitivity in 15 min exposure time. KAON 529 suggests that 170nm wavefront error will	Near-IR imager

		suffice.	
5.2	J-band relative *photometric* accuracy (between primary and companion) of 5% at 0.6" for $\Delta J = 3$ for a $V \leq 17$ ($J \leq 15.9$) asteroid (asteroid size < 0.2") with a proper motion of ≤ 50 arcsec/hour		Near- IR imager (no coronagraph because many asteroids will be resolved)
5.3	Target sample ≥ 300 asteroids in ≤ 4 yr. Leads to requirement of ≥ 25 targets per 11 hour night.	Assumes 3 good nights per year. Needs high observing efficiency: Able to slew to new target and complete the entire observation within 26 minutes on average.	
5.4	Observing wavelengths I through J bands, for optimum companion sensitivity [Source: KAON 529]. J band is best when seeing is good. H band could be used when seeing is poor.		Visible and IR imagers.
5.5	Spatial sampling ≤ Nyquist at each observing wavelength. Pixel sampling of $\lambda/3D$ optimal for photometry and astrometry [KAON 529].		Spatial sampling ≤ Nyquist at the observing wavelength. Pixel sampling of $\lambda/3D$ is optimal at J through H-bands, and $\lambda/2D$ at I through z-band for both photometry and astrometry [see KAON 529].
5.6	Field of view ≥ 3" diameter	AO system passes a >3" unvignetted field of view	Imager fields of view ≥ 3"
5.7	The following observing preparation tools are required: guide star finder for	Guide star finder tool. PSF simulation tool (predict energy and width of central core to within	

	asteroids too faint to use as the only TT star, PSF simulation as function of wavelength and seeing conditions.	10%).	
5.8	The following data products are required: Access to archive with proper identification in World Coordinate System (to within 1 arc sec or better) and with associated calibrated PSF.	Calibrated PSF capability. Accuracy requirement will be discussed in future releases of the SCRD document. Ability to collect AO telemetry data to support the required PSF calibration.	FITS header system capable of handling non-sidereal offsets in reporting object coordinates in the World Coordinate System to within 1 arc sec or better.
5.9	Observing requirements: Observer present either in person or via remote observing rooms, because real-time observing sequence determination is needed.	Classical observing mode or service mode with active observer participation. Remote observing capabilities must allow frequent real-time decisions by observer.	

The requirements for the *asteroid companions orbit determination* science case are summarized in the following table.

Requirements Table 6. Asteroid Companions Orbit Determination driven requirements

#	Science Performance Requirement	AO Derived Requirements	Instrument Requirements
6.1	Companion sensitivity in the near-IR. Same as #5.1	Same as #5.1	Near-IR imager.
6.2	The *companion sensitivity in the visible* shall be $\Delta I \geq 7.5$ mag at 0.75" separation for a $V \leq 17$ ($I \leq 16.1$) asteroid (asteroid size < 0.2") with a proper motion of ≤ 50 arcsec/hour		Visible Imager. Optimum visible wavelength is I through z bands per KAON 529. Note that if the near-IR imager extends down to I band, a separate visible imager would not be needed for this science case.
6.3	*Photometric accuracy*: Same as #5.2	Same as #5.2	
6.4	I-band relative *astrometric* accuracy of ≤ 1.5 mas for a $V \leq 17$ ($J \leq 15.9$) asteroid (asteroid size < 0.2") with a proper motion of ≤ 50 arcsec/hour	Non-sidereal tracking accuracy sufficiently small to achieve I-band astrometric accuracy ≤ 1.5 mas for a $V \leq 17$ ($J \leq 15.9$) asteroid with a proper motion of ≤ 50 arcsec/hour	Uncalibrated detector *distortion* sufficiently small to achieve I-band astrometric accuracy ≤ 1.5 mas for a $V \leq 17$ ($J \leq 15.9$) asteroid
6.5	Target sample size of ≥ 100 asteroids in ≤ 4 years. Leads to requirement of ≥ 25 targets in an 11 hour night.	Needs high observing efficiency: Able to slew to new target and complete the entire observation within 25 minutes on average. Will generally only observe at one wavelength (the one that gives the best astrometric information).	
6.6	Observing wavelengths = I, z, J, H bands. (Note: R-band may become a future requirement if R-band		Imager(s) covering range I, z, J, H bands. Note that if the near-IR imager extends down to I band, a separate visible imager would not

	Strehl > 15%)		be needed for this science case.
6.7	Spatial sampling same as #5.5		Same as #5.5
6.8	Same as #5.6	Same as #5.6	Same as #5.6
6.9	Same as #5.7	Same as #5.7	
6.10	Same as #5.8	See #5.8	
6.11	Observing requirements: 7 epochs per target	Observing model needs to accommodate split nights or some level of flexibility.	

2.5.8 References

Marchis, F., J. Berthier, P. Descamps, et al. 2004b. Studying binary asteroids with NGS and LGS AO systems, SPIE Proceeding, Glasgow, Scotland, 5490, 338.

Marchis, F., Descamps, P., Hestroffer, D. et al., 2005. Discovery of the triple asteroidal system 87 Sylvia, *Nature* 436, 7052, 822.

Marchis, F.; Kaasalainen, M.; Hom, E. F. Y.; Berthier, J.; Enriquez, J.; Hestroffer, D.; Le Mignant, D.; de Pater, I. 2006. Shape, size and multiplicity of main-belt asteroids, *Icarus* 185, 39.

Tanga, Paolo; Consigli, J.; Hestroffer, D.; Comito, C.; Cellino, A.; Richardson, D. C. 2006, Are Asteroid Shapes Compatible With Gravitational Reaccumulation? American Astronomical Society, DPS meeting #38, #65.06

Weaver, H. A.; Stern, S. A.; Mutchler, M. J.; Steffl, A. J.; Buie, M. W.; Merline, W. J.; Spencer, J. R.; Young, E. F.; Young, L. A. 2006, Discovery of two new satellites of Pluto, Nature, 439, 943.

3 Science Cases: Science Drivers

The following eight science cases are defined as Science Drivers (SD). They will place important constraints on the operational modes of the final NGAO system, but are generally less technologically challenging than the KSDs listed in the previous section.

3.1 QSO Host Galaxies

This science case involves very accurate subtraction of the bright central point-source in a QSO, so as to do detailed imaging and possible spectroscopy of the surrounding host galaxy. Because the central point source flux can be up to 200 time brighter than the galaxy flux a half-arc-sec away, this is very challenging. Indeed the full factor of 200 in contrast may not be fully achievable with the NGAO system as specified by the "key science driver" requirements, because the sources are intrinsically fainter than the other high-contrast science cases considered here (planets around low-mass stars, and companions to asteroids).

Nevertheless the QSO Host Galaxy science case is compelling scientifically, and for at least some quasars on the lower end of the contrast scale the NGAO system will yield exciting insights.

The main challenges for this science case are: very accurate PSF subtraction, to eliminate light from the central non-thermal point source, and (possibly) the design of a coronagraph optimized for QSO host galaxy observations.

3.1.1 Scientific Background

At present, the most detailed quantitative studies of quasar host galaxies have been done with HST imaging. AO observations are beginning to play an increasingly important role, particularly due to the inherent advantages of observing in the near-IR, where the underlying host galaxy structure can be more clearly revealed and where the central AGN point source is less prominent than in the optical. However, even for low-redshift quasars, temporal variability of the AO PSF can make it difficult or impossible to extract quantitative information about the host galaxy structure for radii smaller than 1" (Guyon et al. 2006). Thus, even for low-redshift quasars, determining accurate bulge luminosities and profiles is at or beyond the limits of current capabilities, and for high-redshift quasars (z beyond about 2), even the most basic detection of host galaxies has often proved very difficult with current-generation AO (Croom et al. 2004). HST/NICMOS has been used for quasar host galaxy imaging in the H band, and has the advantage of an extremely stable PSF, but Keck NGAO will offer better spatial resolution by a factor of four.

Key observational goals in this area include:

- At low to moderate redshifts ($z < 1$): detailed structural measurements of quasar hosts

and bulge/disk decompositions from AO imaging, using GALFIT or similar tools, to extend the black hole mass/bulge mass correlation and examine the relationship between quasar activity and galaxy mergers. Integral-field unit observations to study emission line velocity fields and outflows. IFU observations can be used to determine the evolution with redshift of the M-σ relation, for example by measuring bulge velocity dispersions with the Ca II triplet for Seyfert 1 galaxies at z~1.

- At high redshifts (z > 1): detection of host galaxies in AO images, measurement of asymmetry/lopsidedness parameters to investigate the relationship to the host galaxy merger history, and measurement of integrated magnitudes and colors to constrain the overall stellar population.

3.1.2 Expected NGAO Performance

For observations of quasar host galaxies, we consider a simplified simulation of a quasar at z=2 with a central AGN point source magnitude of K' = 17 and an elliptical host galaxy with magnitude of K' = 18.7 mag and half-light radius 0.65". A simulated image of the quasar as seen with NIRC2 at 0.01"/pixel was created, for a total exposure time of 3600 sec and with noise added using the current NIRC2 specifications. The PSF was modeled as a double-Gaussian with core FWHM = 0.053" and halo FWHM = 0.5", and with 30% of the total flux in the core for current LGS AO and 72% for NGAO. Radial profiles were extracted for the simulated AGN image and also for a simulated PSF star observation having S/N equal to the AGN image. As shown in Figure 13, the host galaxy is essentially undetectable with the current LGS AO observation, but could be significantly detected with NGAO because of the greatly improved PSF structure. It should be noted that this simulation does not take temporal variability of the PSF into account: for a realistic observation with current LGS AO the host galaxy would be considerably more difficult to detect than even this simulation suggests. With a highly stable PSF, NGAO can play a leading role in the study of AGN host galaxies at high redshift.

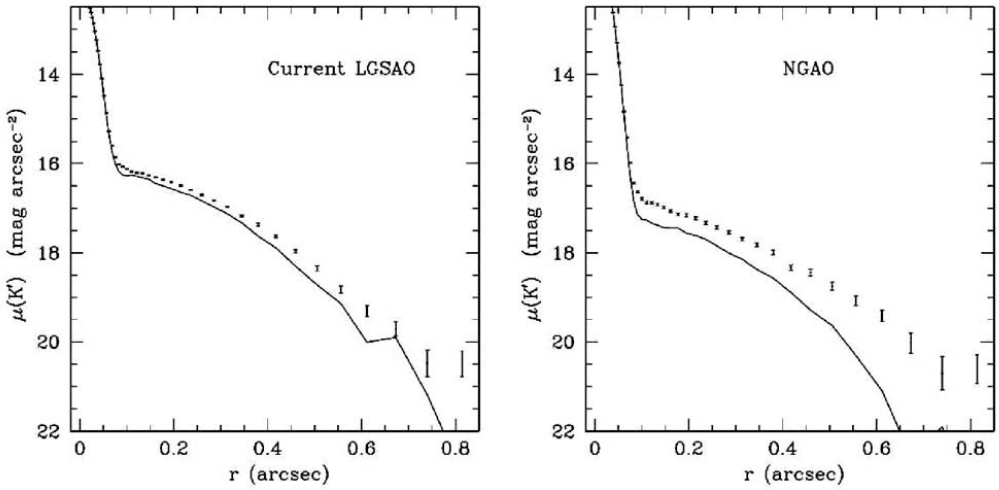

Figure 13. Simulated K' observation of a z = 2 quasar with current LGS AO and with NGAO.
Simulations are for a 1 hour exposure with NIRC2 and assuming the same background level. The solid curve is the PSF profile measured from a simulated PSF image with noise added, and scaled to the same peak flux as the quasar nucleus, and the points with error bars are the radial profile of the quasar plus host galaxy. The host galaxy is nearly undetectable with current LGS AO but can be significantly detected with NGAO.

3.1.3 Proposed observations and targets

- For low-redshift samples such as the PG quasar sample (z~0.1-0.3), typical H-band magnitudes are ~12-14 mag for the AGN point source, and 13-15 mag for the host galaxy.

- For high-z quasars: at z=2, typical bright quasars have K~16-18 mag. Luminous elliptical host galaxies (~2L*) would have K~19 mag with half-light radii of ~0.7 arcsec.

3.1.4 Summary of Requirements

The requirements for the *QSO Host Galaxy* science case are summarized in the following table. The typical QSO that we are considering is at redshift 2. Typical galaxy sizes are 0.5 to 2 arc sec. Contrast ratios between the central point source and a galaxy region ½ arc sec away range from 50 to 200 or more. The scientific goals are the following: 1) measure colors and magnitudes for the point source; 2) measure morphology and surface brightness profile for the galaxy; 3) obtain spectrum of point source; 4) obtain spatially resolved spectrum of galaxy in order to study its kinematics and stellar populations. In order to accomplish these things, accurate PSF subtraction will be crucial.

Additional trade studies will be described in future releases of this document. 1) Wavelength trade: contrast between central point source and host galaxy will be minimized at longer wavelengths (e.g. K band) because central point source is blue and because PSF stability will be higher; however width of PSF core will be larger. 2) Quantitative simulations will be performed in order to optimize PSF subtraction of the central point source, which can be 200 or more time brighter than the host galaxy at 0.5 arc sec separation. 3) Benefits of a specialized coronagraph to reduce light from central point source will be studied.

Requirements Table 7. QSO Host Galaxies Derived Requirements

Future releases of this document will quantify the requirements for PSF subtraction and stability, required spatial resolution, and coronagraph design. The following table outlines the issues and should be viewed as a place-holder.

#	Science Performance Requirement	AO Derived Requirements	Instrument Requirements
7.1	Number of targets required: to be specified in future versions of this document	Sky coverage fraction >30% for 50% enclosed energy within 0.05 arc sec at J band	
7.2	Required wavelength range: 0.85 – 2.4 microns		Near IR IFU spectrograph; near IR and visible imagers.
7.3	Required spatial resolution will be discussed in a future	Desirable to use central QSO point source as one of the tip-tilt reference stars, if possible.	PSF must be oversampled in order to achieve required subtraction accuracy.

	release of this document. Will be determined by considerations of PSF subtraction accuracy. Hence required resolution will be higher than in the high-z galaxy science case.		Quantitative requirements will be discussed in future releases of this document.
7.4	Photometric accuracy and PSF knowledge required for subtracting the central point source in order to characterize the host galaxy must be adequate to obtain host galaxy colors to 20% for a contrast ratio of up to 200 at a distance of ½ arc sec from the point source.	Requires excellent PSF stability and knowledge; future releases of this document will discuss the quantitative requirements. Will have implications for required AO wavefront error, AO stability, and required signal to noise ratio.	Required calibration stability and accuracy, zero-point stability and knowledge, quality of flat-fielding will be discussed quantitatively in future releases of this document. PSF must be oversampled in order to achieve required subtraction accuracy. Quantitative requirements will be discussed in future releases of this document.
7.5	SNR for spatially resolved spectroscopy of the host galaxy will be determined by accuracy of PSF subtraction and by minimization of scattered light from the central point source.		May benefit from specialized coronagraph design to block light from central point source.
7.6	Required observation planning tools (e.g. guide stars); PSF simulation tools to plan for whether PSF subtraction will be good enough to see the host galaxy		
7.7	Required data reduction pipeline for IFU		

3.1.5 References

Croom, S. M., et al. 2004, ApJ, 606, 126
Guyon, O., Sanders, D. B., & Stockton, A. 2006, astro-ph/0605079
Peterson, B. M., et al. 2004, ApJ, 613, 682
Silge, J. D., Gebhardt, K., Bergmann, M., & Richstone, D. 2005, AJ, 130, 406
Woo, J.-H., Treu, T., Malkan, M. A., & Blandford, R. D. 2006, astro-ph/0603648

3.2 Gravitational Lensing

Authors: Elizabeth McGrath, Tommaso Treu, Laura Melling, and Phil Marshall
Editor: Claire Max

3.2.1 Introduction

Massive clusters and galaxies produce a local perturbation of the Robertson-Walker metric that distorts our view of background objects. Gravitational lensing is achromatic and preserves surface brightness. Under appropriate circumstances, if the deflector is dense enough and the impact parameter is small enough, multiple images of the background source appear to the observer. This regime is called strong gravitational lensing. Strong gravitational lensing is extremely useful for the study of the high redshift universe for two main reasons: i) the astrometry of the lens configuration depends on the mass distribution of the deflector and on angular size distances, and thus can be used to "weigh" galaxies/clusters, determine the structure and substructure of dark matter halos, and/or to measure cosmography; ii) the background source is highly magnified both in terms of apparent size and apparent luminosity, so that lenses act as natural gravitational telescopes; magnification is quite significant, typically in the range of 10 to 25 in luminosity.

Precision astrometry is the name of the game for gravitational lensing. So far the Hubble Space Telescope has been the unchallenged leader in this field. Laser guide star adaptive optics has the potential to change the field. The large mirror-size of Keck can deliver a factor of four improvement in angular resolution over HST if high Strehl ratios can be achieved with NGAO. Furthermore, coupling an AO system with integral field spectrographs will open the way for high spatial resolution studies of dynamics and chemistry of galaxies in the distant universe and for detection and spectroscopy of the first galaxies and sources of reionization at a redshift $z > 7$-8. As illustrated by the simulations shown below, Keck with NGAO is better than HST for these purposes and will dominate the subject after the demise of HST.

3.2.2 Scientific background and context

Gravitational lensing provides a unique opportunity to explore the high-redshift universe and to map the evolution of dark and light matter over cosmic time. In particular, gravitational lensing is useful for the study of early-type galaxies, whose centrally concentrated mass profiles make them ideal lensing candidates. These galaxies are often excluded from magnitude-limited, high-redshift galaxy surveys that focus on blue and emission-line-dominated galaxies, but their formation and evolution is of great importance since more than half of all luminous matter is contained within such objects in the present-day (e.g., Fukugita, Hogan, & Peebles 1998). Topics of interest include how and when mass is assembled to form early-type galaxies, the nature of the dark matter halos in which they reside, the star formation history and its role in shaping the total mass distribution in early-type galaxies, and the structural and dynamical evolution of early-type galaxies.

The advantages of gravitational lensing are that 1) it provides a direct measurement of the total mass of the lensing galaxy, and 2) it serves as a "gravitational telescope" to magnify

background sources, providing very detailed structural and kinematical knowledge of faint, high-redshift galaxies. NGAO can provide unprecedented resolution and Strehl ratios at near-IR wavelengths, which corresponds to an increased ability to reconstruct the gravitational potential of the lensing galaxy as well as the structure of background galaxies.

3.2.3 Galaxy versus Cluster Lensing

It is useful to separate two regimes: cluster/group lensing and galaxy size lensing. The angular size is set by the Einstein radius, which in turn scales as the velocity dispersion squared. Hence typical galaxies will have Einstein radii of order 1", while massive clusters in the same redshift configuration will have Einstein radii of order 30" (Figure 14).

Furthermore, clusters – with their longer caustics – have much higher chances than galaxies to lens multiple background objects and in general to be strong lenses. So clusters are rarer in the sky but they are very efficient lenses. Galaxies are more common in the sky, but they are much more unlikely to be lenses. From a practical point of view, galaxy and cluster scale lenses require different strategies for detection and scientific exploitation, and have different instrumental requirements. Galaxy scale lenses have the more stringent requirements in terms of spatial resolution and Strehl ratios, while cluster scale lenses are more demanding in terms of field of view. Therefore they will be treated separately in this document. The intermediate regime, group size lensing, is a very poorly known subject. In general NGAO will be useful for group size lensing as well, but with intermediate requirements between galaxy and cluster scale lensing for spatial resolution and field of view. Therefore we do not discuss group size lensing in this document.

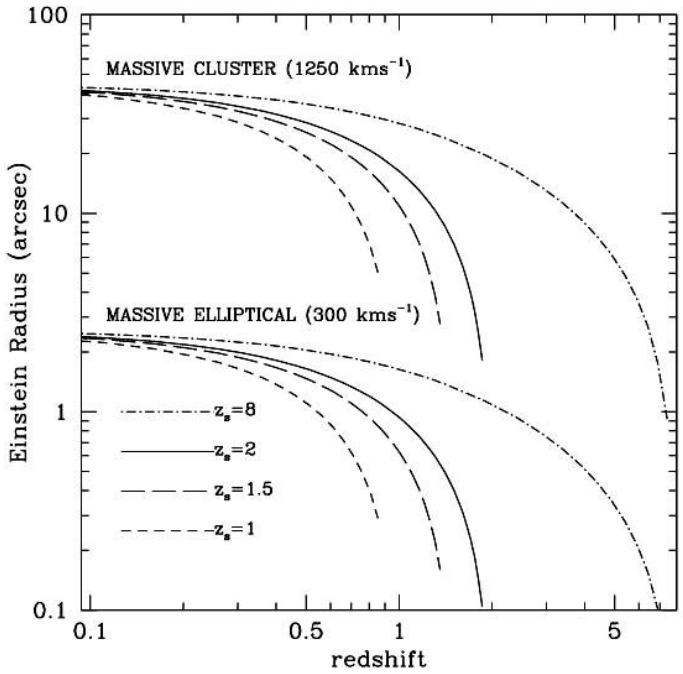

Figure 14. Typical angular scales of cluster-size lensing and galaxy-size lensing.
The curves show the size of Einstein radius for a massive cluster (velocity dispersion 1250 km/s) and a massive elliptical (300 km/s) as a function of deflector redshift. A field of view of 3-4" is well matched to galaxy-size lensing, while a field of 1-2' is well matched to cluster-scale lensing.

3.2.4 Scientific goals

The goals of this study are as follows.

Lensing by galaxies:
Traditional lensing exploits the preservation of surface brightness in order to model the potential of the lens and determine the intrinsic surface brightness profile of the source. By exploiting lensing achromaticity as well, kinematic observations of the source can lead to an improved model of the lens potential and provide super-resolved information of the source velocity field. This is an area where NGAO has a potential to excel, providing far more detail than ever before observed in the structure and kinematics of high-z galaxies. For example, with the magnification power of lensing and the high-Strehl, high-resolution provided by NGAO, we can extend the Tully-Fisher relation to higher redshifts and to galaxies with V_{max}<100 km/s. Furthermore, with improved lens potentials, we can study the distribution of dark and light matter in the elliptical lens galaxies and how it evolves with redshift. This information can then be combined with studies of the fundamental scaling relationships in order to disentangle their stellar population and mass-assembly histories. The following are primary goals for NGAO studies of galaxy-scale lensing:

- Determine the individual stellar and dark-matter mass structures of E/S0 lens galaxies out to z~1.
- Detecting substructure in the dark matter halo of the lensing galaxy through local perturbations in extended multiply lensed images (e.g., Koopmans 2005).
- Quantify evolution with time, and trends with galaxy mass, of the internal mass structure of E/S0 galaxies.
- Combine studies of the mass structure of E/S0 galaxies with studies of their scaling relations (e.g., Fundamental Plane), to disentangle their stellar-population and mass-assembly histories.
- Use lens galaxies as natural magnifying glasses to study the lensed blue emission-line galaxies with super-resolution. This includes morphology studies as well as resolved kinematics and star formation history/chemistry of faint spiral and irregular galaxies. Using NGAO + lensing, the effective diffraction limit in the source plane will typically be ~0.005". This means that galaxies at z=2 (angular distance 1.7Gpc) can be studied with the same detail as a galaxy in the Virgo cluster (17Mpc) in 0.5" seeing.
- Measuring time delays of AGN variability between multiply lensed sources in order to determine H_0 to high precision. If relative photometric precision of order a few percent can be achieved across the field, monitoring of variable lensed sources (such as AGN) can be used to determine cosmological parameters. Effectively, every time delay acts as a standard rod. For every system, angular size distances can be obtained with 10-15% and therefore there are real prospects of determining the Hubble Constant to 5% precision if a sample of a few dozen time-delays can be obtained. NGAO would be exceptionally good at this since one needs to do photometry of sources separated by less than 1 arc sec.

Lensing by clusters:
Some of the most interesting questions here include determination of cluster halo mass profiles, substructure, and shape, which can be compared with numerical simulations to further constrain models of large scale structure. In addition, clusters can be used as gravitational telescopes to identify the first galaxies/ quasars and to study their luminosity function to faint limits. With typical magnifications of order 20, searches for zJH dropouts can be extended three magnitudes deeper than is possible without gravitational telescopes. The primary goals of cluster-scale lensing studies can be summarized as follows:

- Detection of extremely high-z galaxies along critical magnification lines (see Figure 15).
- Spatially resolved kinematics, chemical composition, and star-formation rates of lensed background galaxies.
- Mass distribution within clusters from precise positions of multiple images and arcs.

Most clusters show strong lensing when imaged deeply enough at high spatial resolution. For example, in relatively shallow HST images (~1 orbit WFPC), Sand et al. (2005) found 104 giant arcs in 128 clusters. The NGAO system will have a similar performance, and thus a success rate close to 100% can be assumed, with a density of multiply imaged sources of a few per square arcminute. In extreme cases a density of 10 per square arcminute can be achieved (see Abell 1689 in Figure 16).

As is the case for galaxy size lenses, NGAO will not be competitive for finding cluster lenses, so the main mode of operation would be follow-up of known clusters. Current and future surveys (X-ray, red sequence) will find thousands of high redshift clusters. Targets will be abundant, and high resolution follow-up will be the domain of NGAO.

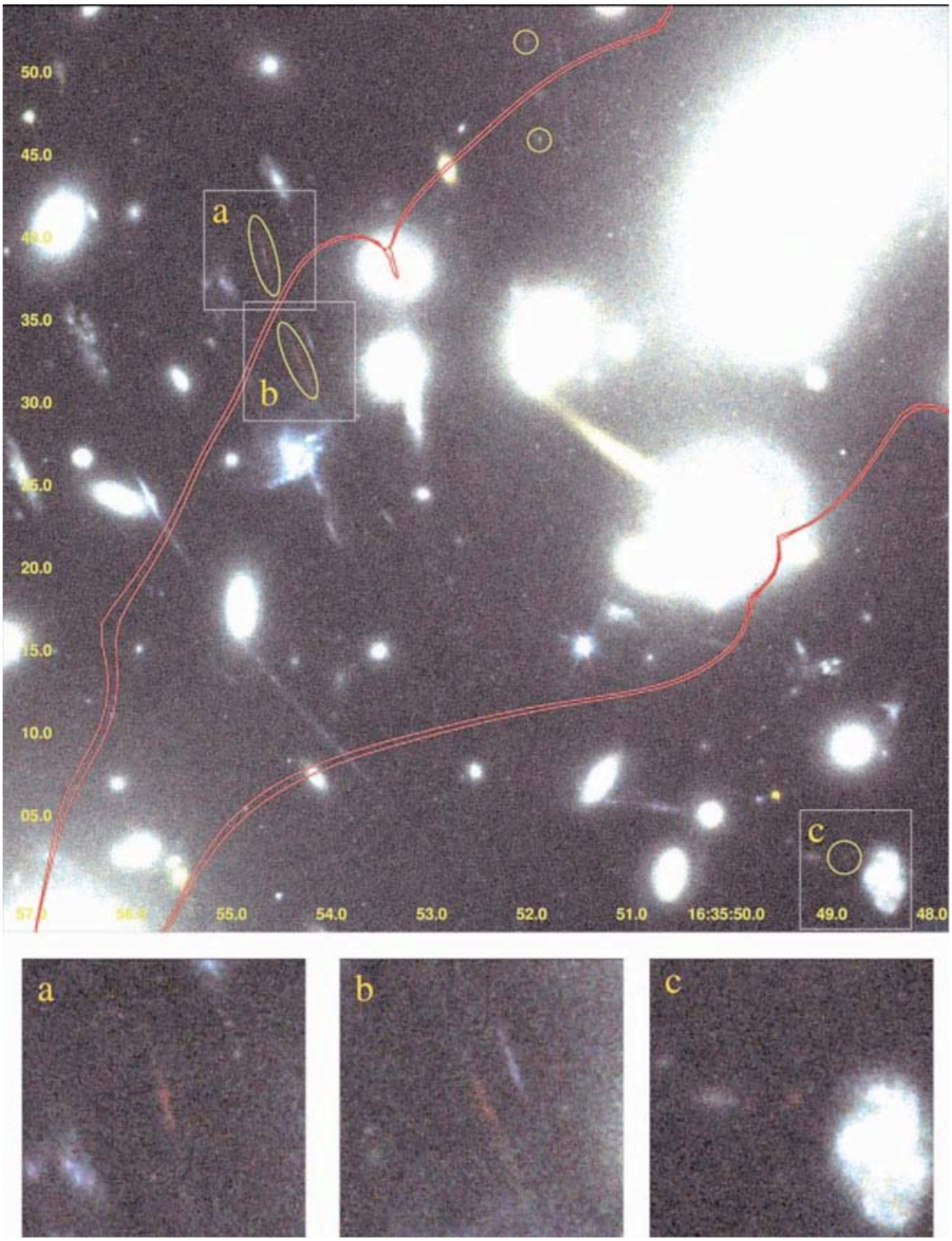

Figure 15. Pseudocolor image of highly magnified lensed sources in the Abell cluster 2218.
The red curves show the critical lines of infinite magnification for sources placed at z=5.576 and 7.0 (from Kneib et al. 2004). Images a, b, and c show a multiply imaged source at z~7. The unlabeled circles at the top of the image mark the multiply imaged source found by Ellis et al. (2001) at z=5.576.

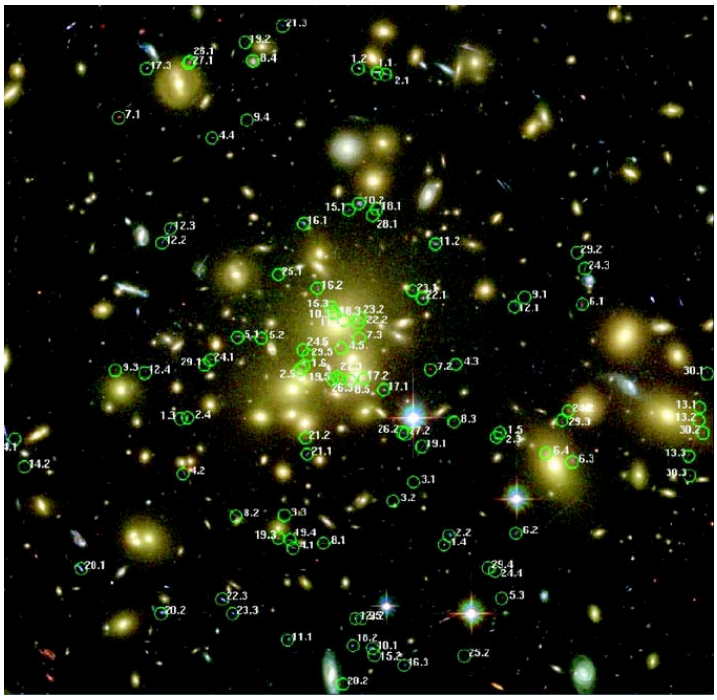

Figure 16. Searching for multiple images in cluster lensing.
At HST-like depth and resolution there are many multiple images of background sources for each massive cluster. The case of Abell 1689, an enormous cluster with an Einstein radius of 50" is shown (the image is approximately 3' on a side); 106 multiple images have been detected here (Broadhurst et al. 2005).

3.2.5 Comparison of NGAO with Current LGS AO and with HST-NICMOS

Figure 17 shows the lens system as observed with NICMOS (top row), NGAO with an upgraded version of NIRC2 (middle row), and the current Keck II LGS AO system with NIRC2 (bottom row). We simulate observations in the J, H and K band. For NICMOS in the J and H band (F110W and F160W) we used the NIC-1 camera because the pixel scale is very similar to that of NIRC2 (0.043" vs. 0.04"). In K band the closest configuration we could find for HST was NIC2 with the F222M filter. We show the results of this simulation even though it is not competitive, because Hubble has a high thermal background and was not optimized for observations in K band. For NGAO we used PSFs from simulations by Donald Gavel. We assumed the science instrument was an upgraded version of NIRC2 with half the background currently measured, assuming that this can be improved in the next generation AO system. For LGS AO, we assumed natural seeing of 0.5" and Strehl ratios of 0.15, 0.2 and 0.3 respectively for J, H, and K. The exposure time is 3600s in all cases. Each image is 4" on a side. Details of the simulations are given at the end of this Gravitational Lensing subsection.

From Figure 17 it is apparent that NGAO performs markedly better than both NICMOS and the current LGS AO system, as confirmed with real data in Marshall et al. (2007). At J and H bands NICMOS performs better than the current LGS AO system (largely due to lower background), whereas at K band LGS AO performs better than NICMOS. For NGAO the gain in resolution and collecting area more than offsets the extra background seen by NGAO with respect to NICMOS.

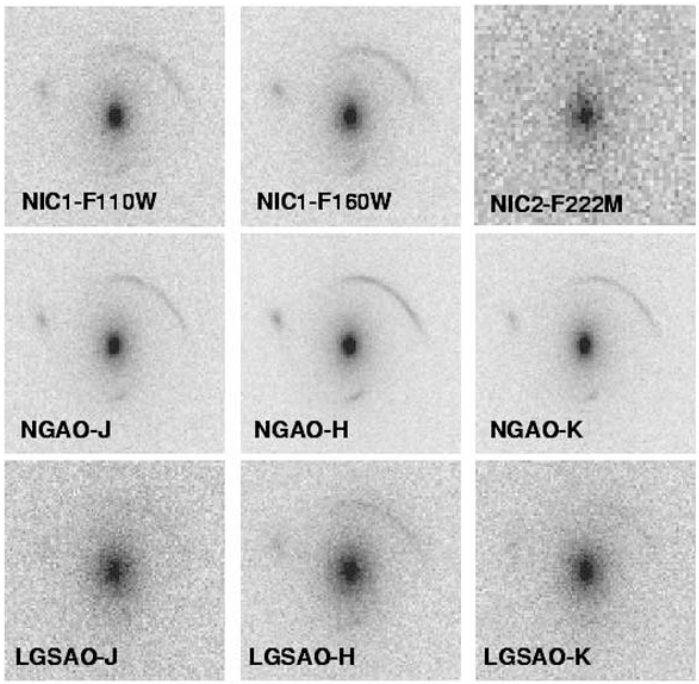

Figure 17. Simulated observations of a gravitational lens.
The simulations are for NGAO (middle row), HST-NICMOS (top row) and the current LGS AO system (bottom row). Each image is 4" on a side and the exposure time is 3600s. For NGAO we adopted the same detector properties as NIRC2 and half the background. The lens is an L* elliptical at z=0.8 and 250km/s velocity dispersion. The background source is a galaxy at z=7 with 0.05" half light radius, and J H K AB magnitudes of 25, 24.2, 24.4, as obtained for a few billion solar masses of a young stellar population (see text for details). Note that NGAO is superior in all cases.

Quantitative estimates of the uncertainties on the source parameters are shown in Figure 18 (68% and 95% contours). Those are obtained by measuring the likelihood in the full multidimensional space of lens and source parameters using a Markov Chain Monte Carlo sampler. The signal to noise ratio of the NIC2-F222M image was too faint to derive any useful constraints on the source properties. Similarly the signal to noise ratio of the Keck LGS AO-J band image was sufficiently low that the method failed to converge at the right minimum.

As is apparent from Figure 18, the proposed NGAO system strongly reduces the uncertainty in measurements of lensed galaxy size and mass. For example the derived uncertainty in size of the lensed galaxy at H band was a factor of four smaller with NGAO than with current LGS AO, and more than a factor of two smaller with NGAO than with NICMOS.

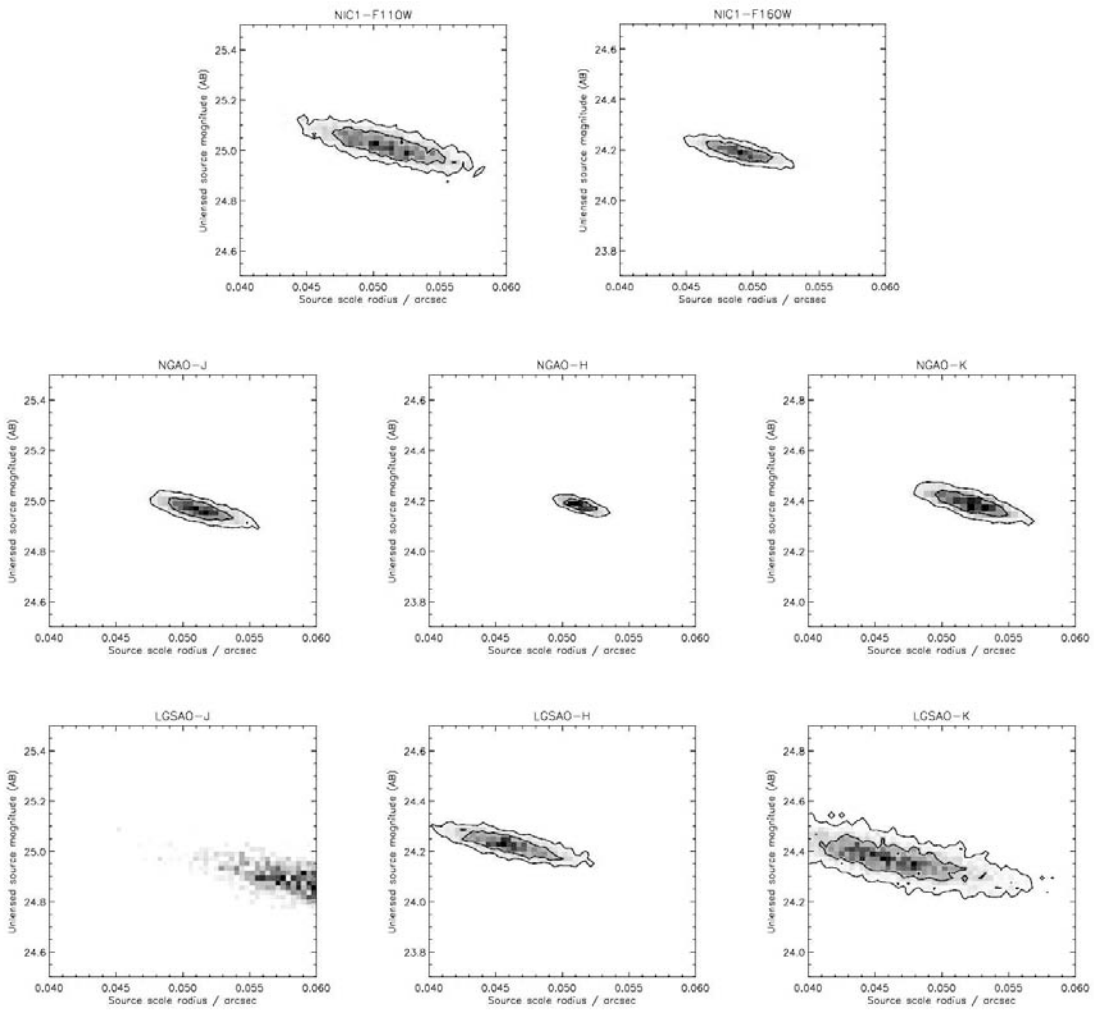

Figure 18. Reconstructed 68% and 95% confidence contours for the lensed source parameters, from a Markov Chain Monte Carlo algorithm.
The contours for NGAO are a factor of six smaller than for LGSAO and half the size of those for NICMOS. Note also that the half radius of 0.05 arcsec is clearly resolved and precisely measured. The SNR of the simulated data is too low for LGSAO-J and NIC2-F222M to obtain meaningful results.

Likewise the uncertainty on the velocity dispersion decreases by a factor of 6 going from LGS AO to NGAO, and by a factor of 2 going from NICMOS to NGAO in J and H bands. Formal statistical uncertainties of better than 0.1% on the velocity dispersion can be achieved with NGAO; this is a stunning achievement for any AO system.

Summarizing these results, for typical galaxy lensing cases the proposed NGAO system is expected to perform four to six times better than the current LGS AO system in its ability to correctly recover the key properties of the lensed galaxies.

3.2.6 Proposed observations and targets

3.2.6.1 Lensing by galaxies

Observations will focus on previously detected strong lenses from surveys such as the CFHT-Strong Lensing Legacy Survey (SL^2S), the Sloan Lens ACS (SLACS) survey, CLASS, and others. There are currently about 100 confirmed galaxy lenses in the SLACS survey and about 100 more from other surveys (e.g., SL2S, COSMOS). By the time these surveys are complete, and in time for NGAO science, many hundreds will be known. From these, a sample of >50 sources will be selected. As these are generally located in less dense stellar fields, this sample imposes a sky coverage requirement (see section 3.2.7.9).

High Strehl imaging will be used for determining geometry and hence the total mass of the lens. It will also be used for detecting substructure signatures in the dark matter halo, monitoring for time delays, and in studying the structure of the lens. Integral field spectroscopy will be essential to perform kinematic studies of the source, but also of the lens if shorter wavelengths (e.g., I, z-band) are available. If the Strehl is good at J, then absorption line kinematics can be used with the redshifted Ca triplet to obtain a velocity dispersion map of the lens. Together with the lensing geometry this will place very powerful constraints on the distribution of mass and light that will be unmatched by any other current or planned facility (e.g., Czoske et al. 2008).

3.2.6.2 Lensing by clusters

Galaxy clusters serve as excellent gravitational telescopes, providing extremely high magnification (10-50x) along critical lines, allowing one to study faint, extremely high-z ($z > 5$) galaxies (e.g., Ellis et al. 2001; Kneib et al. 2004; Santos et al. 2004; Stark et al. 2007). The best targets come from well-studied massive clusters, where the mass profile is already known well enough to predict where these critical lines will be. These include some of the Abell clusters. For kinematic studies of extremely high-z galaxies we ideally require I-, z- and J-band spectroscopy, where Ly α is redshifted into the observed bands for $z>5$ galaxies. For $2 < z < 5$ sources, [OII] can be observed in J- through K-band. Morphological information can best be obtained from imaging in J through K-bands where Strehl is at a maximum.

We assume that the target clusters, which can extend over several arc min, will first be imaged with other instruments, e.g. MOSFIRE at Keck or similar instruments elsewhere.

3.2.7 AO requirements

Spectroscopy: Wavelengths 0.8 – 2.4 μm
Imaging: Wavelengths 0.8 – 2.4 μm

3.2.7.1 Wavefront error

170 nm or better

3.2.7.2 Encircled energy

50 mas at J band for 30% sky coverage.

3.2.7.3 Contiguous field requirement

Imaging: A 1 arcmin contiguous field is useful for cluster lenses in order to reconstruct the mass profile of the cluster. An acceptable alternative is smaller fields of view (30") that can be combined to form a larger mosaic. During Preliminary Design phase, we will investigate several options for obtaining such contiguous field images, including the use of seeing-limited instruments, and GLAO or MCAO at other telescopes.

Spectroscopy: IFU configuration. It is desirable to line up IFUs linearly along a lens arc. Assume that the IFUs are rectangular in spatial format, and that they are placed along an arc with their long dimension parallel to the arc. Spacing between adjacent IFUs shall be no more than one IFU field of view in the longer dimension:

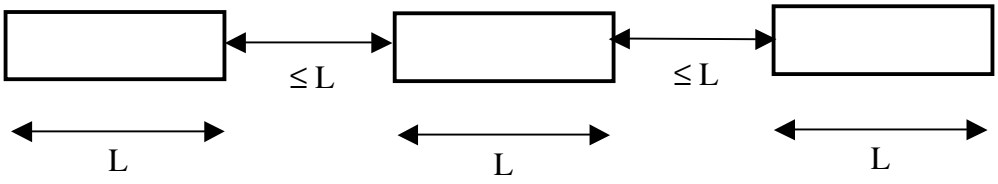

3.2.7.4 Photometric precision

Relative photometry to 0.1 mag. Absolute photometry to 0.3 mag.

3.2.7.5 Astrometric precision

Astrometric accuracy will be a consideration for the cosmography application. Requirements will be discussed in a future release of this document.

3.2.7.6 Polarimetry

N/A

3.2.7.7 Contrast

N/A

3.2.7.8 Backgrounds

Requirement: < 30% above unattenuated telescope + sky. Goal: < 20% above telescope + sky.

3.2.7.9 Sky coverage fraction

At least 30% sky coverage with encircled energy radius < 50 mas at J band.

3.2.8 Other key design features

3.2.8.1 Required observing modes

There are no special requirements for observing modes. This program could be carried out either in flexible queue-based scheduling, or classical mode.

3.2.8.2 Observing efficiency

Observations will typically be ~3 hr per source. If the field of view is large enough, we will dither on-target every ~10-15 minutes. Dithering and re-acquisition (if necessary) of the target should therefore not take longer than ~1 minute. If the field of view is too small to dither on-target, we may need to dither off-source (>5") to obtain sky background measurements. These will need to be performed every ~15 minutes, so the dither and re-acquisition should not exceed ~1 minute.

3.2.9 Instrument requirements

3.2.9.1 Required instruments

Primary: Near-IR IFU with R~5000 and field of view ~3"
Secondary: Near-IR imager with 30" field of view
Secondary: Visible imager (I and z bands)
Secondary: Visible IFU, R~5000 (I and z bands)

3.2.9.2 Field of view

Spectroscopy: For galaxy-scale lensing, with the lens at $0.5 < z < 1$ and the background galaxy at $1 < z < 2$, Einstein rings and arcs are 2-6" in diameter. Therefore, the minimum field of view would be 6" in diameter in order to fit an entire lens system in a single frame. For IFU fields of view smaller than this, one would use mosaicing to reconstruct the whole lens image. The nominal requirement of 3" was chosen because it would not require an excessive amount of mosaicing for most targets.

Imaging: For galaxies lensed by galaxies, require FOV at least 15" diameter. For galaxies lensed by clusters, imager should have a larger field of view (30") so that a minimum number of observations are required to mosaic the entire cluster lens system (~1-2 arcmin diameter). During Preliminary Design phase, we will investigate several options for obtaining these large contiguous field images, including the use of seeing-limited instruments, and GLAO or MCAO at other telescopes.

3.2.9.3 Field of regard

The field of regard for galaxy-galaxy lensing is determined by the availability of adequate tip-tilt guide stars. For group and cluster lenses, however, arcs will be spread out over a larger radius from the lensing center of mass. For groups, typical Einstein rings are 3-7" in radius, while for clusters, R_e~10-50". For a multiple IFU instrument, we therefore require at least a 50" radius field of regard, with IFUs able to be placed near the edge of this field in a ring configuration. Tip-tilt guide star selection will be trickier near the centers of massive galaxy clusters; therefore it is ideal to have a field of regard larger than 50" in order to obtain guide stars near the edge of the cluster. Field of regard for the imager is the same as for the (multiple) IFU instrument.

3.2.9.4 IFU multiplicity

For studies of galaxy-galaxy lensing, a single, high-resolution OSIRIS-like IFU is ideal. Multiple IFUs could also be used with one IFU head monitoring the PSF, one gathering sky

background information, etc. For cluster lensing, multiple IFU units could be used to obtain kinematic information of each sub-component along a lens arc.

3.2.9.5 Wavelength coverage

Spectroscopy: Wavelengths 0.8 – 2.4 μm
Imaging: Wavelengths 0.8 – 2.4 μm

Ideally, this project would use the shortest wavelength possible in order to obtain the best resolution for the background galaxy (or arcs). However, at redshifts $1 < z < 2$, Hα is visible at H and K-bands, and [O II] is visible at I through J-bands. Either of these lines can be used to obtain kinematical information of the background galaxy, while excluding the foreground lens. For extremely high-z, highly-magnified galaxies found in the cluster line-of-sight, shorter wavelengths are required (I and z-band), as Ly α, used for kinematic studies of actively star-forming galaxies, falls into these wavebands.

3.2.9.6 Spaxel size

Nominally 50 mas or less. Optimum sampling will be discussed in later releases of this document.

3.2.9.7 Spectral resolution

In order to accurately resolve the structure of distant lensed galaxies, we require a 20 km/sec Gaussian width (50 km/sec FWHM) for a background galaxy located between $1 < z < 2$. This implies a spectrograph with R~5000. Optimization of spectral resolution for the spectrograph will await the System Design study for the instrument.

3.2.10 Summary of requirements

The requirements for the *gravitational lensing science case* are summarized in the following four tables.

Requirements Table 8a. Imaging studies of distant galaxies lensed by galaxies
Goal: use imaging to screen potential lensed-galaxy targets for more detailed and lengthy spectroscopic study.

#	Science Performance Requirement	AO Derived Requirements	Instrument Requirements
8a.1	Sensitivity: SNR ≥ 3 per pixel (100 per source) for a z = 1 – 2 galaxy in an integration time ≤ 1/2 hour.	Background due to emissivity less than 30% of unattenuated (sky + telescope).	
8a.2	Target sample size of ≥ 200 galaxies, with density on the sky of 10 per	Overhead less than 10 min between targets.	10 per square degree implies that you will only be able to observe one target at a time –

#	Science Performance Requirement	AO Derived Requirements	Instrument Requirements
	square degree. Survey time ~ 3 years.		average of 1 in every ~19'x19' patch.
8a.3	Observing wavelengths = I through K (to 2.4 μm). Emphasis is on shorter wavelengths. Thermal part of K band less important.		
8a.4	Spatial resolution better than 50 mas at J band, for 30% sky coverage.	Need a good model of the PSF or a simultaneous image of a PSF star. Need a figure of merit for goodness of the PSF: how well the model fits the "real" PSF in two dimensions. Will quantify in future releases of this document.	Nyquist sampling of pixels at each wavelength.
8a.5	Field of view > 15" diameter for survey. Bigger is better. Some degradation between center and edge of field is tolerable. Will quantify in future releases of this document.		
8a.6	Relative photometry to ≤ 0.1 mag for observations during a single night		
8a.7	Absolute photometry ≤ 0.3 mag		
8a.8	Sky coverage at least 30% with enclosed energy radius within 0.07 arc sec at H or K.		
8a.9	Dithering and offset considerations: 1) Initially should be able to center a galaxy to ≤ 10% of science field of view. 2) Should know the relative position of the galaxy after a dither to ≤ 20% of pixel size.		

#	Science Performance Requirement	AO Derived Requirements	Instrument Requirements
8a.10	The following observing preparation tools are required: PSF simulation and exposure time calculator		
8a.11	The following data products are required: accurate distortion map (to 1% of the size of the galaxy, or 0.01 arc sec rms)		

Requirements Table 8b. Spectroscopic studies of distant galaxies lensed by galaxies

#	Science Performance Requirement	AO Derived Requirements	Instrument Requirements
8b.1	SNR ≥ 10 for a z = 1 – 2 galaxy in an integration time ≤ 3 hours for a Gaussian width 20 km/sec Gaussian width (50 km/sec FWHM) with a spatial resolution of 50 mas	Background due to emissivity less than 30% of unattenuated (sky + telescope).	R ~ 5000 (or whatever is needed to achieve 20 km/sec sigma on these targets)
8b.2	Target sample size of ≥ 50 galaxies, with density on the sky of 10 per square degree. Survey time ~ 3 years.	Number of IFUs: at least one, plus preferably one to monitor the PSF and one to monitor the sky. The extra two IFUs could be dispensed with if there were other ways to monitor the PSF and the sky background.	
8b.3	Observing wavelengths = J, H and K (to 2.4 μm) required, with emphasis on J band. Goal: also use z and I bands.		
8b.4	Spectral resolution: whatever is needed to get 20 km/sec radial velocity Gaussian sigma		
8b.5	Spatial resolution 50 mas at J band		

#	Science Performance Requirement	AO Derived Requirements	Instrument Requirements
8b.6	Velocity determined to ≤ 20 km/sec Gaussian sigma for spatial resolutions of 50 mas	Required level of PSF knowledge will be assessed in future releases of this document.	
8b.7	Field of view: Typical lens is 2 to 6 arc sec diameter. For IFU fields of view smaller than the lens size, one would use mosaicing. Desirable to take in blank sky in addition to the lens (if possible). Requirement: FOV ≥ 3" diameter. Goal: ≥ 4" diameter.		Requirement: IFU FOV ≥ 3" diameter. Goal: ≥ 4" diameter.
8b.8	Simultaneous sky background measurements		Preferably sky determination within the field of view of the IFU. Less preferably, through use of offsetting to sky or via a separate IFU looking at sky.
8b.9	Relative photometry to ≤ 0.1 mag for observations during a single night		
8b.10	Absolute photometry ≤ 0.3 mag		
8b.11	Sky coverage at least 30% with enclosed energy radius within 50 mas at J band.		
8b.12	Dithering and offset considerations: 1) Initially should be able to center a galaxy to ≤ 10% of science field of view. 2) Should know the relative position of the galaxy after a dither to ≤ 20% of spaxel size.		
8b.13	Target drift should be ≤ 10% of spaxel size in 1 hr		

#	Science Performance Requirement	AO Derived Requirements	Instrument Requirements
8b.14	The following observing preparation tools are required: PSF simulation and exposure time calculator		
8b.15	The following data products are required: calibrated spectral data cube		

Requirements Table 9a. Imaging studies of distant galaxies lensed by clusters

To be added in future releases of this document. Will be similar to Table 8a. Typical size of the highly magnified region of a galaxy cluster is 1 arc min. Will require low AO and instrument background: lens arcs from z ~ 7 are at most Vega magnitude 23 or 24 in H (brightest arcs). Typical size small (half light radii 0.1 arc sec). Astrometric accuracy will be a consideration for the cosmography application.

Requirements Table 9b. Spectroscopic studies of distant galaxies lensed by clusters

To be added in future releases of this document. Will be similar to Table 8b. There is a deployable IFU application here for closer galaxies with giant lensed arcs. The latter are several arc sec long, and the desired field of regard is about an arc min. There are usually 3 to 5 multiple arcs within a square arc min. But each might be long, requiring more than 1 IFU per arc. When this is taken into account, the optimum is ≤ 10 IFU units in a square arc min.

3.2.11 References

Broadhurst T. et al. 2005, ApJ, 621, 53

Czoske, O., Barnabe, M., Koopmans, L. V. E., Treu, T., & Bolton, A. S. 2008, MNRAS, 384, 987

Ellis, R. S., Santos, M. R., Kneib, J.-P., & Kuijken, K. 2001, ApJL, 560, L119

Fukugita, M., Hogan, C. J., & Peebles, P. J. E. 1998, ApJ, 503, 518

Kneib, J.-P., Ellis, R. S., Santos, M. R., & Richard, J. 2004, ApJ, 607, 697

Koopmans, L. V. E. 2005, MNRAS, 363, 1136

Marshall, P.J. et al. 2007, ApJ, 671, 1196

Sand, D.J., Treu T., Ellis R.S., & Smith G.P. 2005, ApJ, 627, 32

Santos, M. R., Ellis, R. S., Kneib, J.-P., Richard, J., & Kuijken, K. 2004, ApJ, 606, 683

Stark, D. P., Ellis, R. S., Richard, J., Kneib, J.-P., Smith, G. P., & Santos, M. R. 2007, ApJ, 663, 10

3.3 Astrometry Science

Authors: E. McGrath, C. Max
Contributors: B. Cameron

In this section we discuss important science issues that can be addressed with astrometry using NGAO (with the proviso that astrometry at the Galactic Center has already been treated elsewhere, see §2.3). Astrometry Science will be analyzed in more detail in future versions of the Science Case Requirements Document, to be released during the Preliminary Design phase. A full Table of Astrometric Science Requirements for input into the System Requirements Document will also be developed during PDR phase.

3.3.1 Introduction

Adaptive optics is a powerful tool for accurate astrometry. AO increases the precision of positional measurements by shrinking the point-spread function (PSF) and boosting the signal-to-noise ratio. These enhancements open up new phase space for discovery. The possible astrometric applications span a wide range of Galactic and extragalactic environments, including detection of unseen binary companions via astrometry, the study of crowded stellar fields near the black hole in the Galactic Center (see §2.3), internal and global kinematics in globular clusters, proper motion studies of nearby neutron stars and black hole binaries, the search for intermediate mass black holes in globular clusters, counterparts of transients in the Galactic Plane and in nearby galaxies, characterizing the progenitors of bright supernovae, and understanding the host galaxies of gamma ray bursts in the most distant galaxies.

3.3.2 Scientific Goals

3.3.2.1 Proper Motion Studies of Nearby Compact Objects

The space velocities of compact objects (e.g. pulsars, magnetars, and black hole or neutron star binaries) can directly inform us of about origins and constrain their lifetimes. At birth, neutron stars are imparted a "kick" from the initial supernova explosion. Measuring their current proper motion allows one to extrapolate back to their formation site, to characterize that site, and thereby potentially to derive an age for the compact object, given the distance traveled since its initial "kick". Furthermore, by pinning down their birth places, one can determine what the likely progenitor star's initial mass and composition may have been, by comparison with other stars in the same environment. Distances can sometimes be determined through parallax measurements, but one needs a thorough understanding of the proper motion before such studies can be undertaken (e.g., Walter & Lattimer 2002). Once the distances to these compact objects are known, we can calculate their radii (in the case of neutron stars, at least) from the black-body spectrum and the distance, and hence calibrate their energy output.

These questions are particularly interesting for magnetars: neutron stars with extremely high magnetic fields (of order 10^{15} gauss) that are thought to be possible engines for Gamma Ray Bursts, and are potential cosmic-ray accelerators. While magnetars rarely appear as radio objects, they are observable as gamma ray transients (soft gamma ray repeaters), X-ray

pulsars (anomalous X-ray pulsars), and, most relevant here, as infrared sources. They presumably emit in the optical and UV as well, but cannot be seen because of strong extinction. Magnetars are believed to be only a few x 10^4 yrs old and are some of the most exotic objects in our Galaxy. In particular, it is of interest to determine how these magnetars relate to standard pulsating neutron stars, as they occupy different areas of the so-called P – P dot diagram (Figure 19). By studying their proper motions one can address formation scenarios that predict different physical processes contributing to the initial velocity "kick". These include asymmetric hydrodynamics, magnetic-neutrino processes, and or electromagnetic rocket effect (e.g., Duncan & Thompson 1992). If magnetars are found to have higher space velocities than standard neutron stars, then more than one of these processes may be important. This information can then, in turn, help determine whether there is an evolutionary sequence between the various types of neutron stars, or whether their differences are purely due to their formation mechanism or some other intrinsic process.

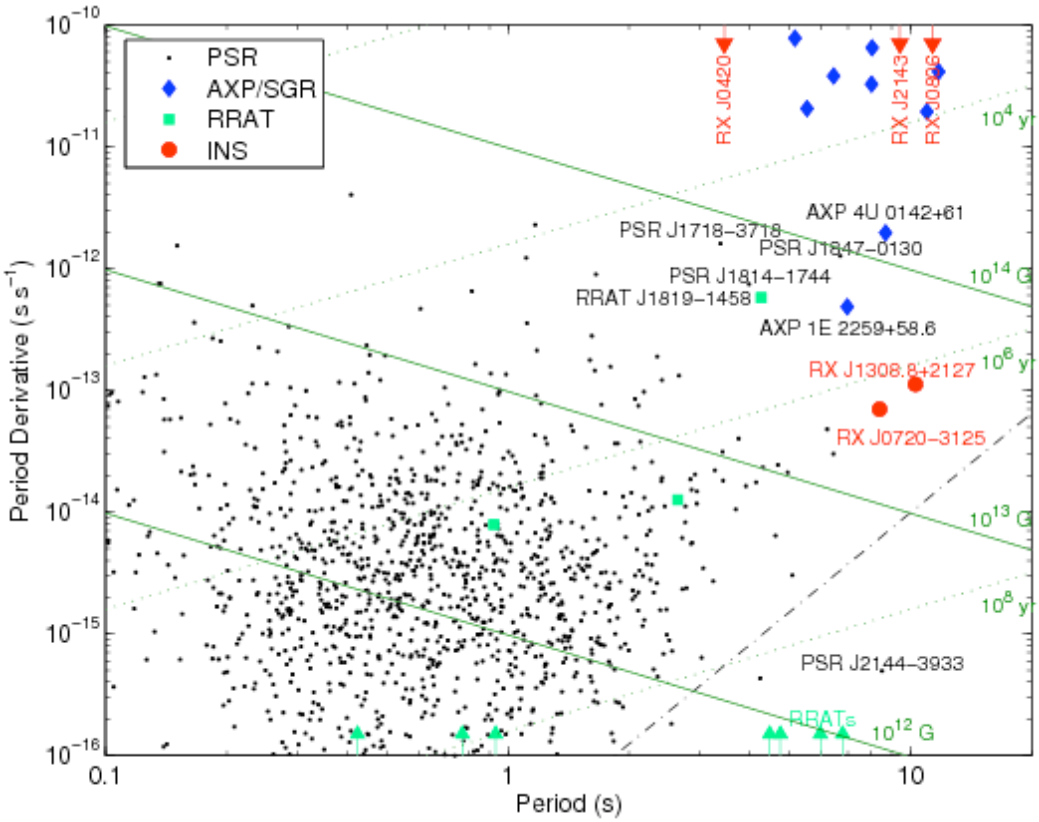

Figure 19. Diversity of Neutron Stars, from the period-period derivative diagram.
Magnetars (blue diamonds) occupy a unique region of this diagram. It is of interest to determine their relationship to standard pulsars with shorter pulsation periods P and faster spindown rates $\dot{P}$. Key for object labels: PSR are standard pulsars, AXP/ SGR are Anomalous X-ray Pulsars and Soft g-ray Repeaters, RRATs are Rotating Radio Transients, and INS are isolated neutron stars. (Courtesy D. Kaplan)

In addition to pulsars, X-ray and black hole binaries are of strong interest for proper motion studies. Most of these are observed to be within the plane of our Galaxy, but a few appear to be located much farther away (e.g., XTE J1118+480; Mirabel et al. 2001). The origin of these

out-of-plane black hole binaries could be either a population of massive stars formed early in the evolution of our Galaxy that follow orbits similar to the globular clusters in the Galactic halo, or a younger population of stars within the disk that were subsequently ejected from the plane via a "kick" during the supernova explosion that formed them. Precise proper motions for such objects would help distinguish between these options. If one can infer a birth location, one can then derive a limit on the age of the black hole and the mass of the progenitor star.

In order to determine the proper motion of an object from one observing epoch to the next, accurate relative astrometry is needed. This requires a set of reference stars that are present in all observations, as well as an accurate method to align the reference frames. Given a field size of between 10" and 30", an adequate number of reference stars (between 5 and 100) should be available, especially in regions near the Galactic plane. The Galactic plane is particularly well suited to NGAO, since future astrometric missions such as SIM and GAIA, which operate exclusively in the optical regime, will not be optimized to observe distant Galactic objects due to the high values of dust extinction and confusion. Magnetars are typically heavily extincted, with A_V~3-30 mag, and have near-infrared magnitudes of K' ~ 19.5 - 22 mag. Hence, NGAO can provide a crucial niche for learning more about these strange objects.

3.3.2.2 Faint Binary Companions

There are several useful applications of astrometry in stellar companion studies. We differentiate among these by the following three primary goals:

- Confirming the orbital association of two or more nearby objects and ruling out field stars with chance alignments by projection effects
- Orbit determination for resolved binaries
- Orbit determination for unresolved (unseen) binaries

In the first case, high levels of astrometric precision are not necessary. In general a few mas accuracy is more than sufficient, and should be readily achievable with NGAO even in sparse fields with few reference stars. For example in isolated stellar systems, Chauvin et al. (2005) were able to obtain an astrometric accuracy of ~15 mas on the VLT with NGS AO plus a Lyot coronagraphic camera. This was enough to confirm or deny associations between the primary star and potential faint brown dwarf companions based on the change in their angular separations over time, by comparing them with the known proper motion of the primary (Figure 20).

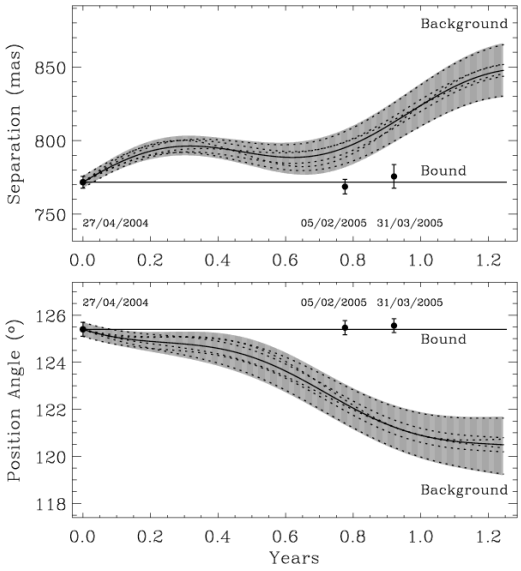

Figure 20. Offset positions of planetary companion to 2MASSW J1207334-393254.
The expected variation of offset positions, if the "companion" is a background object, is shown (*solid line*) with errors *(shaded region)*.

Orbit determination for resolved binaries is discussed in the context of Extrasolar Planets in section 2.4 and for Minor Planets in our Solar System in section 2.5, to which we refer the reader for further details.

Orbit determination in cases where one cannot directly observe the companion is by far the most challenging regime for astrometry science in sparse fields. Radial velocity studies of nearby stars have been very efficient at finding unresolved planetary companion candidates. To date, 225 candidate planetary systems have been found in this manner (see e.g., www.exoplanet.eu). However because the orbital inclination is unknown, radial velocity studies can only place lower limits on the mass of the companion. It is necessary to follow up on these radial velocity measurements by other means in order to confirm the mass of the companion object. For extremely close companions, even with high-resolution, direct imaging is not possible. Instead, the aim here is to measure the wobble of the primary star in the two tangential dimensions, yielding the orbital inclination, and hence the true mass of the companion.

Relative astrometric accuracy as good as ~50 μas has been demonstrated to be achievable at the VLT with AO, in measuring the separation of a bright visual binary (HD 19063; Neuhäuser et al. 2007) to try and detect a planet around one of the parent stars. This level of precision is sufficient to detect the astrometric wobble due to a planetary companion, which would manifest itself as a periodic change in the separation of the binary stars. While we expect this science case to be particularly challenging for NGAO, it may be possible in a few select fields where there are many reference stars and we can keep the systematic errors under control.

3.3.2.3 Astrometry and Globular Clusters

It has been clear for more than a decade that globular clusters do not consist merely of passively evolving old stars. The complexity of their stellar populations, kinematics, and chemical abundances has shown that globular clusters can yield clues to the merger and star formation history of galaxies, and in turn that they suffer tidal disruption from the galaxies around which they live. For the decade or more to come, key questions will involve the relation of globular cluster evolution to galaxy formation, understanding the relative ages of globular clusters, tracking their formation environment, and understanding if clusters and their galaxies are connected by a common star formation and chemical enrichment history.

Much can be learned about Galactic globular clusters with the help of the high astrometric accuracy that will be obtainable with Keck NGAO, of order 0.1 mas or even better. Both the internal kinematics and the motion of Galactic globular clusters as a whole are already measurable via astrometry with accuracy of ~ 1 mas/yr. For example WFPC2 on HST was used quite successfully with mas accuracies to measure the rotation of 47 Tuc on the sky (Anderson and King 2003). Recently ACS has been used with 0.04 mas/yr accuracies against background galaxies to measure the space motion of NGC 6397 (Kalirai et el. 2007), where it was found that this globular cluster must have made frequent passages through the Milky Way's disk.

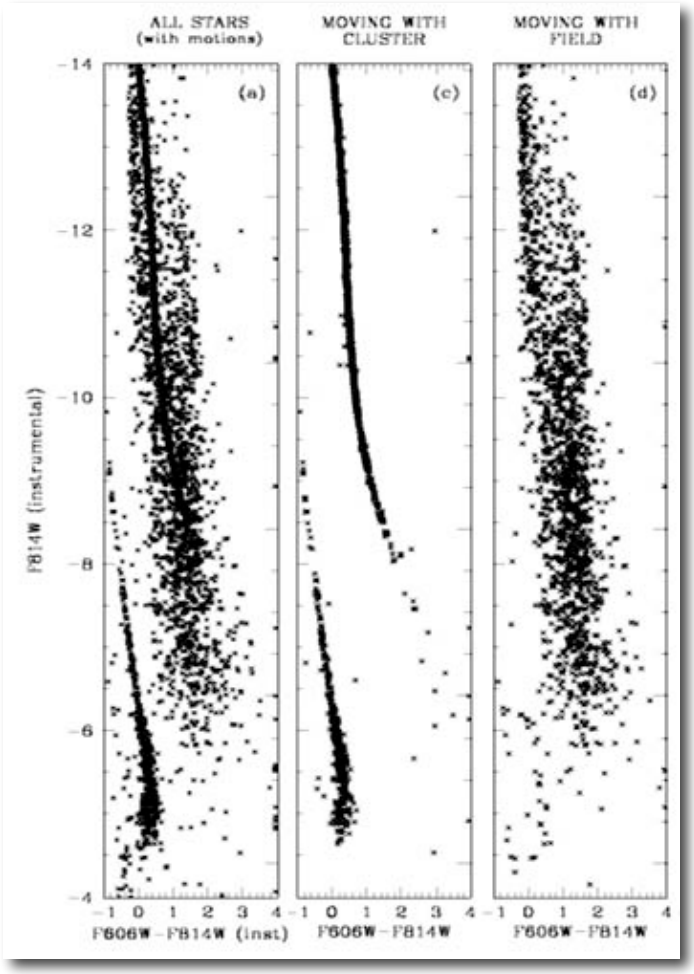

Astrophysical issues that will be addressed by NGAO astrometry include:

1) Ruling out field stars in order to determine cluster membership (e.g. Anderson et al. 2008). Once field stars have been eliminated, one can obtain highly superior color-magnitude diagrams to determine stellar populations, their ages, and their chemical abundances. Figure 21 shows a particularly successful example of this process.

Figure 21. Color magnitude diagrams for stars in or near the Galactic globular cluster NGC 6297

(From Anderson et al. 2008) When proper motions were used to eliminate foreground and background field stars, the diagnostic quality of the color magnitude diagram (center) increased dramatically: a very narrow main sequence and white dwarf cooling sequence were clearly seen.

2) Measuring stellar orbits (Mackey and Gilmore 2004) and overall anisotropies internal to the cluster (Drukier et al. 2003);

3) Determining the space motion of clusters as a whole (e.g. Kalirai et el. 2007 and many others), to decode the dynamics of the major events in which they formed;

4) Correlating kinematics within the cluster with other observed parameters such as the complex chemical abundance patterns within ω Cen (Gnedin et al. 2002), to further understand the processes that have influenced cluster evolution.

5) Finally and most speculatively, NGAO may have a role to play in the search for intermediate-mass black holes in globular clusters, by using spatially resolved integral field spectroscopy to measure the kinematic effects of the black hole on surrounding stars.

Measuring stellar kinematics within globular clusters shares many similarities with studying stellar kinematics at the Galactic Center: the fields are very crowded, but doing repeated measurements for many hundreds of stars at a time allows a joint astrometric solution that is more accurate than it would have been, had fewer stars been present. The globular cluster environment has the added advantage that small background galaxies or QSOs can often be used to establish a local reference frame. The smaller point spread functions and added Strehl stability of NGAO will result in astrometric measurements within clusters that are considerably better than those achieved with Keck and VLT AO to date.

3.3.2.4 Follow-up of Transient Events

In coming decades, synoptic survey telescopes such as PanStarrs and LSST will discover many new and (hopefully) important classes of transient events. NGAO has several roles to play in this new and very rapidly developing field:

1) Discover, characterize, and understand supernova progenitors. Gal-Yam et al. (2007) used Keck laser guide star AO in conjunction with other observations to identify the progenitor of Supernova 2005gl, a Type IIn supernova in a nearby (d=66 Mpc) galaxy. In his discovery paper, Gal-Yam also outlined an ambitious and exciting program to show the relationship once and for all between the "zoo" of different types of supernovae and the varied group of star types that have been proposed as supernova progenitors. The ambitious scope of this endeavor is nicely illustrated in Figure 22. Adaptive optics in general, and NGAO in particular, has a key role to play in this effort.

2) Follow-up of transient events in or near the Galactic Plane. As the new synoptic survey telescopes discover transient events near the plane of the Galaxy, NGAO and its infrared imaging capability will be ideally suited to identifying the sources responsible for this transient emission. NGAO will be able to beat down the effects of crowding and confusion better than any other facility. Its infrared wavelengths will penetrate through the dust in the plane. Once potential counterparts have been identified, NGAO's integral field spectrograph(s) will enable it to measure their radial velocities and spectral characteristics. If the events occur close enough to the Solar System, NGAO will be able to measure proper motions of the counterparts as well.

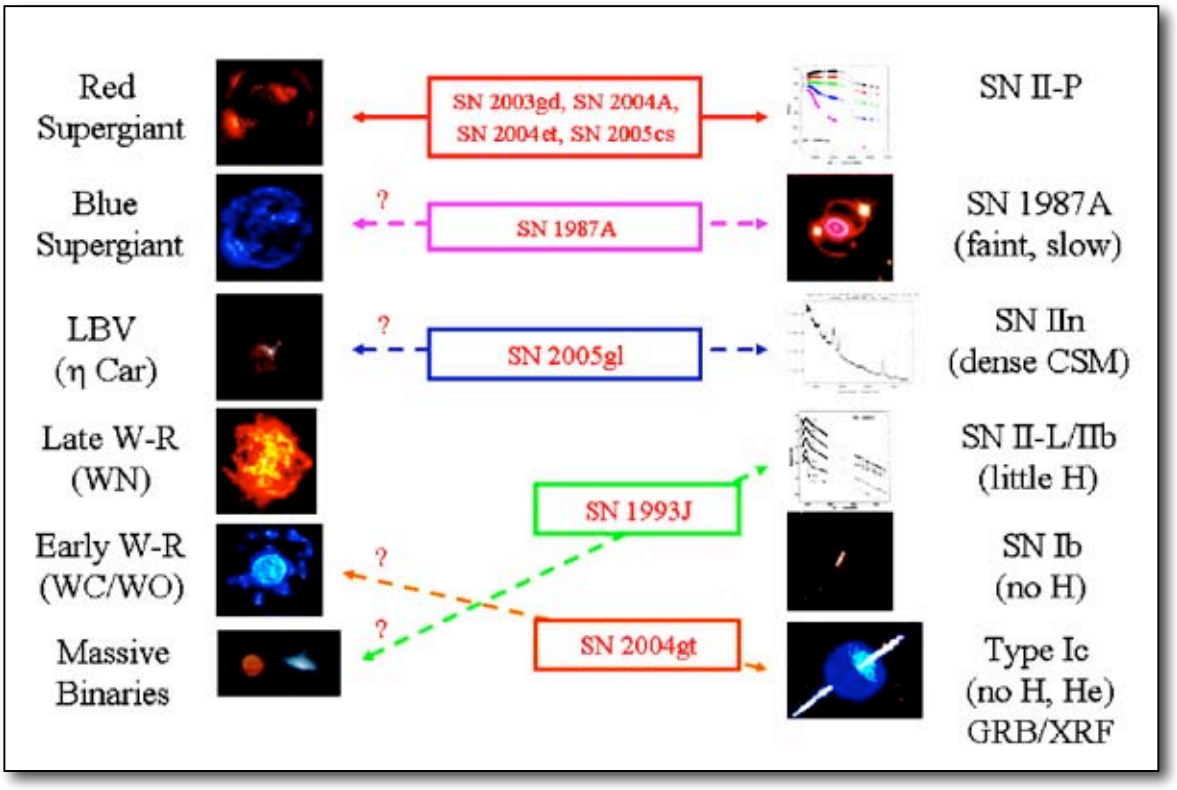

Figure 22. The "Progenitor-Supernova Map" of Avishai Gal-Yam
(From Gal-Yam et al. 2007) This graphic was designed to motivate a comprehensive program to identify the progenitor stars of all the varied supernova types. NGAO will be well positioned to make key contributions to this effort.

3) Characterizing the host galaxies of gamma-ray bursters. Although the optical flashes are very short and the afterglows of gamma-ray bursts fade over a period of weeks and months, NGAO can be used to characterize the host galaxies of gamma-ray bursters. Information can be obtained on galaxy morphology (disk, bulge, etc.) and the ages and metal abundances of stars in the galaxy (from stellar population synthesis). This is particularly important for the "short hard" gamma-ray bursts, for which little is known about their origins and environment.

3.3.3 Anticipated Astrometric Accuracy

One can estimate the precision of a single epoch of data by computing the distance from a target star to each of the reference stars (the 'grid') in our image. If data are limited by random errors, the Allan deviation (the square root of the variance after averaging over various timescales) of each of these series of differences should decrease as $1/\sqrt{t}$ (Figure 23). If the Allan deviation ceases to decrease fashion then the data are limited by systematics.

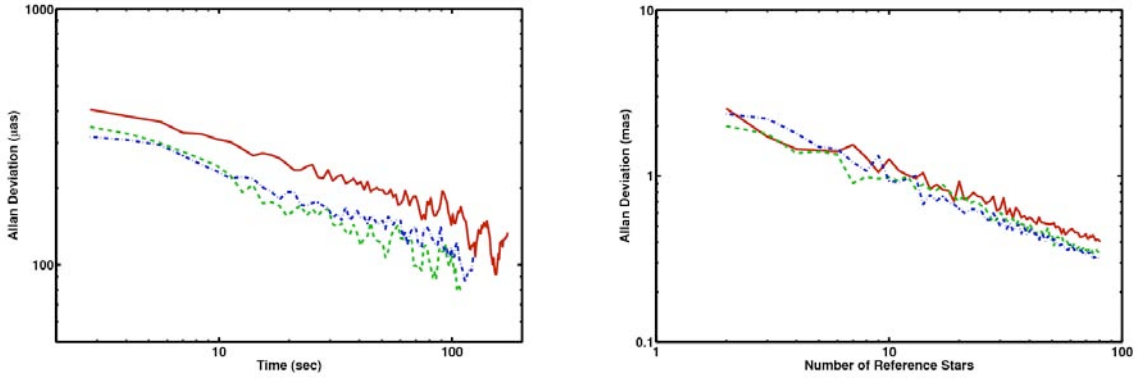

Figure 23. Astrometric Accuracy for Bright Targets

These data are from an NGS AO run at Palomar Observatory. In only 3 minutes of observing time, we can achieve an astrometric accuracy of 100 mas. (Courtesy B. Cameron)

As Figure 23 shows, for bright targets one can reach an astrometric accuracy of 100 μas in 3 minutes of integration time with current NGS AO at Palomar. Furthermore, using the time-averaging technique, one can achieve <100 μas accuracy over a series of observations spread out over 2 months or longer (Figure 24), even on fainter targets (K_s>14 mag, Figure 25). This is encouraging for NGAO as we push to both fainter targets, and to higher astrometric precision on bright targets (e.g., for extra-solar planet detection). In fact, there appears to be no systematic difference between achievable astrometric accuracy with either NGS or LGS AO, as the limiting source of error in a single conjugate system is the differential atmospheric tilt. We can therefore expect even better performance with NGAO as this source of error is diminished.

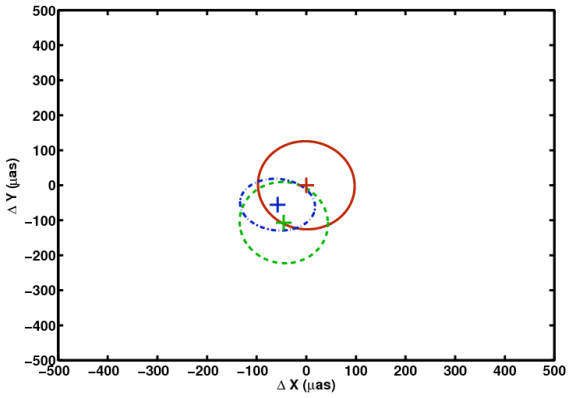

Figure 24. Astrometric precision over a 2 month time-span.

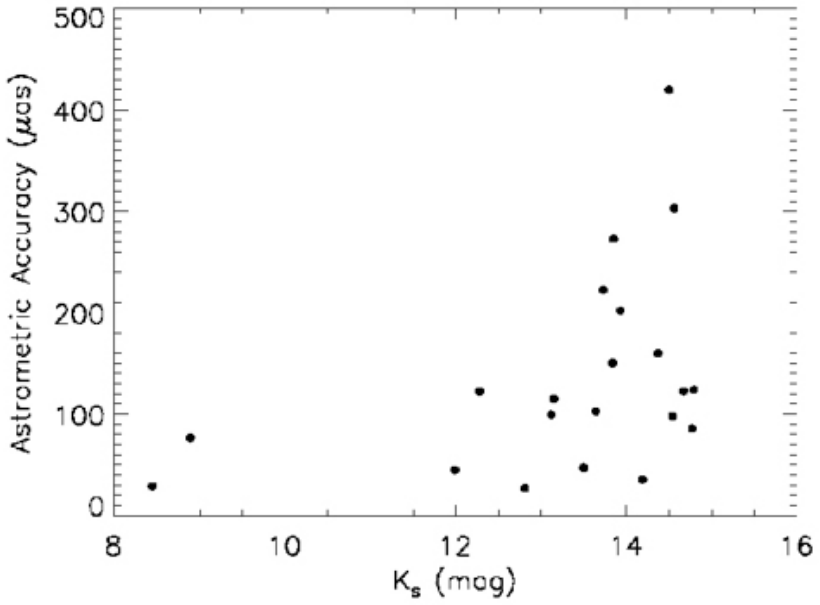

Figure 25. Astrometric accuracy as a function of target brightness.

Requirements Table 10. Astrometry Science Derived Requirements

Table will be added in later releases of this document during PDR phase.

3.3.4 References

Anderson, J. and King, I. R. 2003, AJ, 126, 772

Chauvin, G., et al. 2005, A&A, 438, L25

Drukier et al. 2003, AJ, 125, 2259

Duncan, R. C. & Thompson, C. 1992, ApJL, 392, L9

Gal-Yam, A. et al. 2007, ApJ, 656, 372

Gnedin, O. Y. et al. 2002, ApJ, 568, L23

Kalirai, J. S. et al. 2007, ApJ,657, L93

Mackey and Gilmore 2004

Mirabel, I. F., Dhawan, V., Mignani, R. P., Rodrigues, I., & Guglielmetti, F. 2001, Nature, 413, 139

Neuhäuser, R., Seifahrt, A., Röll, T., Bedalov, A., & Mugrauer, M. 2007, in Proc. of IAU Symposium #240. Eds. W.I. Hartkopf, E.F. Guinan and P. Harmanec. Cambridge: Cambridge University Press, 2007. 261-263

Walter, F. M. & Lattimer, J. M. 2002, ApJL, 576, L145

3.4 Resolved Stellar Populations in Crowded Fields

Author: Claire Max
Contributors: Knut Olsen, Jason Melbourne

3.4.1 Background

The over-riding goal of resolved stellar population studies is to reconstruct the star-forming history of the galaxy by comparing their color-magnitude diagrams with those predicted by stellar evolution codes for stars of varying ages and chemical compositions. The amount of information coming out of such an analysis is strongly increased when the photometric accuracy is high, and when good photometry can be done on fainter and fainter stars. With the help of the Hubble Space Telescope, much progress has been made in reconstructing the stellar population content of Galactic globular clusters and of other galaxies in the Local Group. High-performance AO systems on 8-10 meter telescopes can, in principle, allow yet fainter stars to be measured in the infrared, particularly for stars above the main sequence turn-off, and can allow CMDs to be constructed for regions closer to the most dense regions (e.g. closer to the cores of globular clusters, or in the bulge of M31).

In this section we consider science cases involving photometry of individual stars, in fields such as Local-Group galaxies or Galactic globular clusters for which stellar crowding is the limiting factor in determining the stellar population. We give an overview based on preliminary discussions of the scientific opportunities, as well as a qualitative discussion of the relative strengths and weaknesses of NGAO's Multi-Object AO (MOAO) architecture compared with the Multi-Conjugate AO (MCAO) system being built for Gemini South. The resolved stellar populations Science Driver will be analyzed in more detail in upcoming releases of the Science Case Requirements Document. During the Preliminary Design phase, specific scientific objectives will be selected and the system requirements derived from these objectives will be documented.

3.4.2 Technical Role of NGAO in Resolved Stellar Populations Research

3.4.2.1 General Advantages of AO

Adaptive optics has several technical advantages over seeing-limited images in crowded fields:

1) AO's smaller point spread function reduces the overlap of stars, decreasing the so-called "confusion" caused when an unseen faint star overlaps with a very close brighter star. Crowding introduces photometric error through luminosity fluctuations within a *single* resolution element, due to the unresolved stellar sources in that element.

2) As a result of lower confusion, photometric characterization of all the stars will be more accurate (Olsen Blum & Rigaut 2003).

3) When the Strehl ratio is higher, fluctuations in the photometry are less severe, contributing another factor to improved photometric accuracy.

4) Once the confusion is reduced, fainter stars are revealed for the first time. This can be clearly seen in the two images of the dense star cluster in the Galactic Center shown in Figure 26. Since faint stars are typically less massive than bright ones, the result is that AO allows stellar populations to be measured down to lower masses. Current near-infrared AO systems on 8-10 m telescopes can achieve within two magnitudes of the old turnoff in the outer disk of M31, where the surface brightness is K~19 mags / arcsec^2, and in low surface brightness regions of dwarf satellite galaxies. (K. Olsen, private communication).

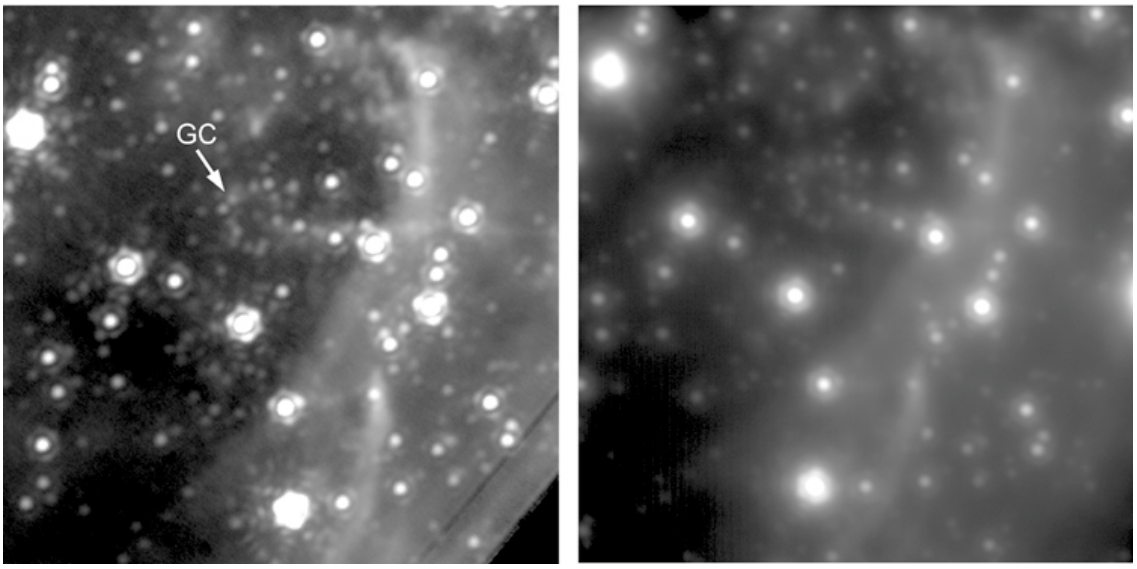

Figure 26. AO observations of stars at the Galactic Center.
Left: Individual stars at the Galactic Center seen with Keck laser guide star AO, in K' band. Right: The same region seen with Keck natural guide star AO. "GC" in the left image shows the position of the black hole, SgrA*. While both NGS and LGS AO allow far more magnitudes and colors to be measured than in seeing-limited images, use of the laser (and in the future use of NGAO's infrared tip-tilt sensing) reveals far more faint stars and improves photometric accuracy in crowded fields. From Ghez et al. (2005).

For stellar population analysis, a goal is to obtain enough individual magnitude and color measurements that there are good statistics in short-lived phases of stellar evolution such as the "red clump" of intermediate-age He-burning stars, or the tip of the red giant branch, or the "AGB bump" in the luminosity function, because many of these regions contain important diagnostic information about stellar population properties.

3.4.2.2 Comparison of Multi-Conjugate and Multi-Object AO, for Stellar Population Studies

Next we consider the strengths and weaknesses of using multi-conjugate AO (MCAO) or multi-object AO (MOAO) for resolved stellar population studies. As the reader will soon see, each has several potential advantages and disadvantages. Further analysis is needed in order to make these comparisons quantitative, and to apply them to the resolved stellar populations science cases.

Field of view: MCAO should provide a more uniform point spread function (PSF) over a considerably wider field than MOAO. (This comes at the cost of somewhat lower peak Strehl ratio.) MCAO's wider field of view should help accumulate the statistics needed to fill in key regions of the color-magnitude diagram, by including the stars in a larger area on the sky. MOAO would have to use multiple small-field-of-view units to increase its area coverage, and even so is unlikely to achieve as much total field area as MCAO.

Knowledge and stability of the point spread function: Good knowledge of the PSF is key to obtaining accurate photometry. It is not yet clear whether MCAO or MOAO will produce better knowledge of the point spread function during a specific exposure. The more uniform PSF of MCAO systems could allow more accurate photometry, provided that the PSF is known sufficiently well as a function of time and as a function of position on the sky. Techniques have been proposed for determining the time variation of the PSF using atmospheric measurements and AO telemetry, but these have not yet been tested with laser guide stars and they need much work to make them function with MCAO or MOAO systems. Methods of determining the PSF self-consistently as a function of position in a crowded field from the *image itself* are being developed and tested now; these would benefit both MCAO and MOAO. Further, it is known that PSF stability improves at higher Strehl ratios. To the extent that MOAO provides higher Strehl than MCAO, the MOAO PSF should be more stable.

Lower confusion and the ability to measure fainter stars: Because the Strehl ratio is predicted to be higher in MOAO systems, these should have improved sensitivity and contrast between the PSF core and the broad wings, which improves photometric accuracy and allows measurements to be made in more crowded fields. In addition, MOAO's higher Strehl ratio should enhance the ability to perform photometry on fainter stars. Thus *within* MOAO's smaller field of view, it should obtain superior dynamic range to that of MCAO. It becomes a quantitative issue whether this improved dynamic range allows MOAO to make up for its smaller area relative to MCAO, for producing stellar population science.

Preliminary conclusions: Although we have not constructed a quantitative comparison between MCAO and MOAO that takes into account all of these effects, it is likely that the wider area accessible to MCAO systems will be a distinct advantage for specific stellar populations studies. However within the broad scope of "resolved stellar populations" there are also science cases for which MOAO is well suited. These include studies of stellar populations in more dense regions such as those close to globular cluster cores or the bulge of M31. It is for these reasons that the resolved stellar populations science case was classified as a "Science Driver" rather than a "Key Science Driver," as it was just about the only application for which the large field of view of MCAO would have been a clear advantage. During PDR phase, our analysis will focus on identifying and understanding those applications for which the NGAO system and MOAO can bring about distinct and unique scientific advances in the field of resolved stellar populations.

3.4.3 Specific NGAO Science Cases

Detailed studies done for the GSMT Science Working Group (2003) and for Gemini South MCAO (2001) suggest that the Keck NGAO system should make significant contributions to the study of resolved stellar populations in the following extragalactic contexts:

- The nearest dwarf galaxies (at tens of kpc distance)
- M31, the nearest large spiral galaxy (at 850 kpc, where 1 pc = 0.3")
- The M81 - M82 group (1 pc = 0.06")
- Perhaps in some dwarf galaxies and large spiral galaxies (e.g. the Sculptor Group) at distances of 2 – 3+ Mpc (1 pc = 0.11")

Within our own Galaxy, NGAO should be able to probe the stellar mass function in star clusters, including both open clusters (sites of current star-formation) and old globular clusters. For this work, astrometric measurements of proper motions are needed in some cases, in order to determine cluster membership and exclude field stars. In more general terms, NGAO should be able to explore the global mass distribution of stars in relatively dense environments of our Milky Way Galaxy.

Here we give two brief examples of extragalactic results that can be expected from NGAO.

3.4.3.1 Local Group Dwarf Galaxies: Keck LGS Data on KKH 98

KKH 98 is a Local Group dwarf irregular galaxy (). Recently the CfAO Treasury Survey group (Melbourne and Delcanton, 2008) obtained Keck laser guide star AO images (45 min) of this KKH 98 at K', with the goal of studying the age and composition of its stellar population by using Keck data in the infrared coupled with Hubble ACS data at visible wavelengths. Figure 28 shows that the I-K versus K CMD has significantly less scatter than a CMD constructed from Hubble B-I colors, due to the fact that I and K bands are less vulnerable to dust extinction.

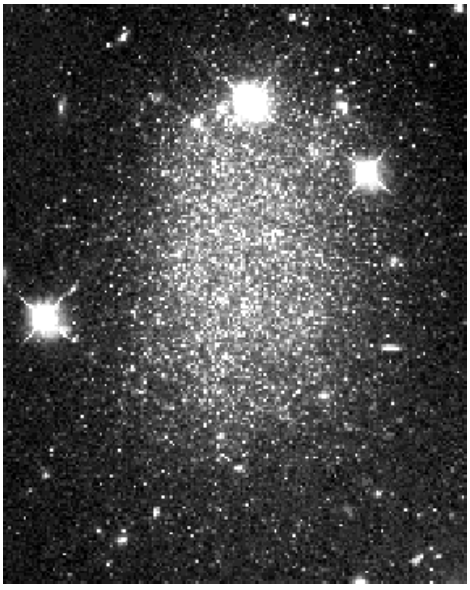

Figure 27 Hubble Space Telescope ACS preview image of the Local Group dwarf irregular galaxy KKH 98.

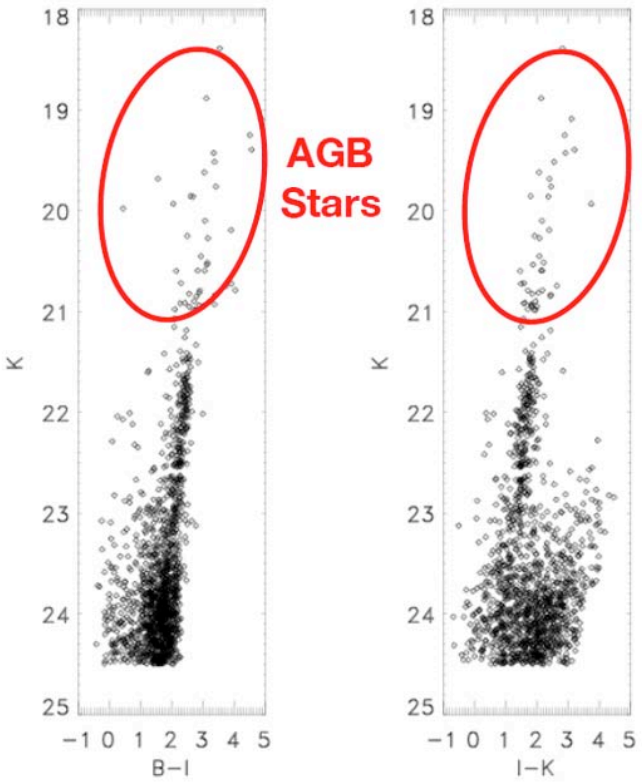

Figure 28. Color magnitude diagrams for KKH 98.

Comparison of CMDs constructed from Hubble B-I colors (left) and from Keck + Hubble I-K colors (right). The upper, AGB portion of the I-K CMD on the right shows significantly less statistical scatter, because the I-K color is less affected by the dusty layers shed by the AGB stars earlier in their lives.

There are 31 dwarf galaxies within 1 Mpc of us. Those that are accessible from Keck's location are prime targets for NGAO stellar population studies. We expect NGAO to provide even more significant results for these objects, and we will carry out quantitative performance simulations for PDR.

3.4.3.2 Simulations of NGAO Performance for the Bulge of M31

Knut Olsen has simulated the color magnitude diagrams retrieved from the bulge of M31, the Andromeda Galaxy, using NGAO. He assumed a one-hour exposure on a 20" x 20" field, and used field-dependent PSFs calculated for NGAO system parameters. First, a mix of stars was picked from model stellar isochrones, and placed in an image. Care was taken to include stars well below the crowding limit. Next the image was convolved with NGAO PSFs, and sky background noise was added. Photometry was performed using the DAOPHOT/ALLSTAR pipeline. PSFs were fit in two ways: one using an average PSF for the whole frame, and the other using the Strehl ratio appropriate for each position in the image. The latter is equivalent to assuming that the "PSF knowledge" approaches being pursued by the NGAO project in conjunction with the CfAO come to fruition by the time the NGAO system is commissioned. The final step in the analysis is to derive the best-fit mix of stellar populations using tools that Olsen has tested extensively in his research with HST and Gemini AO.

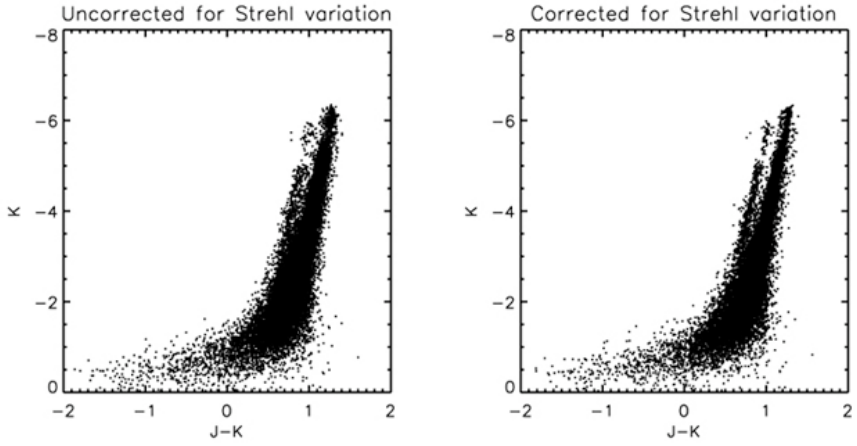

Figure 29. Color magnitude diagrams derived for the bulge of M31.
Left: using the PSFs appropriate to the frame-averaged Strehl ratio, and right: using the field-dependent PSFs that were input to the computation. The advantage of good PSF knowledge is evident in the much improved definition of CMD features in the right frame. From simulations by K. Olsen.

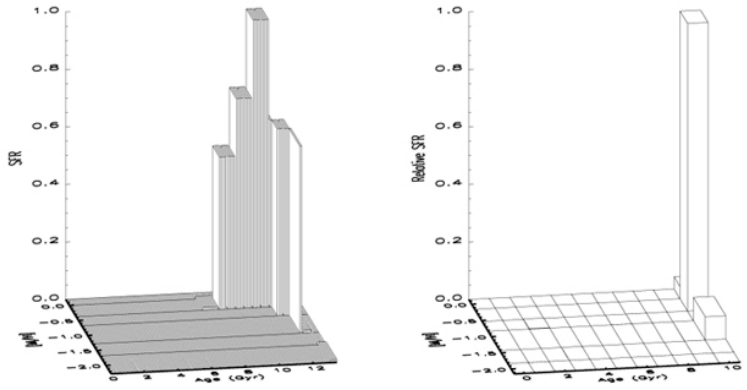

Figure 30. Input (left) and derived (right) color magnitude diagrams for the bulge of M31.
(from simulations by K. Olsen)

The stellar populations that were used as inputs to this calculation are shown in the left panel of Figure 30. Color magnitude diagrams derived from the simulated images are shown in Figure 29, and the stellar population derived from the right-hand color magnitude diagram is shown on the right side of Figure 30. The advantage of good PSF knowledge is evident in the much improved definition of CMD features in the right frame of Figure 29.

3.4.4 Future Work

The resolved stellar populations Science Driver will be discussed in more detail in upcoming releases of the Science Case Requirements Document. During the Preliminary Design phase,

specific scientific objectives will be selected and the system requirements derived from these objectives will be documented.

Requirements Table 11. Resolved Stellar Populations in Crowded Fields derived requirements

Table to be added in later releases of this SCRD document prepared during PDR phase.

3.4.5 References

Ghez, A. et al. 2005, ApJ, 635, 1087

GSMT Science Working Group 2003, "Frontier Science Enabled by a Giant Segmented Mirror Telescope," Supporting Scientific Report 5

Melbourne, J. & Delcanton, J. 2008, in preparation

Olsen, K. A. G., Blum, R. D. & Rigaut, F. 2003, AJ, 126, 452

Rigaut, R. & Roy, J.-R. 2001, "The Science Case for the Multi-Conjugate Adaptive Optics System on the Gemini South Telescope," report number RPT-AO-G0107 version 2.0

3.5 Debris Disks and Young Stellar Objects

Authors: Tom Greene (NASA/Ames), Stanimir Metchev (UCLA), Michael Liu (IfA/Hawaii), Lynne Hillenbrand (Caltech)

Editors: Elizabeth McGrath, Claire Max

3.5.1 Debris Disks

This Science Driver will be discussed in more detail in upcoming releases of the Science Case Requirements Document. Included here is an overview based on the June 2006 NGAO proposal, including a discussion of specific scientific goals for Debris Disks that will be addressed by NGAO. System requirements derived from these goals will be explored and documented during the Preliminary Design phase.

3.5.1.1 Scientific Background

After dissipation of their primordial planet-forming disks of gas and dust, many stars possess debris disks (e.g. Backman & Paresce 1993; Rieke et al. 2005). The dust in debris disks is continually generated from collisions of larger parent bodies that are otherwise undetectable. These parent bodies are the detritus of the planet formation process, and debris disk systems as a whole represent the extrasolar analogs of the asteroid belt and Kuiper Belt in our own solar system.

Theory predicts that planet growth and disk dissipation are intimately linked (e.g., Lissauer 1993). During the post-T Tauri stages of stellar evolution (~10-100 Myr), simulations show that significant debris can arise from large stochastic collisions (e.g., the Earth-Moon formation event) and/or gravitational stirring by recently formed small (Pluto-sized) rocky planets (Kenyon & Bromley 2004). In addition, dynamical interactions between planets and the remaining dust and planetesimals are expected to perturb the orbits of the smaller bodies and to imprint characteristic signatures on the spatial distribution of circumstellar dust (e.g., Roques et al. 1994; Wyatt et al. 1999; Kuchner & Holman 2003). The high prevalence of ring-like and/or clumpy structures seen in scattered light images of debris disks lends supports to this idea (Figure 31). Thus, there is an intimate connection between debris disks and the larger unseen planetesimals and planets that constitute extrasolar planetary systems.

A small fraction of the brightest ($L_{dust}/L_{star} \geq 10^{-4}$) nearest debris disks found by IRAS and ISO have been spatially resolved in scattered light at optical and near-IR wavelengths with HST and/or ground-based natural guide star AO systems. The information gained from these few spatially resolved observations has greatly enhanced our knowledge of the structure of debris disks (e.g., Schneider et al. 1999; Golimowski et al. 2006) and of the physical properties of their constituent dust grains (e.g. Artymowicz 1990; Li & Lunine 2003). The limited data have also posed numerous new questions regarding disk evolution and morphology, such as:

- How do primordial disks transition into debris disks?

- What is the role of planets in this transition?
- How do planets interact with the disks in which they are embedded?
- How significant are stochastic collisions in establishing debris disk properties?

Only about a dozen debris disks have been spatially resolved to date and with limited wavelength coverage --- thus we have only begun to address these central questions. These can be pursued with Keck NGAO through two complementary paths: (1) greatly expanding the resolved census of debris disks and (2) more intensive, multi-wavelength studies of currently resolved systems.

By virtue of its unprecedented angular resolution and stable PSF, Keck NGAO will extend direct-imaging surveys to distances of >100 pc. This will greatly expand the imaging sample due to the disproportionately large number of young (<100 Myr) stars compared to the immediate solar neighborhood; young stellar associations at 100—200 pc contain thousands of sun-like stars. High angular resolution NGAO surveys will harvest a much larger sample of resolved debris disks, opening the door to comparative studies of debris disk properties (e.g. sizes, substructures, and grain properties) as a function of stellar host mass, age, environment, etc. For example, Spitzer mid-IR data reveal remnant debris around at least 10% of Sun-like stars in the 120 Myr old Pleiades cluster (Stauffer et al. 2005), allowing numerous opportunities to scrutinize the outcomes of planet formation in a coeval, homogenous environment. Such a survey will offer the first comprehensive external view of what the solar system may have looked like at a young age.

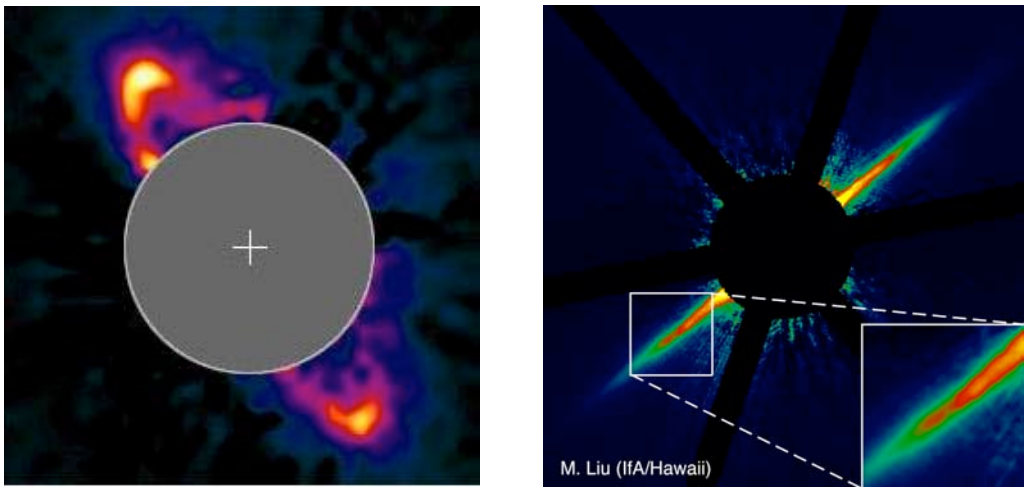

Figure 31. The HR 4796A (Schneider et al 1999) and AU Mic (Liu 2004) debris disks.
Both observations are resolved in near-IR scattered light, using HST (2.5" across) and Keck natural guide star AO (10" across), respectively. The observed ring-like structures, clumps, and gaps are frequently attributed to perturbations by unseen planetary companions. The Keck image of AU Mic represents the current state-of-the-art for ground-based AO, which is limited to the very brightest, edge-on disks. Keck NGAO will enable a much larger sample of debris disks to be imaged, with the necessary multi-wavelength coverage to study their constituent properties.

3.5.1.2 Proposed observations and targets

3.5.1.2.1 Debris disk demographics

One key path to understanding properties and evolution of debris disks is to assemble a much larger census of spatially resolved systems, spanning a wide range of the physical parameter space of age, stellar host mass, formation environment, planet content, etc. The most easily detectable signature of circumstellar dust disks around main- sequence stars is integrated-light thermal emission from optically thin dust at mid-IR and longer wavelengths. New samples of debris disks are presently being furnished through various observing programs conducted with the Spitzer, which offers orders of magnitude improved sensitivity over IRAS and ISO.

While imaging studies of debris disks have been pursued with ground-based AO, the current results are very limited. Keck NGAO will represent a significant new capability for high-contrast imaging of circumstellar dust disks in scattered light. Figure 32 illustrates the expected improvement with simulated deep H-band images from a high Strehl (small FOV) NGAO system, a multi-conjugate NGAO system, and the current Keck natural guide star AO system. The simulation is based on a scattered light model of a massive Kuiper Belt analog around a solar-type star, analogous to conditions that may have existed during the epochs of late planet formation and heavy bombardment in the young (10-300 Myr) solar system (Dominik & Decin 2003; Kenyon & Bromley 2005). The angular scale of the simulations is chosen to correspond to the distance (133 pc) of the 120~Myr old Pleiades open cluster, an ideal population for studying debris disks in the post planet-formation stage.

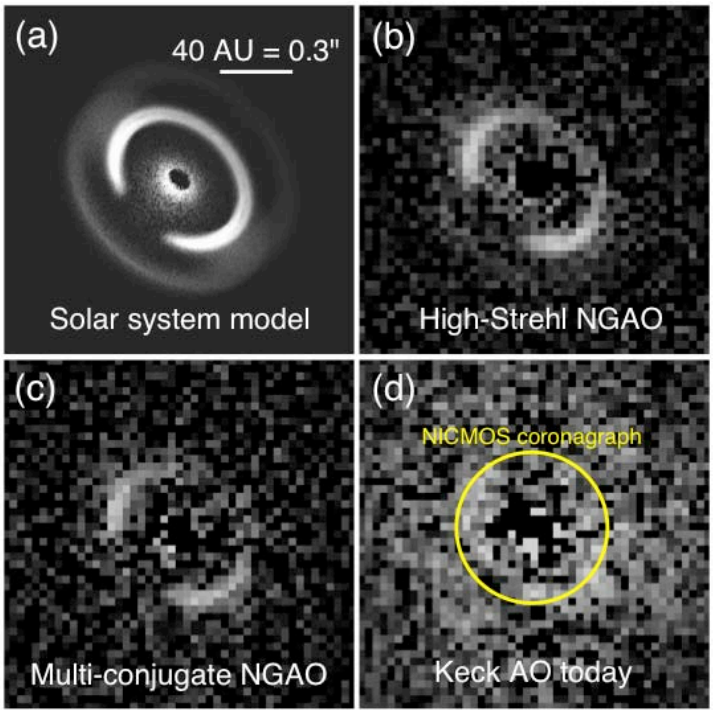

Figure 32. Simulated H-band images of two variants of Keck NGAO, compared to the present-day Keck AO system. Based on a scattered light model of solar-system debris (S. Wolf, private commun.) seen at the distance of the Pleiades cluster (133 pc, 120 Myr). The fractional luminosity of the scattered light is $10^{-3.5}$ relative to the central star, comparable to mid-IR Spitzer observations of Pleiades G-type stars (Stauffer et al 2005). The bright ring in the model corresponds to grains in 1:1 resonance with an outer giant planet (Neptune). Images represent PSF-subtracted 3-hour integrations taken under median, time-varying seeing conditions at Mauna Kea, with Fried length r0 sampled from a log-normal distribution with 21 cm mean and 0.48 dex standard deviation. Strehl ratios of simulated images are 82% (panel b), 47% (panel c), and 28% (panel d). The AO images are binned to 31 mas/pix to enhance the signal-to-noise per resolution element and are shown with the same linear grayscale. The size of the smallest coronagraph available on HST is overlaid on panel (d) to illustrate the new phase space that will be opened at <0.3" separations by NGAO.

In addition to resolving larger numbers of debris disks, Keck NGAO can extend debris disk studies to lower mass stars. Most of present-day debris disk science has concentrated on A-G type stars, because of their larger bolometric luminosities and hence relatively brighter debris disks. However, very little is known about debris disks around M dwarfs, as only a handful of examples have been identified. Past IR~AS and ISO searches for debris disks have largely neglected and/or overlooked low-mass stars, due to sensitivity limitations and choice of science focus. The greater far-IR sensitivity of Spitzer will enable more debris disks around late-type stars to be discovered. These will be prime targets for future investigations in scattered light with the Keck NGAO system, as their primary stars will be too faint for high contrast natural guide star AO. The scientific potential of the M dwarfs is demonstrated by the young star AU Mic, the first identified M dwarf debris disk system (Liu et al 2004; Kalas, Liu & Matthews 2004). Adaptive optics near-IR and HST optical imaging achieves a spatial resolution of ~0.4 AU (Liu et al. 2004; Krist et al. 2005a; Metchev et al. 2005. Fitzgerald et al. 2007) and reveals a rich variety of substructure, suggestive of planetary companions.

Disks around substellar objects are also potential science targets for high-contrast, high-angular resolution imaging. Ground-based and space-based IR photometric studies have already identified many optically thick disks around young brown dwarfs in the nearest (~150 pc) star-forming regions (e.g. Liu et al. 2003; Luhman et al. 2005). Spatially resolved imaging of their disks, which is expected to be within the resolving power of the Keck NGAO system in the red part of the visible band, will open a window into studying the properties and evolution of circum-sub-stellar disks.

3.5.1.2.2 Evolution of low-mass planets and planetesimals through disk substructure

Intensive study of the most observable (nearest and brightest) systems is an important means to advance our understanding of debris disks. Spatially resolved high-contrast, multi-wavelength imaging offers a unique opportunity to study their circumstellar material and their embedded low-mass planets.

High resolution Keck NGAO optical imaging will be a powerful diagnostic tool. Scattered light imaging studies are best performed at shorter wavelengths, where the lower sky brightness and favorable scattering properties of sub-micron dust grains allows optimal imaging contrast between the parent star and the circumstellar dust. Previous ground-based AO observations of debris disks have mostly focused on H-band observations, a necessary compromise since current AO performance at shorter wavelengths is poor. Keck NGAO will overcome this limitation, enabling near diffraction-limited imaging in the red with angular resolution ~0.015" at modest Strehl ratios.

NGAO optical imaging will be a powerful means to identify and diagnose the substructure in debris disks. This new capability can reveal dynamical signatures (rings, gaps) in disks due to embedded planets out to three times greater distances than previous studies. Similarly, it will allow scrutiny over smaller physical scales around nearby systems. The majority of resolved debris disks to date show substructure down to the limit of detectability, suggesting that even higher angular resolution imaging will be fruitful. Such embedded low-mass planets

(~Neptune) have too large orbital separations to be detectable by radial velocity surveys and are too faint to be directly imaged. Hence, observation and theoretical modeling of disk substructure is a unique probe of the outer regions of other solar systems.

An additional benefit of visible AO imaging studies arises from the relation between the scattering properties of grains and their size. Grain scattering efficiency peaks for incoming radiation of wavelength $\lambda \sim 2\pi a$, where a is the grain diameter. If we can extend the capabilities of the Keck NGAO to wavelengths as short as 0.6 μm, we would gain sensitivity to circumstellar grains as small as 0.1 μm. Such small grains are common in primordial circumstellar disks and may dominate the outskirts of the debris disk around late-type stars, where they are blown on highly eccentric orbits by stellar radiation pressure (e.g. Augereau et al. 2001, 2006; Strubbe & Chiang 2006). Visible-wavelength AO capability on Keck will thus be an important asset for measuring the outer radii of these extrasolar Kuiper Belt analogs, an elusive parameter that is often difficult to constrain from long wavelength far-IR/mm unresolved observations.

Finally, Keck NGAO near-IR data will provide an excellent match in angular resolution and contrast with HST optical data, enabling high precision multi-wavelength color measurements. Such data are sensitive to the grain size distribution, porosity and composition; spatially resolved maps will allow for comparative studies of the properties of circumstellar material in different systems. Sub-mm resolved imaging from ALMA of the brightest systems will trace the dust emission properties, providing complementary information to scattered light data. The value of such studies resides not just in ascertaining the properties of the dust grains. Such measurements are needed to ascertain the physical effects acting on the grains, which depend on the grain sizes, and thus are crucial to understand the linkage between disk substructure and embedded low-mass planets.

3.5.1.3 Comparison of NGAO w/ current LGS AO

Current debris disk studies with natural guide star AO are limited to only the brightest, edge-on disks, and current LGS AO does not yet have sufficient Strehl or PSF stability for strong debris-disk science. Keck NGAO will provide a precise, stable PSF for high contrast imaging in the near-IR, suitable for detecting fainter, smaller and or non-edge-on systems. Keck NGAO will also add diffraction-limited imaging in the red, a novel and powerful capability.

3.5.1.4 AO and instrument requirements

Essential: Near-IR and optical imagers.

Desirable but not absolutely essential: Polarimetry, PSF reconstruction from AO telemetry, near-IR detector with substantially lower read noise and/or more dynamic range than NIRC2.

Requirements Table 12. Debris Disks derived requirements

Table will be added in later releases of this document.

3.5.1.5 References

Artymowicz et al. 1990, Advances in Space Research, 10, 81

Backman, D. E., & Paresce, F. 1993, in Protostars and Planets III, 1253--1304

Beichman, C. A., et al. 2005, ApJ, 622, 1160

Decin, G. et al. 2003, ApJ, 598, 636

Dominik, C. & Decin, G. 2003, ApJ, 598, 626

Els, S. G. et al. 2001, A&A, 370, L1

Fitzgerald, M. P. et al. 2007, ApJ, 670, 536

Golimowski, D. A. et al. 2006, AJ, 131, 3109

Kalas, P., Liu, M. C., & Matthews, B. C. 2004, Science, 303, 1990

Kenyon, S. J. & Bromley, B. C. 2005, AJ, 130, 269

Kim, J. S., et al. 2005, ApJ, 632, 659

Krist, J. E. et al. 2005, AJ, 129, 1008

Kuchner, M. J. & Holman, M. J. 2003, ApJ, 588, 1110

Li, A. & Lunine, J. I. 2003, ApJ, 590, 368

Liou, J. & Zook, H. A. 1999, AJ, 118, 580

Lissauer, J. J. 1993, ARAA, 31, 129

Liu, M. C., Najita, J., & Tokunaga, A. T. 2003, ApJ, 585, 372

Liu, M. C. 2004, Science, 305, 1442

Augereau, J. C., Nelson, R. P., Lagrange, A. M., Papaloizou, J. C. B., & Mouillet, D. 2001, A&A, 370, 447

Augereau, J.-C. & Beust, H. 2006, A&A, 455, 987

Liu, M. C., Matthews, B. C., Williams, J. P., & Kalas, P. G. 2004, ApJ, 608, 528

Luhman, K. L., et al. 2005, ApJL, 631, L69

Metchev, S. A., et al. 2005, ApJ, 622, 451

Plavchan, P., Jura, M., & Lipscy, S. J. 2005, ApJ, 631, 1161

Plets, H. & Vynckier, C. 1999, A&A, 343, 496

Rieke, G. H. et al., ApJ, 620, 1010

Roques, F. et al. 1994, Icarus, 108, 37

Schneider, G., et al. 1999, ApJL, 513, L127

Stauffer, J. R., et al. 2005, AJ, 130, 1834

Strubbe, L. E. & Chiang, E. I. 2006, ApJ, 648, 652

Wyatt et al. 1999, ApJ, 527, 918

3.5.2 Young Stellar Objects

This science driver will be discussed in more detail in upcoming releases of the Science Case Requirements Document. Included here is an overview based on the June 2006 NGAO proposal, including a discussion of specific scientific goals for Young Stellar Objects that will be addressed by NGAO. System requirements derived from these goals will be explored and documented during the Preliminary Design phase.

3.5.2.1 Scientific Background

The most broadly accepted scenario for low mass star formation starts with the gravitational collapse of a dense core within an opaque molecular cloud. As collapse proceeds, the core flattens along its rotational axis and forms a central protostar, a circumstellar disk, and an infalling envelope (e.g., Terebey et al. 1984; Shu et al. 1987, 1993), all on timescales of less than a few hundred thousand years. The subsequent evolution of the circumstellar material – from initial formation of the protostar through to a bona fide pre-main-sequence star surrounded by an optically thin, post-planet building, disk – is associated with concomitant evolution in the spectral energy distribution (SED). SEDs peak first at far infrared and sub-millimeter wavelengths and later at shorter near-infrared wavelengths, as the system moves from dominance by cold dust to warmer dust (Lada 1987; Adams et al. 1987; Andre et al. 1993).

Establishing this SED evolutionary scenario has greatly advanced the understanding of low mass star formation, but major puzzles remain. In particular, there is much conflicting evidence in three areas:

- the geometry of circumstellar material, especially in the early "Class I" phase;
- the accretion mechanism and resulting properties of the central stars themselves, especially in the early "Class I" phase;
- the origin and nature of material that is outflowing in jets and winds.

Seeing-limited images at I-band (Eisner et al. 2005) and in the near-IR (Tamura et al. 1991; Whitney et al. 1997) have shown that Class I systems in the nearby (d = 140 pc) Taurus-Auriga dark clouds have large, extended circumstellar envelopes which are resolved in scattered light (Figure 33). Model fits to the imaging data along with the spectral energy distributions for these objects indicate that they are surrounded by both massive disks and envelopes, with envelope matter infalling at high rates. Recent optical (White & Hillenbrand 2004) and near-IR (Doppmann et al. 2005) high resolution spectroscopic studies have confirmed that the central stars of some Class I objects appear to be accreting matter from the disk onto the star at the high rates expected from infalling envelope material, but many others are not, suggesting that disks may have widely varying (and perhaps episodic) accretion rates.

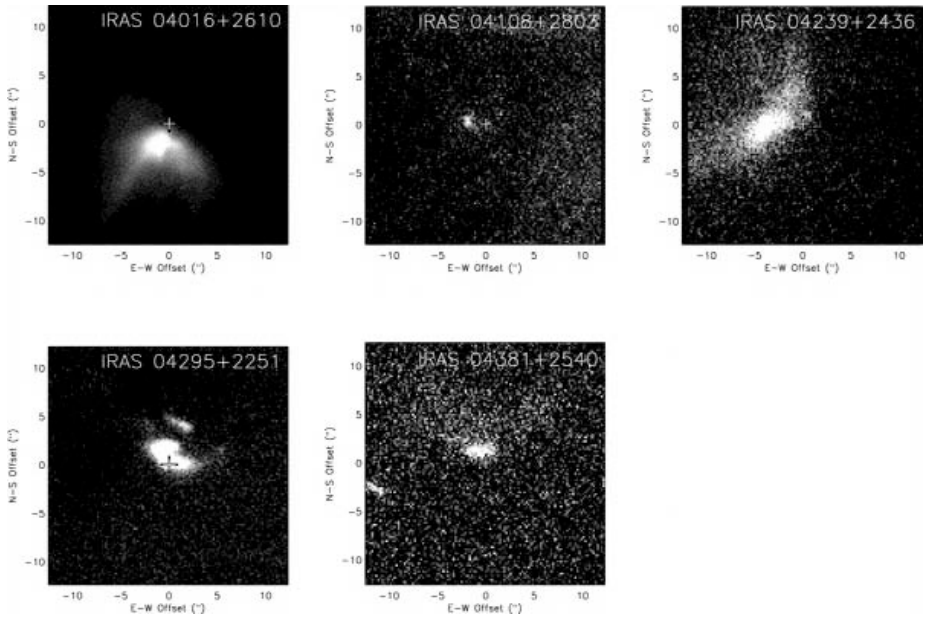

Figure 33. Seeing-limited (0.5-0.6") I-band (0.8 μm) images of protostars in Taurus-Auriga
The resolved scattered light structure from the circumstellar environment is shown (Eisner et al., 2005). Each image is 30" on a side, with the "+" symbol indicating the centroid of the mm-continuum dust emission.

3.5.2.2 Observations and targets

Diffraction-limited AO imaging with Keck will help greatly in resolving the protostellar/circumstellar environment and its connection to the early evolution of the young stars themselves. Existing model fits are not well constrained (Eisner et al. 2005), hampered by seeing-limited spatial resolution and limited wavelength coverage. In particular, multi-color high resolution AO observations from visible-to-near-IR wavelengths would help separate the effects of grain properties (size, composition) from those of the envelope density distributions. Resolved optical and near-infrared imaging from Keck NGAO can be combined with integrated-light SEDs and resolved sub-mm/mm interferometric imaging (e.g. from CARMA and ALMA) to constrain better the physical properties of the circumstellar environment such as the viewing inclination, disk mass, outer size, mass accretion rate, and disk scale height (Figure 34).

The ability to make AO-assisted polarization measurements would further improve the uniqueness of model fits (Whitney et al. 1997), providing more certainty to the nature of these objects. NGAO polarization requirements will be investigated during Preliminary Design phase. Mid-IR AO spectroscopy would trace the spatial distribution of grain properties in the disk and enable a new level of geometric modeling. Finally, high dispersion single-object AO spectroscopy would enable study of both infalling and outflowing material at these early evolutionary stages. In particular, the kinematics of the outflows are relatively unprobed, but observable with Keck NGAO at the spatial scales necessary to separate continuum from various line emission regions, e.g. H2 and [FeII] in the near-infrared or [SII] and [OI] in the optical. Implications for the most desirable spectral resolution will be investigated during Preliminary Design phase.

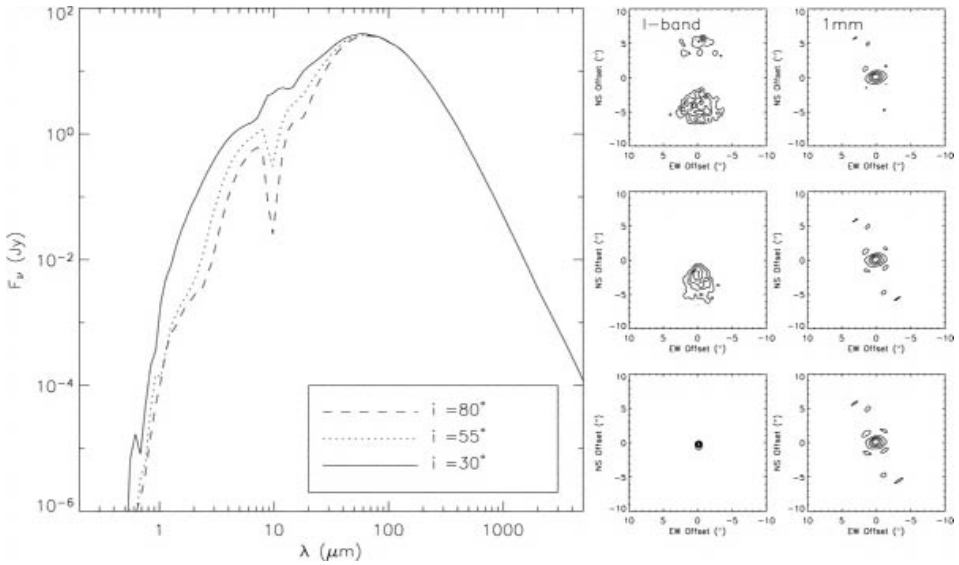

Figure 34. Integrated-light SEDs for circumstellar disks.
I-band scattered light images, and millimeter continuum images for a flared disk model at a range of viewing angles (i increases from the bottom to top panels). Models that are close to edge-on exhibit deeper absorption at mid-IR wavelengths and higher extinction of the central star. For small inclinations (i ~ 30), the central star is visible and dominates the I-band emission. For moderate inclinations, asymmetric scattered light structure is observed, while for nearly edge-on orientations a symmetric, double-lobed structure is seen (Eisner et al. 2005).

More importantly, stable diffraction-limited imaging would extend studies from the handful of Class I objects in Taurus-Auriga that have been studied thus far to many more, e.g. in the more distant ρ Oph, Serpens, and Perseus (140 - 330 pc) regions as well as in even further regions which are undergoing high mass star formation. This would allow some of the first direct measurements of the circumstellar envelopes of high mass protostars, and model fits would provide unique insights into their matter distribution and accretion properties (Figure 35). This would allow the detailed statistical study of the similarities and differences in the formation of high and low mass stars and their circumstellar systems. In Orion alone there are at least 20 objects with Class I (protostar) SEDs and associated nebulosity.

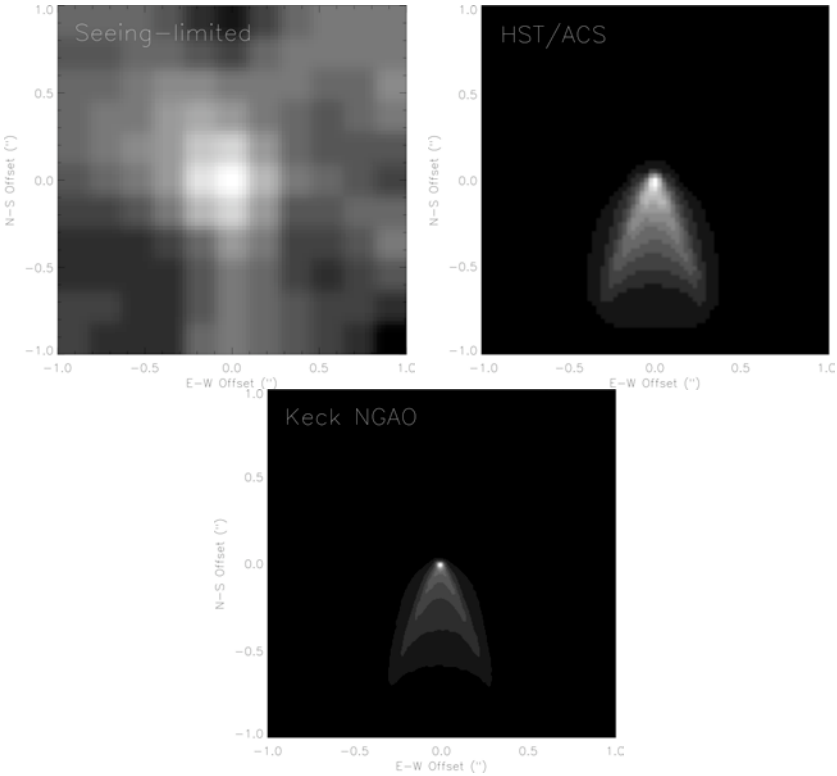

Figure 35. Simulated I-band images for a model of the circumstellar dust around a Class I object at a distance of 1 kpc.
As observed by seeing-limited Keck/LRIS (left), HST ACS/HRC (middle), and Keck NGAO (right). The model consists of a massive disk (0.1 $M_{\odot}$) embedded in a massive envelope (5 x 10^{-3} $M_{\odot}$) with an outflow cavity, observed at an inclination of 55°. Each image is 2" on a side. (Figure courtesy of J. Eisner.)

3.5.2.3 Comparison of NGAO w/ current LGS AO

Diffraction-limited studies of protostars are very challenging for current LGS AO. Imaging of such complex morphologies requires a stable and/or well-known PSF to be able to distinguish circumstellar structure from imaging artifacts, and for quantitative modeling of imaging data. High-resolution multi-wavelength imaging is critical to probe the circumstellar grain properties; this is likewise not possible with current LGS AO.

By their very nature, these objects are in high extinction regions, where optical tip-tilt star availability is poor. In addition, while some of the sources themselves are optically visible, their extended morphologies are not well suited for tip-tilt sensing. Near-IR tip-tilt sensing is required, also not available with current LGS AO.

3.5.2.4 AO and instrument requirements

Essential: Diffraction-limited optical and near-IR imager. Diffraction-limited near-IR IFU spectrograph. The small field of view of current OSIRIS is not well suited for this program. [It may be more desirable, for example, to use one of the deployable-IFU heads with its field of 1" x 3".]

Desirable but not absolutely essential: Imaging polarimetry, near-IR echelle spectroscopy, mid-IR spectroscopy.

Detailed studies of AO and instrument requirements will take place during the Preliminary Design phase.

Requirements Table 13. Young Stellar Objects derived requirements

Table will be added in later releases of this document.

3.5.2.5 References

Adams, F. C., Lada, C. J., & Shu, F. H. 1987, ApJ, 312, 788

André, P., Ward-Thompson, D., & Barsony, N. 1993, ApJ, 406, 122

Doppmann, G. W., Greene, T. P., Covey, K. R., Lada, C. J. 2005, AJ, 130, 1145

Eisner, J. A., Hillenbrand, L. A., Carpenter, J. M., & Wolf, S. 2005, ApJ, 635, 396

Lada, C. J.. 1987, IAU Symp. 115: Star Forming Regions, 115, 1

Shu, F. H., Adams, F. C., & Lizano, S. 1987, Ann Rev Astron & Astrophys, 25, 23

Shu, F. H., Najita, J., Galli, D., Ostriker, E., & Lizano, S. 1993, in Protostars and Planets III, 3

Tamura, M., Gatley, I., Waller, W., & Werner, M. W. 1991, ApJL, 374, L25

Terebey, S., Shu, F. H., & Cassen, P. 1984, ApJ, 286, 529

White, R. J., & Hillenbrand, L. A. 2004, ApJ, 616, 998

Whitney, B. A. Kenyon, S. J., Gomez, M. 1997, ApJ, 485, 703

3.6 Size, Shape and Composition of Minor Planets

Author: Franck Marchis
Editors: Claire Max, Elizabeth McGrath

3.6.1 Scientific background and context

While space missions largely drove early progress in planetary astronomy, we are now in an era where ground-based telescopes have greatly expanded the study of planets, planetary satellites, and the asteroid and Kuiper belts. Ground-based telescopes can efficiently perform the regular observations needed for monitoring planetary atmospheres and geology, and can quickly respond to transient events.

The study of the remnants from the formation of our solar system provides insight into the proto-planetary conditions that existed at the time of solar system formation. Such information has been locked into the orbits and properties of asteroids and Kuiper Belt objects. The study of binary (and multiple) minor planets is one key path to revealing these insights, specifically by studying their kinematics and geological properties. There are no space missions currently planned to study these binaries. This important inquiry is only accessible to ground-based telescopes with AO.

3.6.2 Scientific goals

High angular resolution studies are needed of large samples of binary asteroids to understand how their enormous present-day diversity arose from their formation conditions and subsequent physical evolution, through processes such as disruption and re-accretion, fragmentation, ejecta capture, and fission. Specifically one can study:

- Formation and interiors of minor planets by accurate estimates of the size and shape of minor planets and their companions
- Mass, density, and distribution of interior material by precise determination of the orbital parameters of moonlet satellites
- Chemical composition and age, by combining high angular resolution with spectroscopic analysis

3.6.3 Proposed observations and targets

Spatially resolved imaging of large asteroids is critical in order to derive reliable statistical constraints on large collisions throughout the Main Belt. Observations of the 15 or 20 largest asteroids would provide the statistics necessary to put much stronger constraints on the frequency of major collisions. We estimate that 20 Main Belt asteroids will be resolved with sufficient resolution with NGAO in R-band (33 in V-band) to obtain mapping comparable to that already done for 4 Vesta.

Table 5 summarizes the number of asteroids resolvable from visible to near-IR, categorized by domain and population. Thanks to NGAO's high angular resolution in V and R bands, ~800 main-belt asteroids could be resolved and have their shape estimated with a precision of better

than 7%. With the current AO system ~100 asteroids, located only in the main-belt, can be resolved. The determination of the size and shape of even a few Trojan asteroids will be useful to estimate their albedo. For Near Earth Objects (NEAs), the large number of resolvable objects is a result of very close approaches to Earth.

Table 5
Number of asteroids resolvable with Keck NGAO in various wavelength ranges and populations (assuming on-axis observations).

Populations by brightness (numbered and unnumbered asteroids)					
Orbital type	Total number	V < 15	15 < V < 16	16 < V < 17	17 < V < 18
Near Earth	3923	1666	583	622	521
Main Belt	318474	4149	9859	30246	88049
Trojan	1997	13	44	108	273
Centaur	80	1	1	2	2
TNO	1010	1	2	0	2
Other	3244	140	289	638	870

This research program will have even higher impact if it is combined with the study of binary asteroids. Recent studies suggest that the primary asteroid of most binary asteroid systems has a rubble-pile structure, indicating that they have weak shear strength (Marchis et al., 2006). Consequently their shape is directly related to the angular momentum at their formation (Tanga et al., 2006). One can obtain their mass through determination of moonlet orbits combined with a good shape determination, by direct imaging in the visible (which provides the best angular resolution). Assuming an R band Strehl > 20% so that there is a clear diffraction-limited peak in the PSF, we estimate that between 1000-4000 new binary asteroids could be discovered with NGAO. An accurate shape estimate for ~300 of them (an order of magnitude more than the number of asteroids with currently known shapes) can be attained with NGAO in R band. Six observations taken at various longitudes are enough to accurately reconstruct the 3D-shape of the asteroid. Twelve nights of observations should be considered for the completion of such a program. Dedicated nights are not necessary since this program can be combined with the study of satellite orbits of asteroids using the same instrumentation.

3.6.4 AO requirements

3.6.4.1 Wavefront error

A wavefront error of 140 nm would provide excellent angular resolution in the visible, better than HST and adequate for our program. We expect excellent sensitivity for point source detection. Table 14 of the Keck NGAO Proposal to the SSC (June 2006) indicates that the point source limiting magnitude for such AO system (5σ, 1hr integration) is 29.0 in R band. For comparison, recent observations of Pluto-Charon recorded with ACS/WFC at 0.61 μm (Weaver et al. 2006) allowed the detection of 2 new moons with R = 23.4 (SNR=35). With NGAO in R band with 140 nm of wavefront error, these moons could have been discovered with SNR~47. Such gain in sensitivity will help find more multiple systems, and also to find out if around these multiple systems there is still a ring of dust left over from the catastrophic

collision that formed the multiple system. We are currently carrying out simulations to characterize the science that could be done with 170 nm and 200 nm of wavefront error. Our expectation is that there will not be a "cliff" in science output as the wavefront error degrades, but rather a gradual decrease in the number of moonlets detected and in the number of primary asteroids whose shapes can be measured. Future releases of this Science Case Requirements Document will compare the science performance for 140, 170, and 200 nm of wavefront error.

3.6.4.2 Encircled energy

N/A

3.6.4.3 Contiguous field requirement

Required FOV is ≤ 2 arc sec. There is no requirement for a larger contiguous field.

3.6.4.4 Photometric precision

Accurate photometry will lead to a better estimate of the size and shape of the moonlets, which will give strong constraints on their formation mechanism (e.g. one would be able to tell if the moonlet is synchronized and displays an equilibrium shape under tidal forces). The proposed method is to detect photometric changes due to its potential lack of sphericity over the moonlet's orbit, as we see different faces of the moonlet. With current AO systems, the photometric accuracy on the moonlet is rather poor. The accuracy of the flux estimate of the 22 Kalliope moonlet, orbiting at 0.6 arc sec with $\Delta m=3$, was only ~20% with Keck LGS AO. Assuming the same sky background and detector noise as with current Keck LGS AO, NGAO in the near IR is predicted to yield a photometric accuracy of 5% or better for the same observing situation.

3.6.4.5 Astrometric precision

The astrometric measurements for our program are relative to the primary. The maximum angular separation between the secondary and the primary is 0.7 arc sec. We require the visible instrument to provide images with at least Nyquist sampling. The relative position of the secondary, estimated by a Moffat-Gauss fit, cannot be better than a 1/4 of a pixel (since the primary is resolved). The residual distortion over the field of the detector should not be more than 1.5 mas. Uncharacterized detector distortion will be the limiting factor in these astrometric measurements.

3.6.4.6 Contrast

At the current time the faintest and closest moonlet discovered around an asteroid is Remus, orbiting at 0.2-0.5" (350-700 km) around 87 Sylvia with Δm (peak-to-peak) = 3.5. The detection of this moonlet is challenging with current Keck AO, and also with the VLT NACO system. For instance, it was detected (SNR > 3) on 10 images out of 34 recorded over 2 months with the VLT. A better contrast will increase the detection rate, allowing us to see fainter and closer moonlets but also to get a better photometric measurement on those already known. Coronagraphic observations cannot be considered in our case: the central source is not point-like so the effect of the mask will be negligible. It is assumed that the distance to

the primary of a satellite is driven by tidal effects, but at the moment theoretical work fails to agree on the age of an asteroid and the position of its moonlet. This is mostly due to the lack of observed systems in which a moonlet orbits at less than 1000 km ($a / R_p < 8$). Two orders of magnitude gain in the detection limit ($\Delta m = 5.5$ at 0.5 arc sec) would lead to the possibility of detecting a half-size moonlet around (87) Sylvia.

3.6.4.7 Polarimetric precision

N/A

3.6.4.8 Backgrounds

Any background equal to or better than current Keck AO will be acceptable. Lower backgrounds are always better.

3.6.4.9 Overall transmission

Comparable to or better than with current LGS AO system.

3.6.5 Other key design features

3.6.5.1 Required observing modes

The capability of efficiently observing moving targets must be included in the design of NGAO, so that implementation of differential guiding when the tip-tilt source is not the object itself (and is moving relative to the target) is possible. The maximum relative velocity to be expected is 70 arc sec per hour.

We also point out that for this science case, the scientific return of the Keck telescope and the NGAO system would greatly improve if some sort of flexible or queue scheduling or service observing were to be offered. With an error budget of 140 nm the NGAO system will achieve a Strehl of ~20% in R- band under moderate seeing conditions. Bright targets like the Galilean satellites (V~6) can be observed even if the seeing conditions are lower than average in the near IR (at separations > 1.2”). Other difficult observations, such as the study of multiple TNOs (V>17) could be scheduled when the seeing conditions were excellent (< 0.7”). Finally, frequent and extremely short (half hour) direct imaging observations of a specific target such as Io, to monitor its activity over a long period of time, would be extremely valuable and are not available on HST. All these programs could be done more easily if flexible or queue or service observing were available at Keck. It would also relax the constraints on the NGAO error budget since it would be possible to take advantage of excellent atmospheric conditions to observe the faintest objects.

3.6.5.2 Observing efficiency

Current observations with Keck AO have a ~25 minute overhead when switching between targets for an on-axis LGS observation of an asteroid. It is very desirable to reduce this overhead. A goal of 10 minutes setup time when switching between LGS targets is desirable. There is no firm requirement, but observing efficiency suffers in direct proportion to the time it takes to switch from one target to the next, particularly when the observing time per target is relatively short. This is an important constraint for this science case, since numerous targets must be observed per night.

3.6.6 Instrument requirements

3.6.6.1 Required instruments

Primary: Visible imager, on-axis, diffraction limited, narrow field, with coronagraph
Secondary: Near IR imager, on-axis, diffraction limited, narrow field, with coronagraph
Secondary: Visible IFU, on-axis, narrow field, R~100
Secondary: Near infrared IFU, on-axis, narrow field, R~1000-4000

3.6.6.2 Field of view

No more than 4 arc sec.

3.6.6.3 Field of regard

Should be determined by the requirement to find adequate tip-tilt stars.

3.6.6.4 Pixel sampling

For both photometry and astrometry, the pixel scale of the imager that yields the best overall performance is $\lambda/3D$ for J, H, and K-bands, or $\lambda/2D$ for R and I-bands. See KAON 529 and for an in-depth discussion of how these values were chosen.

3.6.6.5 IFU multiplicity

Single object mode only. Density of asteroids on the sky is not high enough for multi-object observing.

3.6.6.6 Wavelength coverage

Imaging: Wavelengths 0.7 – 2.4 μm
Spectroscopy: Wavelengths 0.8 – 2.4 μm

For astrometry, neither R nor K-band are ideal choices for the imager. In K-band, this is because the width of the PSF and artifacts that spread out to ~3.3 arcsec confuse the detection of faint asteroid companions. In R-band, this is because the Strehl is not as good and the companions are too faint to be detected accurately. See KAON 529 for more details.

3.6.6.7 Spectral resolution

There are spectroscopic features at visible wavelengths (e.g. the absorption bands of pyroxene at 0.85 - 1 μm). For these bands, which are relatively broad, a spectral resolution of R~100 is desirable. This could be accomplished either with a low resolution IFU spectrograph or with narrow-band filters. There are also bands in the near IR. SO_2 frost (bands at 1.98 and 2.12 μm) can be best observed with R~1000. However R~4000 would be acceptable.

3.6.7 Requirements Summary

The requirements for the *asteroid size and shape* (characterize surface and orbital parameters) science case are summarized in the following table. In addition to the requirement of a high resolution visible imager, the slope of the visible spectrum is needed to determine the asteroid age or surface type. This case desires a spectral resolution of R ~ 100 for 0.7 – 1.0 μm wavelength with Nyquist spatial sampling. If R ~ 100 is not available, some of this work can be achieved either with multiple narrow-band filters or with a higher-resolution spectrograph.

Requirements Table 14. Asteroid size, shape, and composition derived requirements

#	Science Performance Requirement	AO Derived Requirements	Instrument Requirements
14.1	Target sample size of ≥ 300 asteroids in ≤ 3yrs years. ≥ 10 targets in an 11 hour night	#6.5 is stricter requirement.	
14.2	Observing wavelengths 0.7 – 1.0 μm. Strong preference for R band because optimum to obtain shape of asteroid.	AO system must pass 0.7 to 1.0 micron wavelengths with sufficient sensitivity to satisfy #14.1	Imagers (R through J band) with narrow-band filters or slit spectrograph (R~100), or possibly visible IFU (R~100).
14.3	Spatial sampling same as #5.5	Same as #5.5	Same as #5.5
14.4	Field of view ≥ 1" diameter	Same as #6.8	Same as #6.8
14.5	Ability to measure the spectral slope with R ~ 100 at 0.85-1.0 μm		

14.6	Ability to measure the SO_2 frost bands at R=1000 (R=5000 is acceptable) at 1.98 and 2.12 μm, crystalline ice band at 1.65 microns.		Spectroscopic imaging at R~1000 to 5000 in the H and K bands.
14.7	Same as #5.7	Same as #5.7	
14.8	Same as #5.8	Same as #5.8	

3.6.8 References

Marchis, F., J. Berthier, P. Descamps, et al. 2004b. Studying binary asteroids with NGS and LGS AO systems, SPIE Proceeding, Glasgow, Scotland, 5490, 338.

Marchis, F., Descamps, P., Hestroffer, D. et al., 2005. Discovery of the triple asteroidal system 87 Sylvia, *Nature* 436, 7052, 822.

Marchis, F.; Kaasalainen, M.; Hom, E. F. Y.; Berthier, J.; Enriquez, J.; Hestroffer, D.; Le Mignant, D.; de Pater, I. 2006. Shape, size and multiplicity of main-belt asteroids, *Icarus* 185, 39.

Tanga, Paolo; Consigli, J.; Hestroffer, D.; Comito, C.; Cellino, A.; Richardson, D. C. 2006, Are Asteroid Shapes Compatible With Gravitational Reaccumulation? American Astronomical Society, DPS meeting #38, #65.06

Weaver, H. A.; Stern, S. A.; Mutchler, M. J.; Steffl, A. J.; Buie, M. W.; Merline, W. J.; Spencer, J. R.; Young, E. F.; Young, L. A. 2006, Discovery of two new satellites of Pluto, Nature, 439, 943.

3.7 Characterization of Gas Giant Planets

Author: Imke de Pater and Heidi B. Hammel
Editors: Claire Max, Elizabeth McGrath

3.7.1 Scientific background and context

Characterization of gas giants (Jupiter and Saturn)—including their atmospheres, ring systems and satellites—is a critical step in our understanding of the growing numbers of extrasolar planets. [The following section will describe analogous science cases for the ice giants, Uranus and Neptune.]

3.7.2 Scientific goals

We identify several science goals for the gas giants for which the Keck Observatory, along with HST, has historically been the leader. These are not attainable with any other existing or planned facility that we are aware of. They include atmospheric dynamics and long-term climate change on Jupiter, Saturn, and Titan; volcanic activity on Io; temporal evolution of ring systems; and satellite astrometry.

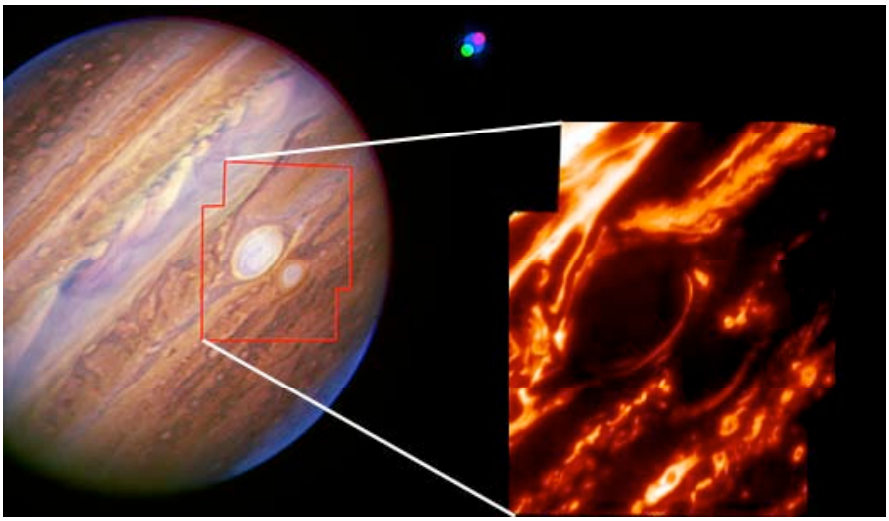

Figure 36. Jupiter's Great Red Spot and new Red Oval with the Keck AO system.
Left: This false-color near-infrared composite of Jupiter and Io was taken in July 2006. The AO system used Io as its reference star. Io itself is visible as the green, blue, and red dots, corresponding to 1.29, 1.65 and 1.58 μm, respectively (Io's blue dot looks larger). The motion of the satellite with respect to Jupiter during the observing sequence is clearly seen. The red outline shows the area covered by the mosaic shown on the right. Right: The two spots were also imaged with AO through a 5-μm filter that samples thermal radiation from below the main cloud deck. Both spots appear dark because clouds block heat emanating from lower elevations, though narrow regions around the spots that are cloud-free show leakage of heat into space.

3.7.2.1 Atmospheric Dynamics and Long-term Climate Change

Jupiter has two red spots Figure 36, the Great Red Spot (GRS, first spotted in the 1600s) and the Red Oval (discovered in December 2005). The latter feature—currently Jupiter's second largest storm—is new, having formed between 1998 and 2000. It was originally white but

turned red in 2005 and is now similar in color to the GRS.

As summarized by Marcus et al. (2007), the oval's color change may have been triggered by a global climate change on Jupiter, as had been predicted (Marcus 2004). This global change may also be the trigger for an atmospheric "global upheaval", characterized by dramatic variations in clouds over a wide range of latitudes, including, for example, eruptions of spots in the North Tropical Belt, a dislocation of the GRS from the South Equatorial Belt, and rifts in clouds.

Observations of the formation and evolution of the new Red Oval uniquely emphasize the importance of continued monitoring of Jupiter. To assess the validity of the claim that global climate change on Jupiter is driving major change on Jupiter, the planet needs to be monitored several times a year at high angular resolution; spectroscopic measurements also are required to determine the vertical structure of the atmosphere, as well as changes therein.

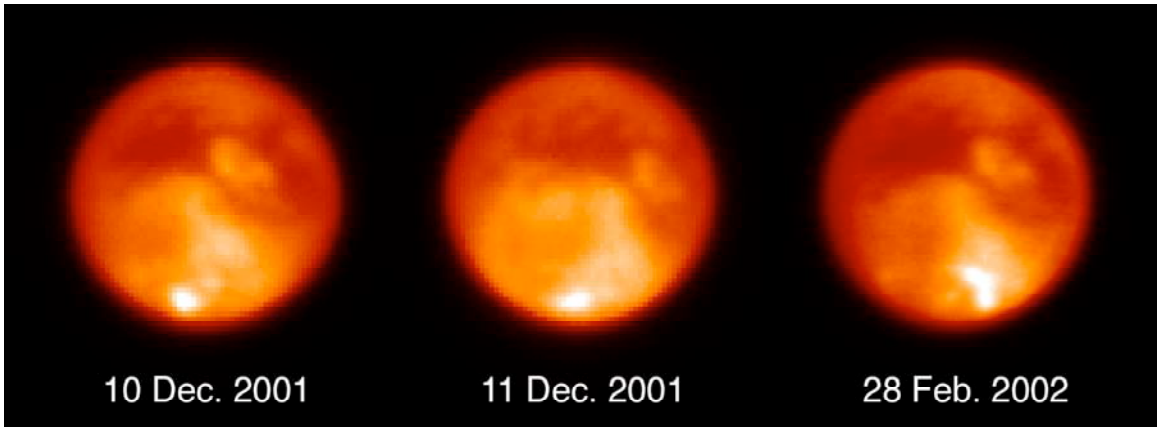

Figure 37. Keck imaging of Titan's Clouds.
These K'-band images of changing methane clouds near Titan's south pole were taken using the Keck AO system in December 2001 and February 2002. Nearly the same face of the moon is viewed in all three images; the disk of Titan subtends just 0.8 arcseconds. The large storm in the Feb. 28 image is over 1400 km (870 miles) long. From Brown et al. 2002.

Significant long-term and short-term changes in the atmospheres of Saturn and Titan are well documented in the literature. These changes include seasonal variations on both objects (Saturn: Barnet et al. 1992a, Olivier et al. 2000, and Moses and Greathouse 2005; Titan: Caldwell et al. 1992, Lorenz et al. 1999, and Roe et al. 2004); the sudden onset of large but short-lived storms on Saturn (Sanchez-Lavega et al. 1991; Barnet et al. 1992b; Beebe et al. 1992); and Titan haze migration, methane recycling, and clouds/rain, for example as in Figure 37(Brown et al. 2002; Ádámkovics et al. 2004, 2006, 2007; Schaller et al. 2006a, 2006b).

Nevertheless, the details of most of these processes, especially the long-term ones, remain elusive due to a lack of continuous data coverage. After the end of the Cassini Saturn mission, ground-based telescopes will be our primary means for observing these bodies and unraveling their secrets (Saturn will be too bright for JWST; studies of whether Titan will also be too bright are underway, but regardless, the spatial resolution of Keck's 10-m aperture will surpass that of JWST's 6.5-m aperture in the near infrared).

The specific goal for long-term climate change studies is continued high-spatial-resolution images in the near infrared over many years and preferably decades. Such data are required in order to characterize the long-term changes of zonal banded structure, haze migration, and the timescales of discrete-feature formation and evolution.

3.7.2.2 Small Satellites and Ring Astrometry

Temporal changes in the rings of Jupiter and Saturn have been noted (in particular in dust components), and should be monitored (this is discussed in more detail in the analogous section for ice-giant systems, 3.8.2.4).

3.7.2.3 Io

Io is a mysterious and intriguing body. It is the most volcanically active body in the Solar System. Its heating and cooling processes are still not well understood, despite numerous spacecraft fly-bys and ground-based monitoring for almost 30 years. OSIRIS and new AO-fed IFUs on Keck present an unprecedented opportunity to advance our knowledge of this fascinating moon through the ability to simultaneously map Io at high spatial and spectral resolution. Io's extreme volcanic activity can be imaged both in reflected sunlight (Figure 38) and in eclipse (Figure 39). Many outstanding questions can be explored with continued Keck imaging and spectroscopy. We list a few below.

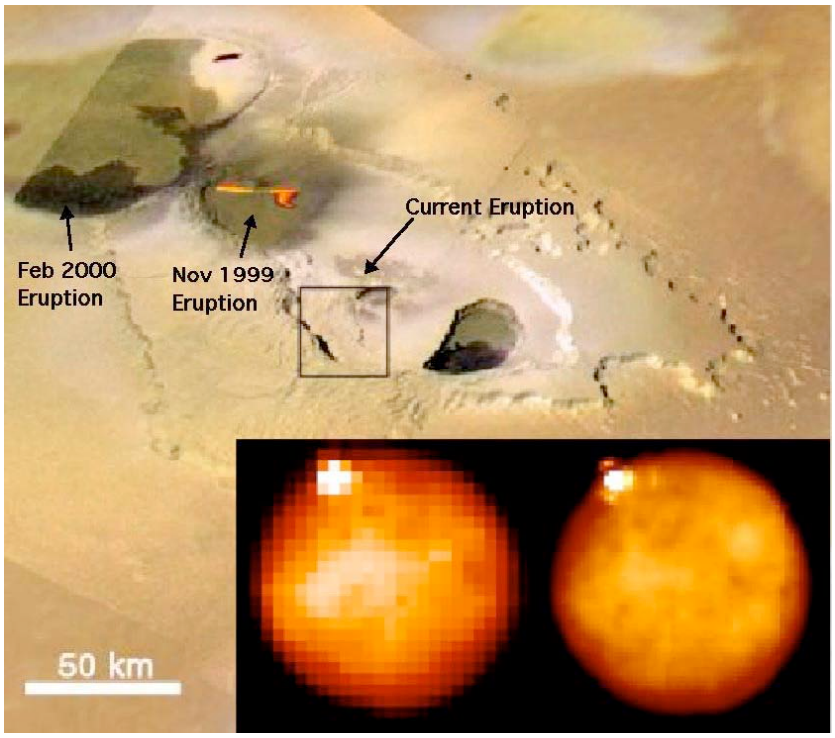

Figure 38. Keck OSIRIS images of Tvashtar erupting on Io.
Two Keck OSIRIS K-band images from 2006 are superposed on a visible image taken by Galileo in November 1999. The pair show the initial detection of a volcano at the 11 o'clock position in low resolution (0.05" pixels, left), with a follow-up high-resolution image (0.02" pixels; right). The estimated position of the Keck volcano is shown as a 1-sigma error box on the Galileo image. From Laver et al. (2007).

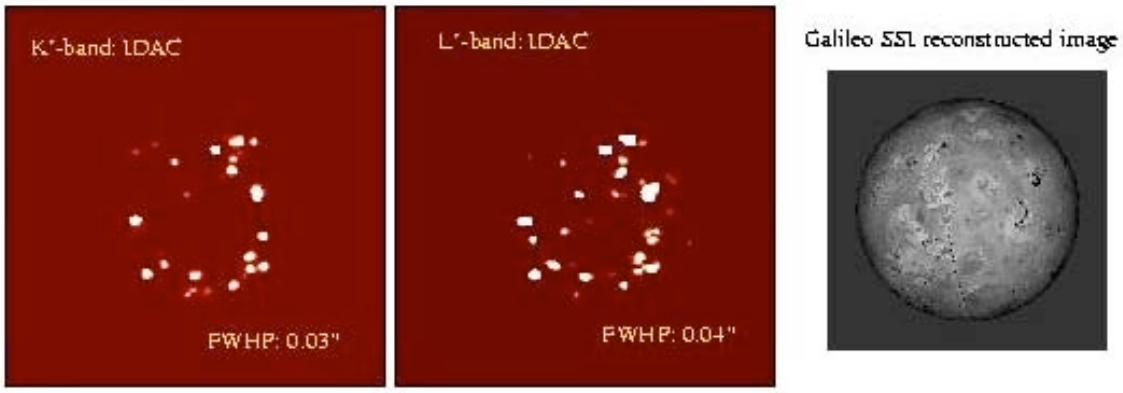

Figure 39. Keck AO images of many volcanoes on Io.
Images of Io in K'- (left) and L'-bands (middle) were taken using the Keck AO system while the satellite was in eclipse; i.e., only thermal emission was detected. The images were deconvolved with the "IDAC" algorithm using a Gaussian beam with a FWHM of 0.03" at K'-, and 0.04" at L'-band. All images have been rotated so Io's north pole is up. On the right side of the figure we show a Galileo visible-light SSI reconstructed image at the time of the observations. From de Pater et al. (2004).

• What form of volcanism dominates on Io, sulfur or silicate? This question can be addressed via spatially resolved measurements of the eruption temperatures. Particularly fascinating are reports of ultra-high temperature (~1800 K) eruptions, suggestive of rocks with extreme high melting temperatures similar to those that may have been present on Earth during its early history.

• Is Io's huge heat flow steady, or does it fluctuate over time? This question is related to tidal dissipation models: some show heat dissipation in the asthenosphere just below the crust, and others show dissipation in the deep mantle.

• Is the tenuous SO_2 atmosphere supported by volcanic activity or through sublimation of surface frost? In other words, what is the relation between Io's gas plumes, its atmosphere, its volcanoes, and its interaction with Jupiter's magnetosphere?

Through continued monitoring with Keck and its unparallel spatial resolution we can solve the fundamental riddles of this enigmatic moon. Ideally, Io should be monitored monthly both in reflected sunlight and in eclipse, to monitor volcanic eruptions and atmospheric gases.

3.7.3 Proposed observations and targets

3.7.3.1 Atmospheric Dynamics and Long-term Climate Change

Jupiter dynamics. To measure winds in cyclones on Jupiter, we require an image cadence spread out over a few hours. Multiple wavelengths will yield altitude discrimination.

Jupiter climate change. At a minimum, a single multi-wavelength imaging set for Jupiter and Saturn should be obtained each year. Spatially resolved spectroscopy of small regions will help to elucidate the physics and chemistry of individual atmospheric features.

Titan. Multi-frequency observations (e.g., with OSIRIS) are needed at least twice a year. Individual regional changes in cloud frequency and composition require the ability to follow changes of periods of days to weeks.

3.7.3.2 Small Satellites and Ring Astrometry

Typically, we require repeated deep images at a single wavelength (typically K' band, where the planet is dark and thus the rings can be traced close in to the planet). For Saturn's outer rings, H and J bands are also required to provide basic color information on the rings. Cadence of these observations will depend on the specific phenomena being studied.

3.7.3.3 Io

Io should be observed as often as is feasible using multi-frequency observations. Observations in reflected sunlight are best done in the visible, and any wavelength longer than about 0.5 μm would be useful. In particular, 0.8 μm or longer would be adequate. For observations of Io in eclipse, one needs to image in K band or longer wavelengths, since one is observing thermal emission from the volcanic activity. Here the thermal IR from 2 to 5 μm would be useful. In the absence of an L' and M' capability, K-band will be key. For the purposes of statistical studies a minimum cadence for Io is once per month. To study the course of individual volcanic eruptions one will need a cadence of days to weeks.

3.7.4 AO requirements

3.7.4.1 Wavefront error

A wavefront error of 140 nm would provide excellent angular resolution in the visible for observations in reflected sunlight, better than HST and adequate for our program. For K-band observations of Io in eclipse a wavefront error of 170 nm will suffice. Future releases of this Science Case Requirements Document will quantitatively compare the science performance for 140, 170, and 200 nm of wavefront error for each of the three science goals discussed here (atmospheric dynamics, small satellites and ring astrometry, and Io vulcanism).

3.7.4.2 Encircled energy

Comparable to current Keck capabilities, or better. To be quantified in future releases of this Science Case Requirements Document.

3.7.4.3 Contiguous field requirement

Jupiter's disk itself is of order 30 arc sec in diameter. Imaging the whole disk of Jupiter or Saturn at once is best done with MCAO, to avoid distortions due to anisoplanatism. Due to the rapidly evolving atmospheric structure and fast rotation periods on the gas giants (a full rotation is of order 10 hours or less), it is extremely difficult to create effective mosaics from many small fields of view unless those FOVs are observed simultaneously. In other words, IFUs can have FOV ~ a few arc sec if enough IFUs can be positioned to cover the required area.

Keck NGAO's strength will be imaging and spectroscopy of specific planetary and ring features. Many of these features will be small, of order a few arc sec, and thus amenable to

imaging spectroscopy with IFU fields of view of several arc sec. However, the largest of these features is the Great Red Spot on Jupiter, which is variably between 8"-13" in E-W diameter. Ideally one would like to image the Great Red Spot by using an IFU with larger field (of order 15 arc sec) or by using multiple abuttable smaller IFUs. There is no firm requirement on how closely abuttable these smaller IFUs must be, but the closer the better for this science case.

The Jupiter and the Saturn ring systems subtend 40 and 47 arc seconds respectively. Thus the same field of view considerations apply as for disk imaging and spectroscopy.

Io subtends 1.2 arcseconds, and Titan subtends only 0.8 arcseconds. Thus, FOVs of 1.5 arcseconds are adequate for both satellites.

3.7.4.4 Photometric precision

Comparable to current Keck capabilities, or better.

3.7.4.5 Astrometric precision

Comparable to current Keck capabilities, or better.

3.7.4.6 Contrast

Comparable to current Keck capabilities, or better.

3.7.4.7 Polarimetric precision

N/A

3.7.4.8 Backgrounds

Comparable to current Keck capabilities, or better.

3.7.4.9 Overall transmission

Comparable to current Keck capabilities, or better.

3.7.5 Other key design features

3.7.5.1 Moving Target Tracking

For planetary science, the capability of observing non-sidereal targets must be included in the design of NGAO. This will require implementation of differential guiding when the tip-tilt source is not the object itself, and when the tip-tilt source is moving relative to the target. The maximum relative velocity for Jupiter is ~16 arcsec/hour (4.5 mas/s), and Io's rate around Jupiter reaches a maximum of ~37 arcsec/hr (10.2 mas/s). Such rates would also permit observations of Saturn (~10 arcsec/hr = 2.9 mas/s) and Titan (25 arcsec/hr = 6.9 mas/s).

Analysis of optimum tip-tilt strategies for the gas giant planets and their moons will be performed in the PDR phase of the NGAO project. The issues are subtle. For example, to image a feature on Jupiter's disk or in its rings, is it sufficient to use one bright moon (e.g. Io)

for the low-order wavefront sensor, or are multiple tip-tilt "stars" needed? If the latter, can these include some "fixed" stars or must they be other moons?

3.7.5.2 LGS on Bright Extended Sources

For very extended objects like Jupiter and Saturn, the system will require the capability of putting Laser Guide Stars on the disk of the planet. The visible light from the planetary disk may then need to be rejected in order to obtain sufficient signal to noise ratio for the LGS wavefront sensors.

3.7.5.3 Required observing modes

For some programs in this science case, e.g., atmospheric monitoring of long times-scales, the scientific return of the NGAO system would greatly increase if some sort of flexible or queue scheduling or service observing were to be offered. Frequent and extremely short (half hour) direct imaging observations of a specific target such as Io to monitor its activity over a long period of time would be extremely valuable. Such programs could be done more easily if flexible or queue or service observing were available at Keck.

3.7.5.4 Observing efficiency

These objects require relative short exposures and multiple wavelengths. Thus, minimizing set-up time between exposures is highly desirable. Ensuring fast switching between wavelength bands would also greatly increase the observing efficiency. These are two different operations, and both should have their execution time minimized.

3.7.6 Instrument requirements

3.7.6.1 Required instruments

Primary: Near IR imager, on-axis, diffraction limited, at least 30 arc sec FOV at K band. At J and H, at least 20 arc sec FOV (goal is 30 arc sec, ~Jupiter diameter).
Secondary: Near IR IFU, diffraction limited, R~1000-4000. Field of view as large as possible (planetary disk sizes are up to 30 arc sec, while the Great Red Spot on Jupiter is up to 13 arc sec in diameter). If (as appears likely) one IFU cannot be built with such a large FOV, it will be desirable to be able to position separate IFUs as closely together as possible to facilitate mosaic creation.

3.7.6.2 Field of view

See above.

3.7.6.3 Field of regard

Should be determined by the requirement to find adequate tip-tilt stars.

3.7.6.4 IFU multiplicity

Depends on FOV of IFU. If small, then multiplicity is required to obtain adequate FOV coverage (see above).

3.7.6.5 Wavelength coverage

Imaging: Wavelengths 0.8 – 2.4 μm

Spectroscopy: Wavelengths nominally 0.8 – 2.4 μm. The spectroscopic utility and advantages of an IFU in the range 0.8 – 1 μm will be explored in future studies.

3.7.6.6 Spectral resolution

For gas giants, the spectroscopic features in the near infrared are dominated by methane absorption features, which are exquisitely sensitive to the vertical distribution of aerosols in the atmosphere. Spectral resolution of R~3000 provides very good coverage of structure of features. Higher resolution provides even better information for specific molecules and isotopes.

3.7.7 Requirements Summary

The requirements for the *Gas Giants* science case (all three goals) are summarized in the following table.

Requirements Table 15. Gas Giants derived requirements

#	Science Performance Requirement	AO Derived Requirements	Instrument Requirements
15a.1	*Capability of tracking a moving target* with rate up ≤ 50 arcseconds per hour (14 mas/second)		
15a.2	*Capability of using at least one tip-tilt star that is moving with respect to the (moving) target planet*. (For example, a moon of Jupiter or Saturn)	Motion of low order wavefront sensor to track tip-tilt star.	
15a.3	*Ability to acquire Io within 5" of Jupiter and to track it to within 2.5" of Jupiter.* Note that this is a goal but perhaps not a rigid requirement: we know we can acquire within 10" today.	May require either a diaphragm or a filter to attenuate the light from Jupiter.	See AO derived requirement at left.
15a.4	*Sensitivity:* comparable to the current Keck system		

15a.5	*Absolute Photometric accuracy:* comparable to the current Keck system (≤ 0.05 mag)	PSF knowledge	Detector flat-fielding requirements, linearity, etc will flow down from required photometric accuracy.
15a.6	*Targets*: Jupiter and Saturn systems, with special focus on Io and Titan	AO system capable of working in the presence of scattered light from nearby extended objects; NGS option for bright moons	Jupiter & Saturn: near-IR imager from 0.8-2.4 μm Io: IFU 0.8-2.4 μ Titan: IFU 0.8-2.4 μm
15a.7	*Observing wavelengths* I, z/Y, J, H, K	AO system must pass these wavelengths to science instruments.	Near- IR imager and IFU spectrometer, λ= 0.8-2.4 μm
15a.8	*Spatial sampling:* for imager, ≤ Nyquist at the observing wavelength		For imager, spatial sampling ≤ Nyquist at the observing wavelength. For IFU, spatial sampling ~λ/D.
15a.9	Imager field of view ≥ 30" diameter at K band, ≥ 20" diameter at J and H bands (goal 30")	AO system passes a >30" unvignetted field of view	Imager field of view ≥ 30" diameter at K band, ≥ 20" diameter at J and H bands (goal 30")
15a.10	IFU field of view as large as possible, up to 15" (Jupiter's diameter is 30", Great Red Spot is 13" diameter)		If IFU FOV is only a few arc sec, desirable to be able to place different IFUs as close together as possible. No firm numerical requirement.
15.11	Moons are very bright: do not allow saturation. Typical brightness: 5 mag per square arc sec.		Either need to use neutral density filters, or have a fast shutter, or have a detector with large wells or very short exposure times (and low read noise). Note: these observations will have high overhead.
15a.12	The following observing preparation tools are required: PSF simulation, target ephemeris, exposure time calculator to enable choice of ND filter and exposure		

	time.		
15a.13	The following data products are required: Calibrated PSF.		
15a.14	Observing requirements: Io and Titan are time domain targets; Io requires ≤ 1 hr notification of volcano activity. Typical timescales for clouds on Titan are of order days to weeks.		

3.7.8 References

Ádámkovics, M., M. Wong, C. Laver, and I. de Pater, 2007. Detection of widespread morning drizzle on Titan. Science 318, 962-965.

Ádámkovics, M., I. de Pater, H. Roe, S. Gibbard, and C. Griffith, 2004. Spatially-resolved spectroscopy at 1.6 μm of Titan's atmosphere and surface. Geophys. Res. Lett. 31, L17S05.

Ádámkovics, M., I. de Pater, M. Hartung, F. Eisenhauer, R. Genzel and C.A. Griffith, 2006. Titan's bright spots: Multiband spectroscopic measurement of surface diversity and hazes. J. Geophys. Res. 111, EO7S06.

Barnet, C. D., Beebe, R. F., and Conrath, B. J. 1992a. A seasonal radiative-dynamic model of Saturn's troposphere. Icarus 98, 94-107.

Barnet, C. D., Westphal, J. A., Beebe, R. F., and Huber, L. F. 1992b. Hubble Space Telescope observations of the 1990 equatorial disturbance on Saturn - Zonal winds and central meridian albedos. Icarus 100, 499-511.

Beebe, R. F., Barnet, C., Sada, P. V., and Murrell, A. S. 1992. The onset and growth of the 1990 equatorial disturbance on Saturn. Icarus 95, 163-172.

Brown, M. E., Bouchez, A. H., and Griffith, C. A. 2002. Direct detection of variable tropospheric clouds near Titan's south pole. Nature 420, 795-797.

Caldwell, J., and 9 colleagues 1992. Titan: Evidence for seasonal change - A comparison of Hubble Space Telescope and Voyager images. Icarus 97, 1-9.

de Pater, I., F. Marchis, B.A. Macintosh, H.G. Roe, D. Le Mignant, J.R. Graham, and A.G. Davies, 2004. Keck AO observations of Io in and out of eclipse. Icarus 169, 250-263

de Pater, I., Laver, C., Marchis, F., Roe, H. G., and Macintosh, B. A. 2007. Spatially resolved observations of the forbidden SO $a\Delta \rightarrow X\Sigma$ rovibronic transition on Io during an eclipse and a volcanic eruption at Ra Patera. Icarus 191, 172-182.

Laver, C., de Pater, I., Roe, H., and Strobel, D. F. 2007. Temporal behavior of the SO 1.707 μm ro-vibronic emission band in Io's atmosphere. Icarus 189, 401-408.

Lorenz, R. D., Lemmon, M. T., Smith, P. H., and Lockwood, G. W. 1999. Seasonal Change on Titan Observed with the Hubble Space Telescope WFPC-2. Icarus 142, 391-401.

Marcus, P. S. 2004. Prediction of a global climate change on Jupiter. Nature 428, 828-831.

Marcus, P.S., X. Asay-Davis, M. Wong, C. Go, and I. de Pater 2007. Why Jupiter has a new red spot. Science, submitted.

Moses, J. I. and Greathouse, T. K. 2005. Latitudinal and seasonal models of stratospheric photochemistry on Saturn: Comparison with infrared data from IRTF/TEXES. Journal of Geophysical Research Planets 110, 9007

Ollivier, J. L., and 6 colleagues 2000. Seasonal effects in the thermal structure of Saturn's stratosphere from infrared imaging at 10 microns. Astronomy and Astrophysics 356, 347-356.

Roe, H. G., de Pater, I., and McKay, C. P. 2004. Seasonal variation of Titan's stratospheric ethylene (C_2H_4) observed. Icarus 169, 440-461.

Sanchez-Lavega, A., and 5 colleagues 1991. The Great White Spot and disturbances in Saturn's equatorial atmosphere during 1990. Nature 353, 397-401.

Schaller, E. L., Brown, M. E., Roe, H. G., and Bouchez, A. H. 2006a. A large cloud outburst at Titan's south pole. Icarus 182, 224-229.

Schaller, E. L., Brown, M. E., Roe, H. G., Bouchez, A. H., and Trujillo, C. A. 2006b. Dissipation of Titan's south polar clouds. Icarus 184, 517-523.

3.8 Characterization of Ice Giant Planets

Author: Heidi B. Hammel and Imke de Pater
Editors: Claire Max, Elizabeth McGrath

3.8.1 Scientific background and context

Extrasolar planet hunting has matured to the point of detecting Neptune-sized bodies around other stars (e.g., Butler et al. 2004; McArthur et al. 2004; Beaulieu et al. 2006; Lovis et al. 2006, and others), yet many aspects of the ice giants within our own Solar System—Uranus and Neptune—remain elusive. Questions whose answers are within our grasp include: what are the natures and timescales of the mechanisms driving atmospheric circulation on an ice giant? By what process are large discrete atmospheric features formed and dissipated? How does seasonally-varying insolation affect the energy balance in an ice giant atmosphere? These questions, which may be answerable for Uranus and Neptune in the coming decades with Keck observations, have direct implications for the atmospheres of ice giants around other stars.

The diverse architecture of these extrasolar planetary systems is influencing theories on planet formation. Such theories start with circumstellar disks, but crucial steps of early planet formation are still not well understood. Planetary ring systems are close analogues to these disks although much smaller in extent; they exhibit similar characteristics such as gaps, clumping, and waves, but are much more accessible to our telescopes and evolve on time scales more commensurate with human lifetimes. The ring systems of the local ice giants are of particular interest due to their clumpy nature and their rapid evolution (the latter discovery based on Keck images), indicative of observable ongoing processes in these systems.

At present, there are only two facilities in the world that are capable of producing images with adequate spatial resolution to effectively assess the dynamics and evolution of ice-giants atmospheres and ring systems: the Keck Observatory and the Hubble Space Telescope. These facilities are complementary, and together have revolutionized our understanding of both Uranus and Neptune, as well as their ring systems.

Looking toward the future, however, Hubble's end of life is likely in the 2012 timeframe. The James Webb Space Telescope has no moving target capability (though a moving-target study is underway). Furthermore, these planets may be too bright for the exquisite sensitivity of JWST's cameras (again, a study is underway to assess its bright-object limitations). No spacecraft are planned to either of these distant worlds until some time after 2035, according to both the Planetary Decadal Survey (NRC 2003) and the recent NASA Solar System Exploration Roadmap (NASA 2007). Thus, the Keck Observatory will soon be unique in its ability to study Uranus and Neptune.

Our goal here is to present those ice giant science goals that will continue to be productive at Keck in the next decade. We then identify the necessary requirements for the NGAO system and instrumentation suite to accomplish this ice-giant science. The gas giants Jupiter and Saturn (and their satellites and rings) present a sufficiently different set of constraints that they were discussed separately in the previous section.

3.8.2 Scientific goals

The ice giants provide a rich arena for scientific studies, and as discussed above, these studies have implications beyond just the two planetary systems themselves. Here we identify four ice giant science goals in which the Keck Observatory has historically been the leader, and which are not attainable with any other existing or planned facility that we are aware of: short-term atmospheric dynamics; long-term climate change; atmospheric vertical structure; and temporal evolution of ring systems.

3.8.2.1 Short-term Atmospheric Dynamics

The zonal wind profiles of giant planets are of critical importance for understanding many aspects of the planets. Several recent studies have used Keck-derived profiles for ice-giant zonal winds to explore the planets' deep convective mixing (Aurnou, Heimpel, and Wicht 2007; Soderlund and Aurnou 2007), as well as the formation of discrete dark atmospheric features on both planets (Deng and LeBeau 2007; LeBeau and Deng 2007).

Keck observations provided the first comprehensive zonal wind profile of Uranus (Hammel et al. 2006b). This could only be accomplished by tracking the small-scale atmospheric features over several contiguous nights (Figure 40). Even so, there are significant gaps in the profile at some latitudes. Keck images are showing increased cloud activity, so with continued monitoring, those gaps can be filled.

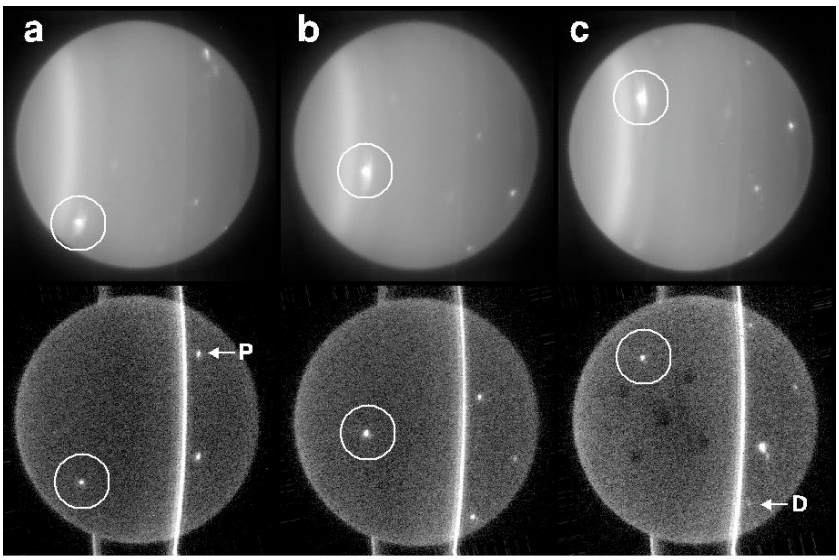

Figure 40. Keck images of Uranus in 2004.
These images of the 3.7"-diameter disk of Uranus were obtained on 4 July (a, b, and c). For each pair, the upper image is H (1.6 μm) and the lower image is K' (2.2 μm). The south pole of Uranus is to the left. An unusual bright feature is circled in each image; tracking such features yields the zonal atmospheric velocity at that latitude. At K', images are dominated by ring flux, and Uranian moons masquerade as northern cloud features (P = Portia; D = Desdemona); unarrowed white spots are small-scale cloud features. Dark splotches in (c) at K' are an artifact caused by residual charge. From Hammel et al. (2005a).

Neptune's wind velocity field reveals a considerable dispersion in relative zonal velocities at the same latitude band, very different from the wind fields in other giant planets (Martin et al. 2007). Such studies require minute-to-minute tracking of small cloud features; Neptune has an astonishing number of such clouds in Keck images (Figure 41).

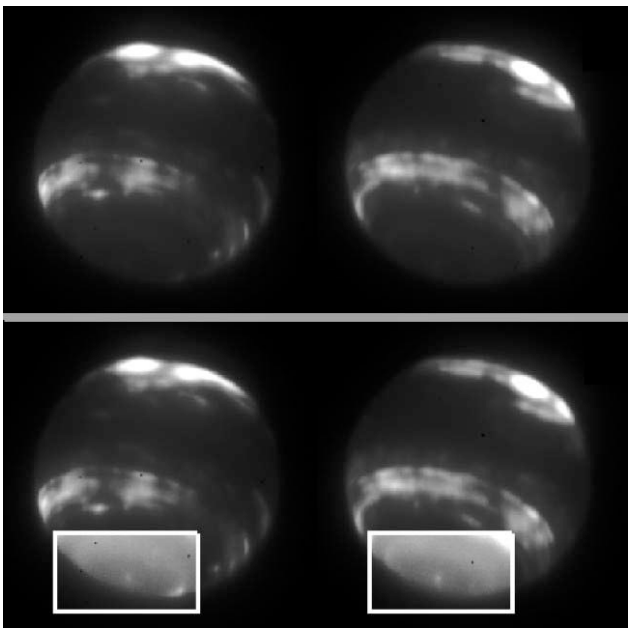

Figure 41. Neptune with Keck in 2005.
The planet's disk subtends only 2.3 arcseconds. Upper pair: these H-band images of Neptune were obtained with the Keck NGS AO system and NIRC2 on 5 July (11:16 UT, left; 13:34 UT, right). They show tropospheric clouds at mid-latitudes in both hemispheres. Lower pair: The south polar regions of the images were enhanced by a factor of 2.6 to show that the zonal circulation pattern continues right to the pole. Similar images, taken in 2001, were used by Martin et al. (2007) to study the detailed structure of the zonal wind profile by tracking dozens of the tiny discrete features. Hammel et al. (2007).

The specific goal for short-term cloud structure studies is continued high-spatial-resolution images in the near infrared to study the formation and evolution of such features on diurnal (hourly) timescales, and to fully map out the detailed zonal wind structures for both planets.

3.8.2.2 Long-term climate change

Obliquity plays an important role in climate change on Earth (e.g., Zachos *et al*. 2001) and Mars (e.g., Nakamura and Tajiki 2002). Uranus, with its pole almost in the ecliptic plane, provides an obliquity extremum. In pre-equinox years, Uranus has been exhibiting increased cloud activity in Keck and HST images (Hammel *et al*. 2005a, 2005b, Sromovsky and Fry 2005), as well as changes in the zonal banded structure, i.e., the "background" atmosphere (Rages et al. 2007). Both are strongly suggestive of seasonally-driven dynamics (Hammel and Lockwood 2007a). Neptune, too, exhibits slight obliquity, and long-term changes in its brightness are suggestive of a role due to solar variation (Hammel and Lockwood 2007b). Once the HST mission is complete, Keck will be the only facility that can continue to observe these atmospheres with spatial resolution that is high enough to determine which zonal bands and clouds are changing in response to insolation variations.

The specific goal for long-term climate change studies is continued high-spatial-resolution images in the near infrared over many years and preferably decades. Such data is required in order to characterize the long-term changes of zonal banded structure, and the longer timescales of discrete-feature formation and evolution.

3.8.2.3 Atmospheric Vertical Structure

TBD

3.8.2.4 Temporal Evolution of Ring Systems

Uranus Ring System. The uranian rings differ markedly from those of the other outer planets. Nine narrow annuli consist of macroscopic particles, ranging in size from ~10 cm to 10 m, with almost no dust (Elliot et al. 1977; Smith et al. 1986). Voyager images revealed many embedded dust belts and the narrow λ ring (Smith et al. 1986; French et al. 1991; Esposito et al. 1991). In 2006, HST images revealed an outer ring system (Showalter and Lissauer 2006), and the rings grew even more intriguing with the Keck discovery of the diverse colors of these new outer rings (de Pater et al. 2006b): the innermost is red, but the outermost is blue, suggesting a dynamical parallel to Saturn's blue E ring, which is generated by Enceladus' ice plumes.

The 2007 Uranus ring-plane crossing (RPX) events provided an unprecedented opportunity to study this ring system (Figure 42). Keck and Hubble images outclassed all other observations with their unparalleled spatial resolution (de Pater et al. 2007).

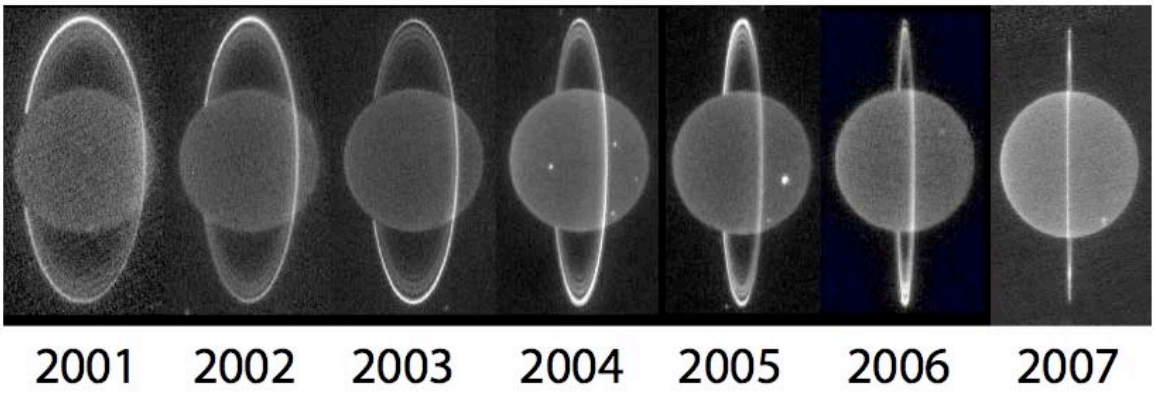

Figure 42. Annual images of the rings of Uranus from Keck.
The last RPX was in 1965, and the next will occur in 2049. White spots in these K'-band images are high-altitude cloud features. Adapted and updated from de Pater et al. (2006).

Figure 43 compares Keck images from 2004 and 2006 with a 2007 dark-side image. The radial extent of the rings appeared to shrink: the ε ring—the dominant feature prior to 2006—faded, and by 2007 was completely invisible. In 2007, the brightest part of the ring system was the ζ ("zeta") ring, which was first detected in 2004 Keck data (de Pater *et al*. 2006a). The rings were exceptionally bright near η ("eta"), which had already been the brightest region on the northern ansa in 2006.

In 2007, the rings were superposed atop each other, but de Pater et al. (2007) extracted a radial scan using an "onion-peel" deconvolution (de Pater et al. 2006a). Figure 44 shows the resulting 2007 profile compared with Keck 2004 data and a Voyager profile.

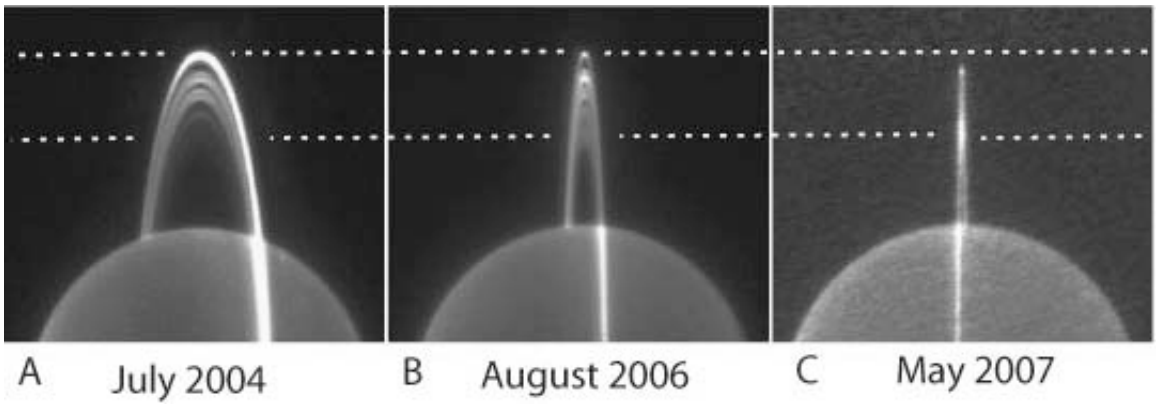

Figure 43. Comparison of the lit and unlit sides of the rings of Uranus.
(A) The lit side in early July 2004. (B) The lit side on 1 August 2006. (C) The unlit side on 28 May 2007. The planet was scaled to the same size in these images. Dotted lines show position of ε ring (upper line) and ζ ring (lower line). de Pater et al. (2007).

Both the older Keck and Voyager profiles differ significantly from the 2007 profile. The brightness of η suggests an optically-thin component, perhaps the 55-km broad outward extension detected via stellar occultations (de Pater et al. 2006a). The region near 45,000 km was nearly devoid of dust according to Voyager, but surprisingly was about half as bright as the η ring in the Keck data, indicative of dust. Even stranger is the ζ ring, which apparently shifted radially from the Voyager epoch to the present. de Pater et al. (2007) concluded that the dust distribution within the system changed significantly since the 1986 Voyager encounter. Although modest changes in dusty rings over 20-year time scales had been noted in other ring systems, Keck observations of the Uranian system revealed changes on much larger scales than had been previously recognized.

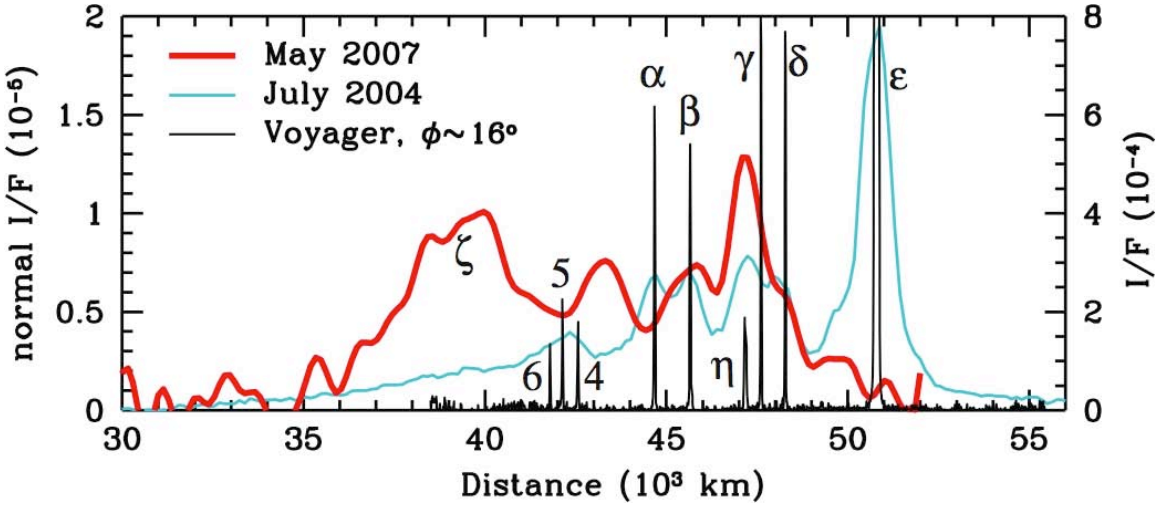

Figure 44. Temporal evolution of the Uranus rings.
Comparison of the 2007 deconvolved (*i.e.*, onion-peeled) radial profile averaged over both north and south sides (red; smoothed radially over ~ 650 km), with the northern profile from 2004 (cyan), and the Voyager profile in backscattered light (black). We shifted the Voyager ε ring to match the Keck profile, compensating for its large eccentricity. The left axis shows the *I*/*F* normal to the ring plane of the 2007 profile. The axis on the right side

shows the measured *I/F* for the 2004 data. The scale for the Voyager data is arbitrary (and off-scale for ε). The Voyager data were smoothed to match the Keck pixel size. From de Pater et al. (2007).

Continued observations of the ring system of Uranus as it opens up after equinox will provide a unique record of these unusual variable rings. No other facility can match the detail in Keck images.

Neptune Ring System. Neptune's ring arcs, too, are unique within the Solar System. Keck AO observations of Neptune's ring system from July 2002 and October 2003 (Figure 45) revealed significant temporal variation since Voyager in 1989 (de Pater et al. 2005). Only arc Fraternité appeared to follow a well-defined mean orbital motion; all other arcs shifted in location and intensity relative to Fraternité. In particular the leading arcs Liberté and Courage were severely diminished in intensity. Voyager sub-arcs Egalité 1 and 2 reversed in relative intensity, suggesting that material migrated between resonance sites. Both the 1998 NICMOS and 2002/2003 Keck data indicated that arc Liberté changed resonance sites. In 2003, Courage was observed ~8° ahead in its orbit, i.e., it had moved over one full resonance site (out of 43 sites).

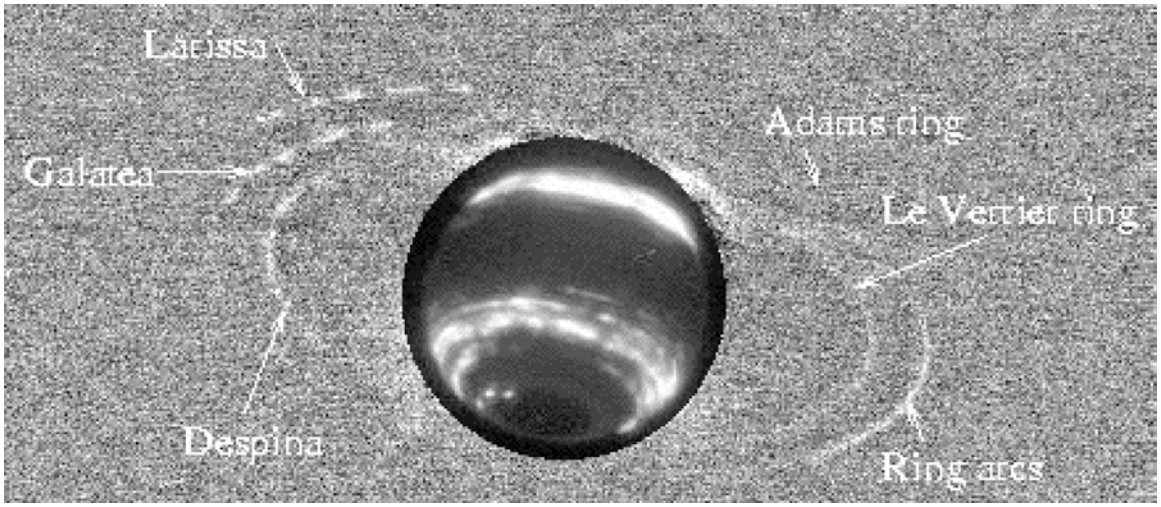

Figure 45. Keck observations of Neptune's rings.
This composite image of July 2002 Keck AO data (K' band, total integration time of 33 minutes) shows satellites, ring arcs, and the complete Adams and Le Verrier rings. The images have been high-pass filtered by subtracting the same image median-smoothed with a width of 50 pixels. This procedure removes diffuse scattered light, and brings out small-scale features. Neptune is highly saturated in this composite exposure; here the saturated planet has been cropped and a 1-minute exposure of Neptune itself is shown in its place. From de Pater et al. (2005).

The red color of the ring arcs (Dumas et al. 2002; de Pater et al. 2005) is consistent with ring arcs being composed of dust, the natural product of moon erosion. If indeed the entire arc system has been decaying over as short a timescale as ~10 years, as the Keck data suggest, the loss mechanism must be acting faster than the regeneration mechanism. No quantitative theory has yet been devised that can describe the rapid dynamical evolution discovered with Keck observations.

Continued observations of Neptune's ring system with Keck are required to determine if some or all ring arcs decay away over time, or if some arcs bounce back into existence near one of their former locations or in a completely new location.

3.8.2.5 Satellite-Ring interactions and astrometry

Interactions between rings and moons manifest themselves in a variety of ways: some moons are known to "shepherd" rings (Cordelia and Ophelia shephard the ε ring); others define their sharp edges (Porco and Goldreich 1987); and yet others can raise sinusoidal patterns on ring edges (French and Nicholson 1995, Showalter and Lissauer 2004).

The precise orbits of moons can be influenced by gravitational torques as well, which could be the cause of variations in the orbits of Galatea (Neptune) and Mab (Uranus). In addition, small moons in the Uranus system, the closely-packed "Portia group," show significant orbital changes over timescales of a few years. This result supports inferences by Duncan and Lissauer (1997) that the system is chaotic, with collisions likely to occur over million-year time scales. The two smallest moons Cupid and Perdita, straddle the orbit of Belinda and are on especially precarious orbits.

Keck can continue to be instrumental in detecting the precise positions of the faint satellites in the ice giant systems.

3.8.3 Proposed observations and targets

Most of the science for all four goals can be readily accomplished with a relatively modest number of observations due to science multiplexing: *i.e.,* the same image that yields measurements of a ring system can also be used for atmospheric feature measurements. The differences between the science goals usually come down to differences in imaging cadence or wavelength coverage: *e.g.,* fifty images in a night for atmospheric dynamical studies versus one image set per year for long-term studies; or repeated deep imaging at a single wavelength for ring studies versus multi-wavelength imaging for atmospheric structure measurements. In this section, we outline the specific requirements for each goal.

3.8.3.1 Short-term Atmospheric Dynamics

Repeated observations at one wavelength (typically H has the best spatial resolution and feature contrast) on one night for very-short-timescale (diurnal) feature tracking and evolution. Moderate timescale feature-tracking for zonal winds with reasonable error bars requires a minimum of four contiguous "nights" (partial nights are perfectly fine, e.g., half nights or third nights – but they still should be four contiguous). Multi-wavelength is preferred for moderate-timescale tracking so that altitude discrimination can be done for discrete features.

3.8.3.2 Long-term climate change

At a minimum, a single multiwavelength set (J, H, and K') should be obtained each year. More is desirable, especially for Uranus which has been exhibiting secular change in the

brightness of its banded structure as equinox has been approaching. A monthly sample would be the maximum for this science goal.

3.8.3.3 Atmospheric Vertical Structure

TBD. This will be determined in later releases of this document and during the PDR phase.

3.8.3.4 Ring Systems

Typically, many repeated images at a single wavelength (typically K', where the planet is dark and thus the rings can be traced close in to the planet). Sometimes sets of H-band data are use in order to provide basic color information on the rings. Timing is important (see below), but for both planets, these times can be determined months in advance.

Uranus. Data need to be collected at specific times depending of the location of the ring periapse, and when Uranus is close to equinox, the locations of the satellites.

Neptune. Specific timing is important for Neptune ring imaging as well, since the arcs cannot be imaged very close to Neptune, only at their elongation points – though imaging at other ties should be done to capture possible emergence of new arcs.

3.8.3.5 Satellite-Ring interactions and astrometry

The observing requirements for satellite and ring astrometry are identical to those needed for short-term atmospheric dynamics.

3.8.4 AO requirements

3.8.4.1 Natural Guide Star AO Capability

NGS AO capability should be built into the LGS AO instrumentation. NGA AO will significantly increase the efficiency of the observatory, since it could be implemented on nights that LGS AO is not feasible (whether due to weather, LGS equipment, or other issues). Keck's current NGS AO has been optimized to perform diffraction-limited imaging on the extended ice giants Uranus and Neptune. It would be criminal to lose this capability when the system is upgraded: Keck is the *only* facility that can provide near-infrared imaging on these distant planets with 40-50 mas spatial resolution, which is critical for the science outlined here. We strongly recommend that the current Keck NGS capability or its equivalent be retained within the NGAO design.

3.8.4.2 Wavefront error

A wavefront error of 140 nm would provide excellent angular resolution in the visible, better than HST and adequate for our program. Future releases of this Science Case Requirements Document will compare the science performance for 140, 170, and 200 nm of wavefront error.

3.8.4.3 Encircled energy

Comparable to current Keck capabilities, or better.

3.8.4.4 Contiguous field requirement

Required FOV is 15 arcseconds. This is driven by the breadth of the Uranus ring system, which subtends roughly 13 arc seconds from ansa to ansa. The planet itself subtends 3.4 arcseconds. Neptune subtends about 2.3 arcseconds, and its ring system is 8 arcseconds from ansa to ansa.

3.8.4.5 Photometric precision

Comparable to current Keck capabilities, or better.

3.8.4.6 Astrometric precision

Comparable to current Keck capabilities, or better.

3.8.4.7 Contrast

Comparable to current Keck capabilities, or better.

3.8.4.8 Polarimetric precision

N/A

3.8.4.9 Backgrounds

Comparable to current Keck capabilities, or better.

3.8.4.10 Overall transmission

Comparable to current Keck capabilities, or better.

3.8.5 Other key design features

3.8.5.1 Moving Target Tracking

The capability of observing moving targets must be included in the design of NGAO. This will require implementation of differential guiding when the tip-tilt source is not the object itself, and when the tip-tilt source is moving relative to the target. The maximum relative velocity for Uranus is 5.0 arcseconds per hour (1.4 milliarcseconds per second); Neptune is 3.6 arcsec/hr (1.0 mas/s).

3.8.5.2 Required observing modes

For some programs in this science case (e.g., atmospheric monitoring of long times-scales), the scientific return of the NGAO system would greatly increase if some sort of flexible or queue scheduling or service observing were to be offered. Frequent and extremely short (half hour) direct imaging observations of a specific target such as Neptune, to monitor its activity over a long period of time, would be extremely valuable. Such programs could be done more easily if flexible or queue or service observing were available at Keck.

3.8.5.3 Observing efficiency

These objects require relative short exposures and multiple wavelengths. Thus, minimizing set-up time between exposures would be highly desirable. Ensuring fast switching between wavelength bands would also greatly increase the observing efficiency. These are two different operations, and both should have their execution time minimized.

3.8.6 Instrument requirements

3.8.6.1 Required instruments

Primary: Near IR imager, on-axis, diffraction limited, 15-arcsec FOV
Secondary: Near IR IFU, on-axis, diffraction limited, 15-arcsec FOV, R~1000-4000

3.8.6.2 Field of view

Preferred 15 arcseconds FOV. Minimum: 5 arcseconds.

3.8.6.3 Field of regard

Should be determined by the requirement to find adequate tip-tilt stars.

3.8.6.4 IFU multiplicity

Depends on FOV of IFU. If small, then multiplicity is required to obtain adequate FOV coverage (15 arcseconds).

3.8.6.5 Wavelength coverage

Imaging: Wavelengths 0.8 – 2.4 μm
Spectroscopy: Wavelengths 0.8 – 2.4 μm

3.8.6.6 Spectral resolution

For ice giants, the spectroscopic features in the visible through near infrared are dominated by methane absorption features, which are exquisitely sensitive to the vertical distribution of aerosols in the atmosphere. Spectral resolution of R~3000 provides very good coverage of structure of features. Higher resolution provides even better information for specific molecules and isotopes.

3.8.7 Requirements Summary

The requirements for the *Ice Giants* science case (all four goals) are summarized in the following table.

Requirements Table 16. Ice Giants derived requirements

#	Science Performance Requirement	AO Derived Requirements	Instrument Requirements
16.0	*Capability of tracking a moving target* with	• The planet can be used as tip/tilt guidestar (proper	

	rate up ≤ 5.0 arcseconds per hour (1.4 mas/se)	motion of ≤ 5.0 arcsec/hour). • The AO system requires sufficient field of view for planets and for their seeing disks (>5 arcsec). • The tip-tilt residual error will be less than 10 mas (limited by resolved primary) while guiding on one planet at 5.0 arcsec/hr (1.4 mas/sec).	
16.1	*Sensitivity:* comparable to the current Keck system		Near-IR imager, 0.8 - 2.4 μm
16.2	*Photometric accuracy:* comparable to the current Keck system		Near- IR imager
16.3	*Targets:* Uranus and Neptune systems	AO system (both LGS and NGS) capable of correcting on extended objects. • Uranus = 3.4 arcsec • Neptune = 2.3 arcsec	Near-IR imager, 0.8 – 2.4 μm
16.4	*Observing wavelengths:* J, H, K		Near- IR imager
16.5	*Spatial sampling:* ≤ Nyquist at the observing wavelengths		Spatial sampling ≤ Nyquist at the observing wavelength
16.6	*Field of view:* ≥ 15" diameter	AO system passes a >15" unvignetted field of view	Imager fields of view ≥ 15"
16.7	*Observing requirements:* one run per semester with at least 4 contiguous (partial) nights; both targets can be studied during one run		
16.8	The following *observing preparation tools* are required: PSF simulation, target ephemeris, exposure time calculator to enable choice of ND filter and exposure		

	time.		
16.9	The following *data products* are required: Calibrated PSF.		
16.10	*Observing requirements:* some science goals would be well suited to queue or service observing modes		

3.8.8 References

Aurnou, J., Heimpel, M., and Wicht, J. 2007. The effects of vigorous mixing in a convective model of zonal flow on the ice giants. Icarus 190, 110-126

Beaulieu, J.-P., and 72 colleagues 2006. Discovery of a cool planet of 5.5 Earth masses through gravitational microlensing. Nature 439, 437-440.

Butler, R. P., and 7 colleagues 2004. A Neptune-Mass Planet Orbiting the Nearby M Dwarf GJ 436. Astrophysical Journal 617, 580-588

de Pater, I., S. Gibbard, E. Chiang, H. B. Hammel, B. Macintosh, F. Marchis, S. Martin, H. G. Roe, and M. Showalter (2005). The dynamic neptunian ring arcs: gradual disappearance of Liberté and a resonant jump of Courage. Icarus 174, 263-272.

de Pater, I., S. Gibbard, and H. B. Hammel (2006a). Evolution of the dusty rings of Uranus. Icarus 180, 186-200.

de Pater, I., H. B. Hammel, S. G. Gibbard, and M. R. Showalter (2006b). New dust belts of Uranus: One ring, two ring, red ring, blue ring. Science 312, 92-94.

de Pater, I., H. B. Hammel, M. R. Showalter, and M. A. van Dam (2007). The Dark Side of the Rings of Uranus. Science.

Deng, X., and R.P. LeBeau, " Dynamic Simulations of Potential Dark Spots in the Atmosphere of Uranus", 39th Annual Meeting of the Division for Planetary Sciences, Orlando, FL, October 7-12, 2007.(abstract)

Dumas, C., Terrile, R. J., Smith, B. A., and Schneider, G. 2002. Astrometry and Near-Infrared Photometry of Neptune's Inner Satellites and Ring Arcs. Astronomical Journal 123, 1776-1783 Duncan and Lissauer 1997

Elliot, J. L., Dunham, E., and Mink, D. 1977. The rings of Uranus. Nature 267, 328-330.

Esposito, L. W., Brahic, A., Burns, J. A., and Marouf, E. A. 1991. Particle properties and processes in Uranus' rings. In "Uranus", pp. 410-465.

French, R. G. and Nicholson, P. D. 1995. Edge waves and librations in the Uranus epsilon ring. Bulletin of the American Astronomical Society 27, 857

French, R. G., Nicholson, P. D., Porco, C. C., and Marouf, E. A. 1991. Dynamics and structure of the Uranian rings. In "Uranus", pp. 327-409.

Hammel, H. B., and G. W. Lockwood (2007a). Long-term atmospheric variability on Uranus and Neptune. Icarus 186, 291-301.

Hammel, H. B., and G. W. Lockwood (2007b). Suggestive correlations between the brightness of Neptune, solar variability, and Earth's temperature. Geophysical Research Letters 43, L08203.

Hammel, H. B., I. de Pater, S. G. Gibbard, G. W. Lockwood, and K. Rages. New cloud activity on Uranus in 2004: First detection of a southern feature at 2.2 microns. Icarus 175, 284-288 (2005a).

Hammel, H. B., I. de Pater, S. Gibbard, G. W. Lockwood, and K. Rages. Uranus in 2003: Zonal winds, banded structure, and discrete features. Icarus 175, 534-545 (2005b).

Hammel, H. B., M. L. Sitko, D. K. Lynch, R. W. Russell, T. Hewagama, and L. Bernstein. Mid-infrared ethane emission on Neptune and Uranus. Ap. J. 644, 1326-1333 (2006).

Hammel, H. B., M. L. Sitko, G. S. Orton, T. Geballe, D. K. Lynch, R. W. Russell, and I. de Pater. Distribution of ethane and methane emission on Neptune. *Astron. Journal* **134**, 637-641 (2007).

LeBeau, R.P., and X. Deng, 2007. Toward Capturing the Many Motions of Neptune's Original Great Dark Spot. Bul. Amer. Astron. Soc., in press.

Lovis, C., and 13 colleagues 2006. An extrasolar planetary system with three Neptune-mass planets. Nature 441, 305-309.Martin et al. 2007

Martin, S.C., I. de Pater, H.G. Roe, S.G. Gibbard, B.A. Macintosh, and C.E. Max, 2007. Near-IR Adaptive Optics imaging of Neptune's upper atmosphere in 2001. Icarus, to be submitted.

McArthur, B. E., and 11 colleagues 2004. Detection of a Neptune-Mass Planet in the ρ1 Cancri System Using the Hobby-Eberly Telescope. Astrophysical Journal 614, L81-L84.

NASA 2007. NASA Solar System Exploration Strategic Roadmap, updated 12 February 2007. http://solarsystem.nasa.gov/multimedia/downloads/SSE_RoadMap_2006_Report_FC-A_med.pdf

Nakamura, T. and Tajika, E. 2002. Stability of the Martian climate system under the seasonal change condition of solar radiation. Journal of Geophysical Research (Planets) 107, 5094

NRC 2003. The "Planetary Decadal Survey." New Frontiers in the Solar System: An Integrated Exploration Strategy. http://www.nap.edu/catalog.php?record_id=10432#toc

Porco, C. C. and Goldreich, P. 1987. Shepherding of the Uranian rings. I - Kinematics. II - Dynamics. Astronomical Journal 93, 724-737.

Rages, Kathy A.; Hammel, H. B.; Sromovsky, L. (2007). Uranus: Direct Comparison of Northern vs. Southern Hemispheres at Equinox. Bul. American Astronomical Society, in press.

Smith, B. A., and 10 colleagues 1986. Voyager 2 in the Uranian system - Imaging science results. Science 233, 43-64. Showalter and Lissauer 2004

Showalter, M. R. and Lissauer, J. J. 2006. The Second Ring-Moon System of Uranus: Discovery and Dynamics. Science 311, 973-977.

Soderlund, Krista M.; Aurnou, J. M., 2007. Effects of Deep Convective Mixing on the Ice Giants Bull. American Astronomical Society, in press.

Sromovsky, L. A. and Fry, P. M. 2005. Dynamics of cloud features on Uranus. Icarus 179, 459-484.

Zachos, J. C., Shackleton, N. J., Revenaugh, J. S., Pälike, H., and Flower, B. P. 2001. Climate Response to Orbital Forcing Across the Oligocene-Miocene Boundary. Science 292, 274-278.

3.9 Backup Science

Authors: Elizabeth McGrath, Claire Max

3.9.1 Scientific background and context

This section addresses science cases that can be accomplished when one must shift to NGS-mode operations if the lasers cannot be propagated (e.g. due to cirrus). It also includes less-demanding examples of LGS science that can be done when the laser power available is lower than nominal due to hardware problems. The derived requirements for Backup Science will largely involve science preparation and operations issues. The primary AO requirement is that the field of regard for the NGS wavefront sensors be large enough to provide an acceptable amount of sky coverage. Unless a flexible queue-based schedule is adopted for the Keck Observatory, it is crucial to plan for backup science operations that will provide results in these most difficult observing scenarios in order to ensure a minimal amount of wasted shutter time. This is particularly important for extragalactic science.

3.9.2 Extragalactic NGS science

The main challenge facing NGS extragalactic science is the limited amount of sky coverage provided by current systems. Unlike other science fields, extragalactic observations tend to be focused away from the plane of our Galaxy, and therefore in less-dense stellar fields. The goal of NGAO should be to provide at least as much sky coverage as current NGS systems so that at a minimum, the science currently achievable will remain within grasp if the observer is forced to switch to a backup NGS mode.

Much of the extragalactic science in LGS-mode will rely on the deployable IFU, with ≥ 6 individual units. In NGS backup mode, we will have only one IFU unit available in the narrow field of the AO relay. Therefore, the number of targets observable to the same limiting flux density within a given night will decrease by a factor of six in NGS-mode. Individual science cases will have more nuanced requirements on sky coverage, but to first order an acceptable NGS sky coverage would be one-sixth of that achievable in LGS mode.

3.9.3 Seeing-limited observations

In many circumstances, when a suitable NGS guide star is unavailable, science cases could benefit from having a seeing-limited imager, such as the acquisition camera. By utilizing the large collecting power of the Keck telescopes, this would provide a large field of view (up to ~3 arcmin) over which large regions of the sky could be surveyed. This could be particularly useful in selecting targets for follow-up with AO imaging or spectroscopy. Requirements to use the acquisition camera in this manner will be detailed in a future release of this document.

3.9.4 Other NGS backup-mode science

There are several other science cases well-suited to NGS backup-mode operations. These include planetary nebulae, circumstellar disks, and other targets with bright natural guide

stars. These are less demanding on the NGS operations and will be described in more detail in a future release of this SCRD.

3.9.5 Proposed observations and targets

For proposed observations, see §2.1.4.

3.9.6 Summary of Requirements

Requirements Table 17. Backup Science Observing Modes: NGS

#	Science Performance Requirement	AO Derived Requirements	Instrument Requirements
17.1	*NGS mode.* NGS as a backup observing mode for when conditions restrict propagation of the lasers.		
17.2	*Sky coverage* ≥5% to ensure at least one-sixth of the off-axis LGS targets will still be observable if it is necessary to go to an NGS backup mode.	Assuming $b=30^o$, For 5% sky coverage: • R=14 mag guide star with 60" diameter field of regard (FOR) • R=15 mag guide star with 45" diameter FOR [Keck Observatory Report No. 208, p. 4-100]	
17.3	Capability to switch between NGS and LGS modes in ≤ 15 minutes (not including target acquisition) to enable flexibility if conditions change.		
17.4	*Sensitivity*. SNR ≥ 10 for a z = 2.6 galaxy in an integration time ≤ 3 hours for a spectral resolution R = 3500 with a spatial resolution of 50 mas	Sufficiently high throughput and low emissivity of the AO system science path to achieve this sensitivity. Background due to emissivity less than 30% of unattenuated (sky + telescope).	

#	Science Performance Requirement	AO Derived Requirements	Instrument Requirements
17.5	Observing wavelengths = J, H and K (to 2.4 μm)	AO system must transmit J, H, and K bands	Infrared single IFU and imager designed for J, H, and K.
17.6	*Spectral resolution* = 3000 to 4000		Spectral resolution of >3000 in IFU
17.7	*Imaging:* Nyquist sampled at H-band		Nyquist sampled IR imager (at H-band)
17.8	Encircled energy 50% in 70 mas for a bright NGS guide star within 10 arc sec	Wavefront error sufficiently low (~170 nm) to achieve the stated requirement in J, H, and K bands.	Optimum spaxel size will be determined during a detailed study of the IFU instrument.
17.9	If a new instrument: IFU field of view ≥ 1" x 3" to allow simultaneous background measurements while observing a 1" galaxy. OSIRIS FOV would be adequate.	Narrow relay passes 1"x3" field	If a new instrument: IFU field of view ≥ 1" x 3" to allow simultaneous background measurements while observing a 1" galaxy. OSIRIS FOV would be adequate.
17.10	Imager FOV ≥ 10" x 10" for galactic center and gravitational lensing science		Imager FOV ≥ 10" x 10"
17.11	Relative photometry to ≤ 5% for observations during a single night, provided the night is photometric	Knowledge of ensquared energy in IFU spaxel to 5%.	
17.12	Should be able to initially center a galaxy to ≤ 10% of science field of view		
17.13	Should know the relative position of the galaxy to ≤ 20% of spaxel or pixel size		
17.14	Target drift should be ≤ 10% of spaxel size in 1 hr		

#	Science Performance Requirement	AO Derived Requirements	Instrument Requirements
17.15	The following observing preparation tools are required: NGS guide star finding tool; PSF simulation and exposure time calculator		
17.16	The following data products are required: calibrated spectral data cube		